

VAPOUR PRESSURES OF SOME INORGANIC
SULPHATES AT HIGH TEMPERATURES

Gomatam V. Jagannathan

A Thesis Submitted for the Degree of PhD
at the
University of St Andrews



1977

Full metadata for this item is available in
St Andrews Research Repository
at:
<http://research-repository.st-andrews.ac.uk/>

Please use this identifier to cite or link to this item:
<http://hdl.handle.net/10023/15500>

This item is protected by original copyright

VAPOUR PRESSURES OF SOME INORGANIC
SULPHATES AT HIGH TEMPERATURES

A Thesis
presented for the degree of
DOCTOR OF PHILOSOPHY
in the faculty of Science of the
University of St Andrews

by

GOMATAM V. JAGANNATHAN M.Sc.

1977



ProQuest Number: 10167401

All rights reserved

INFORMATION TO ALL USERS

The quality of this reproduction is dependent upon the quality of the copy submitted.

In the unlikely event that the author did not send a complete manuscript and there are missing pages, these will be noted. Also, if material had to be removed, a note will indicate the deletion.



ProQuest 10167401

Published by ProQuest LLC (2017). Copyright of the Dissertation is held by the Author.

All rights reserved.

This work is protected against unauthorized copying under Title 17, United States Code
Microform Edition © ProQuest LLC.

ProQuest LLC.
789 East Eisenhower Parkway
P.O. Box 1346
Ann Arbor, MI 48106 – 1346

TL 8860

ABSTRACT

The vapour pressures of some inorganic sulphates at high temperatures were determined by the combined use of the Knudsen effusion, transpiration, and matrix isolation methods. After a detailed comparison with the results of other investigators, it is concluded that the principal vapour species in the case of K_2SO_4 , Rb_2SO_4 , and Cs_2SO_4 are the undecomposed sulphate molecules themselves, and in the case of Li_2SO_4 the decomposition products, Li , SO_2 , and O_2 . The sodium salt also decomposes to some extent into Na , SO_2 , and O_2 , but it is deduced that the vapour concentration of the species Na_2SO_4 is probably greater than was formerly supposed. The decomposition of alkaline earth sulphates is also discussed, especially in the light of the dependence of the Knudsen effusion results upon the size of the orifice used.

On the basis of the vapour constitutions deduced, thermodynamic functions for the important species present are tabulated up to 1400 K or above. Reference is also made to the function of sodium sulphate in the glass-making industry and to the possible mechanism of its corrosive action on furnace walls.

CERTIFICATE

I hereby certify that G.V. Jagannathan has spent eleven terms of research work under my supervision, has fulfilled the conditions of Ordinance No. 16 (St. Andrews) and is qualified to submit the accompanying thesis in application for the Doctor of Philosophy.

P.A.H. Wyatt

DECLARATION

I declare that this thesis is my own composition, that the work of which it is a record has been carried out by myself and that it has not been submitted in any previous application for a Higher degree.

This thesis describes the results of research carried out at the Chemistry Department, United College of St. Salvator and St. Leonard, University of St Andrews, under the supervision of Professor P.A.H. Wyatt, since 1st October 1973.

G.V. Jagannathan

ACKNOWLEDGEMENTS

First of all, I would like to thank my supervisor. Professor Wyatt has been an unfailing source of encouragement and inspiration through out my tenure. I acknowledge without reservation my debt to him and the profit I have gained by our association. I also thank Dr. G.R. Woolley for his help during the course of this research work. My thanks are also due to Dr. Burdett of the University of Newcastle Upon Tyne for his valuable advice regarding the matrix isolation studies.

I am especially grateful to Mr. Rennie and Mr. Clark of the workshop, Mr. Ward and Mr. Linton of the Electronics department, and Mr. West, the glass blower for patiently dealing with one of the most troublesome customers. I thank Dr. J.F. Ireland and other friends who made my stay at St. Andrews quite enjoyable. My thanks are also due to the technical staff of the Chemistry department and to Miss Seonaid McCallum who typed this thesis.

CONTENTS

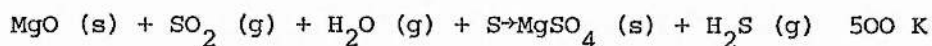
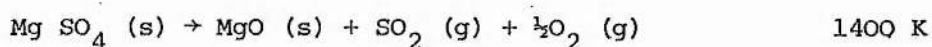
	<u>Page</u>
Introduction	1
Experimental	61
I Alkali metal sulphates	
(A) Results and discussion of muffle furnace experiments	74
(B) Sodium sulphate. Results and discussion of Knudsen effusion experiments	75
(C) Results and discussion of Transpiration experiments.	82
(D) Lithium sulphate. Results and Discussion of Knudsen effusion experiments	89
(E) Results and discussion of Transpiration experiments	95
(F) Rubidium and Caesium sulphates. Results and discussion of Knudsen effusion experiments	103
SUMMARY	113
II Calcium and Magnesium sulphates	
(A) Calcium sulphate. Results and discussion of Knudsen effusion experiments	117
(B) Magnesium sulphate. Results and discussion of Knudsen effusion and Langmuir experiments	138
SUMMARY	
Appendix I - IV	139 - 143
References	144

INTRODUCTION

CHAPTER 1

INTRODUCTION

The high temperature thermodynamic properties of inorganic substances are of great technical importance. The rapid advancement of technology based on the high temperature processes in the traditional fields such as metallurgy, glass and ceramics as well as in the still developing fields of nuclear power, rocket fuel, and semi-conductors has shown the need to have more reliable information about the high temperature thermodynamic properties and behaviour of the substances (which are mostly inorganic) involved in these processes. This information in turn will enable the technologist to calculate with great accuracy the yields of the reactions and to achieve a high degree of economic and production efficiency. A large number of possible routes to produce hydrogen, which is likely to be the future major energy source, are being investigated currently throughout the industrialised world. One of the thermochemical cycles¹ for producing hydrogen from water is based on the sulphate system:



The predicted efficiency for conversion of primary heat into chemical energy in the form of hydrogen by such a cycle is very sensitive to the quality of the thermodynamic data used in evaluating each step. Errors of several kJ in a reaction enthalpy, for example, can effect a change of several percentagepoints

calculated efficiency^{2,3}. A close inspection of available data shows that the thermodynamics of some sulphate cycle steps are not known with sufficient accuracy to rank the cycles properly. While third-law determinations and statistical calculations continue, the free-energy values for many compounds still depend upon the measurement of a chemical or phase equilibrium at a high temperature, if only for checking internal consistency, and here a good feeling for the possibility of chemical complications and even kinetic constraints, is obviously vital. The advances in Mass-spectrometry and the development of Matrix-isolation technique have produced a revolution in our knowledge of the constitution of the vapor phase over high temperature melts and solids. In other words, it is possible now to provide values for all the necessary thermodynamic parameters and vaporisation behaviour of the substances at high temperatures with greater accuracy than before. Jagannathan, Woolley, and Wyatt⁴ have recently reviewed in general terms the entire high temperature field, summarising the main findings of the previous reviews⁵⁻¹¹, the important developments published until 1974, and the present status of the high temperature studies so far carried out on metal sulphates.

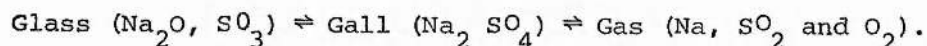
Sodium sulphate is extensively used in the glass manufacturing industry and it is in this compound that interest is centred, although other salts have been included in this study for comparison. The use of sodium sulphate in glass making is discussed briefly below. Work previously reported in this laboratory and elsewhere on the determination of the vapour pressure of this compound will be shown during the course of this introduction to have produced confusing results, and it was for the purpose of introducing some harmony into the somewhat discordant evidence that the present work was undertaken.

The Function of Sodium Sulphate in Glass Making

Sodium sulphate is a component of the raw material mixture ("glass batch") introduced into glass making furnaces. The sodium sulphate acts as a fining agent helping in the dissolution of batch particles and the dissipation of any gas bubbles formed in the process. Qualitative descriptions of the action of sodium sulphate have been produced by Buss¹² and Conroy et al¹³ with the aid of hot stage microscopes. The wetting of the reacting materials by fluxing agents is apparently more favourable in a melt containing sulphate. With insufficient wetting "dry sand groups" form with the participation of lime and dolomite which sinter together and are dispersed throughout the melt as insoluble remains. At temperatures above that of the formation of the first permanent silicate phase, about 1313 K, sodium sulphate is almost completely insoluble in the glass and collects at all melt-solid and melt-gas interfaces. Due to the presence of this highly fluid sulphate liquid at these interfaces the solid aggregates are broken up and dissolution of solid batch particles proceeds at an increased rate and gas bubbles are expelled more rapidly from the melt. In fact this aspect of sulphate behaviour is in some respects reminiscent of that of surface active agents in detergency. Above about 1588 K thermal decomposition of sodium sulphate becomes significant according to Conroy. The products of the decomposition (Na , SO_2 and O_2) are soluble in the glass melt and are transferred across the interfaces between undecomposed sulphate liquid and the glass. This transfer of material upsets the interfacial tensions between the two liquid phases, resulting in development of a vigorous convective motion at all interfaces. Thus in this temperature range a second function develops which produces a significant mixing in the glass. At about 1728 K Conroy believes that the partial pressure of the decomposition

products of sodium sulphate reaches atmospheric pressure, (evidence produced later in this work may cast doubt upon this figure), and a new generation of bubbles develops in the glass. It is then proposed that these bubbles, by virtue of equilibria discussed below, serve a homogenising function in that they transfer soda equivalent (sodium and oxygen) from areas initially high in this component to the melt surface where the final dissolution of silica scum has produced a relatively low soda concentration with respect to silica.

When a bubble develops containing gaseous decomposition products of sodium sulphate it contains sodium monoxide and sulphur trioxide equivalents in some proportion related to the composition of the glass in which the bubble formed. Equilibria are maintained in a three phase system: (1) The glass surrounding the bubble; (2) Molten sodium sulphate ("gall") as droplets in the bubble or as a thin film between bubble and glass; (3) gas phase. This may be expressed as:



When a bubble encounters glass rich in Na_2O , the glass-gall equilibrium is forced to the right as is the gall-gas equilibrium and the bubble will expand. Where silica-rich glass is encountered the glass-gall equilibrium moves to the left, as does the gall-gas equilibrium, and the bubble shrinks. The intermediate sodium sulphate phase controls this three-fold equilibrium since the transported materials must pass through the gall layer. Further, Conroy maintains that the rates at which the reactions proceed to maintain the equilibrium are extremely rapid.

If a melt is cooled to below the decomposition temperature liquid sodium sulphate forms but, since transfer of sodium sulphate into the glass demands decomposition as a pre requisite, the sodium sulphate solidifies as

a separate phase. However, so long as the temperature of the melt is above 1728 K and some undecomposed sodium sulphate persists, then all three sulphate functions (wetting, stirring and soda transfer) operate simultaneously, and melting is completed sooner than with sulphate-free batch. Buss found that the smallest proportion of sulphate to produce effects that were still clearly visible in the miniature melts of his hot stage microscope experiments was 3%.

These then are the reasons for introducing sodium sulphate into the glass batch. It also has disadvantages. It has been observed that large areas of the fire brick within the regenerator towers connected with the glass furnaces have been completely corroded away, and also that a large quantity of sodium sulphate has been found in the towers. How the sulphate reaches the regenerator is not clear. It may be physically blown in by the surface heating of a glass batch or it may have vaporised in the furnace and recondensed in the regenerator. In the latter case it would be important to determine the components of the vapour above sodium sulphate at various temperatures and also their absolute amounts and this provides a strong motivation for the present work.

Of the limited number of methods available for the determination of thermodynamic properties of vapours and condensed phases in equilibrium at high temperatures, two were adopted, the Knudsen effusion and transpiration techniques.

Knudsen Effusion Method 14,15,16

Knudsen's effusion method is based on the kinetic theory of dilute gases¹⁷ by which the molecular flux at a boundary can be estimated for a gas at equilibrium. In its simplest thermodynamical application, the vapour composed of single or more species in equilibrium with its congruently evaporating condensed phase is allowed to flow from an isothermal cell through a small thin-edged orifice into an evacuated space. The vapour pressure of the condensed phase is related by the molecular effusion formula to the temperature T, the mass of a molecule or atom in the vapour, the mass rate of effusion dw/dt , the orifice area B, and the usual natural constants of kinetic theory. Hence, for steady-state effusion

$$P_m = \frac{1}{B} \frac{dw}{dt} \sqrt{2\pi kt/M}$$

and

$$P_m = Z(MT)^{1/2} / 44.33Bt \quad (1)$$

Where Z is the number of moles of material lost in an effusion run of t seconds through an orifice of area B.

Equation (1) is the ideal Knudsen equation which assumes that neither the hole nor the body of the cell exerts an influence on the effusing molecules. However with any effusion orifice of finite length, that is in every practical arrangement, there will be a channelling effect on the vapour. This is accounted for by introducing a further factor into equation (1) thus,

$$P_m = Z(MT)^{1/2} / 44.33 W_B Bt$$

Where W_B is the Clausing factor¹⁸. A more detailed discussion of the Clausing factor will be undertaken later.

The validity of the molecular-effusion formula and its applicability

to the measurement of low vapour pressures were first established by Knudsen's studies on the gaseous flow^{15,16}. Knudsen's experiments established the fact that, under realizable experimental conditions, the molecular-effusion formula is a suitable expression for the effusion of vapour primarily in the micron and lower-pressure regions. In these regions the atoms and molecules in the vapour phase escaping through a small orifice move nearly independently of one another and thereby have no appreciable effect on the equilibrium for which equation (1) is valid. At higher pressures the mean free path is small enough in relation to the orifice dimensions that dependent motion prevails; the gas behaves like a fluid effusing in accordance with the Poiseuille Law¹⁹. Consequently, the molecular effusion formula, and the experimental measurement of the mass rate of effusion of a very dilute vapour comprise a method of estimating the vapour pressures and hence the free energies of vaporisation of slightly volatile substances independently of the vaporisation mechanism. This last fact establishes one of the principal advantages of the effusion method over the free-evaporation or Langmuir method²⁰.

Vapour Saturation in a Knudsen Cell

The process of molecular effusion may be approximated by returning to the equilibrium theory underlying the method itself. The same equilibrium theory which yielded formula (1) yields a mechanical law of evaporation and a law of reflection of molecules at the boundaries of the container. These laws are identical and comprise what is known as the cosine law, which

within the context of kinetic theory is an exact expression for an equilibrium system. One considers a totally closed isothermal system consisting of an inert enclosure, evaporating material, and vapour in which gas phase collisions are absent.

Carlson¹⁴ has dealt with the mathematical formalism exhaustively and has presented the specific formulas to define statistical laws of reflection, restitution, evaporation, flux density, geometry factor of the cell, and orifice. This mathematical formalism provides an underlying structure for Clausing's¹⁸ derivation of transmission coefficients for molecular flow, the analysis of molecular flow by De Marcus²¹, the theory underlying the analysis of vapour saturation by Whitman²² and Motzfeldt²³, and the formalism employed by Balson²⁴.

Whitman²² was the first to take into account the influence of the main body of the cell. However his procedure involving infinite series leaves a solution which is rather inconvenient for practical application. A simpler method of approach by Motzfeldt²³ leads to a solution of more practical use. This method will be considered.

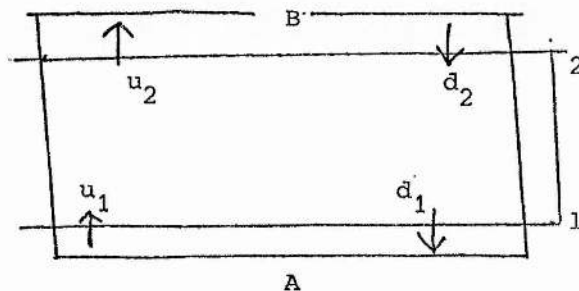


Figure 1

In the diagram plane 1 is close to the evaporating surface and plane 2 is close to the lid. The pressures in these two planes will be considered. At steady state and with no hole the pressure will be evenly distributed throughout the cell. With a finite hole size this no longer will be the case. The upward pressure u will be different from the downward pressure d for each plane, and the pressures will be different for the different planes.

Here it is necessary to introduce another factor, to be discussed in detail later, the coefficient of evaporation or condensation a .

A number of equations may now be derived. The rate of evaporation, which is proportional to αP_{eq} , is equal to the rate of recondensation plus the rate of escape through the hole,

$$a P_{eq} = ad_1 + fu_2$$

where $f = \frac{W_{BB}}{A}$ and A is the evaporating surface area. The upward pressure u_1 is made up of the evaporation from the surface plus the rebounding of molecules coming from above

$$u_1 = a P_{eq} + (1 - a) d_1$$

The downward pressure at plane 2 is due to reflection of upward molecules minus the fraction which escapes

$$d_2 = (1 - f) u_2$$

The upward pressure u_2 is due to the fraction W_A of the molecules heading upwards from the bottom plus the fraction $(1 - W_A)$ of the molecules heading downwards from the top, because this fraction is reflected upward again by the walls of the cell.

$$u_2 = W_A u_1 + (1 - W_A) d_2$$

This is the first time we have met W_A , the fraction of the molecules leaving the bottom of the cell which arrives at the top. The pressure u_2 is equal to the measured pressure P_m and is therefore known. The solution of the above four equations is

$$P_{eq} = [1 + f (\frac{1}{a} + \frac{1}{W_A} - 2)] P_m \quad (2)$$

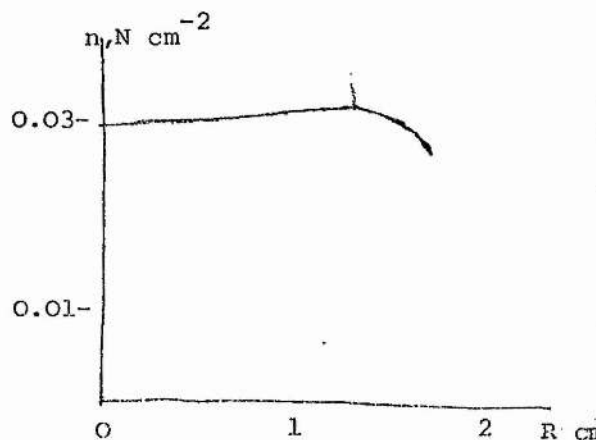
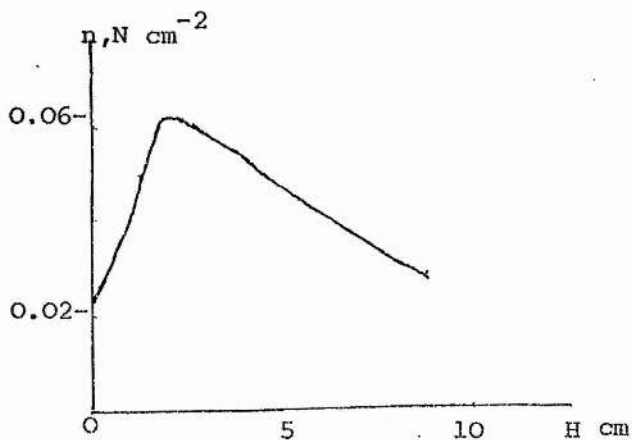
In this derivation some assumptions have been made which are not strictly valid. Pressures across any one plane were considered uniform and scattering at the wall giving rise to factor W_A has been assumed random.

In the limit $f \rightarrow 0$ $P_{eq} \rightarrow P_m$ and if $f = 1 = W_A = W_B$ $P_{eq} = P_m/a$, the equation for evaporation from a free surface. Equation (2) may be rearranged to

$$P_m = P_{eq} - (\frac{1}{a} + \frac{1}{W_A} - 2) P_m f \quad (2a)$$

and plotting P , against $P_m f$ gives a straight line of slope $1 (\frac{1}{a} + \frac{1}{W_A} - 2)$ and intercept P_{eq} , the equilibrium vapour pressure.

Ozhegov and Evseev²⁵ consider a cylindrical tube with a point source of molecular flux at its centre. The distribution of density of incidence of molecular flux on the wall of the tube having parameters, height H 9cm and radius R 2.1cm is shown in Figure 2, and the distribution of density of incidence of molecular flux in the plane of circular cross-section of a tube having the same parameters, in Figure 3.



Clausing¹⁸ has derived correction factors which are applicable to vapour pressure determinations by the Knudsen method employing an effusion orifice of finite length. However these factors cannot be used to calculate the pressure in a cell from the force exerted by vapour effusing from the cell, because the force depends on the angular distribution of the effusing molecules as well as on their number. Freeman and Searcy²⁶ have used Clausing's equation for the angular distribution of the effusing molecules to calculate suitable correction factors. A few values reported by these authors are given below for comparison.

L/r	K	K'
0	1	1
0.2	0.9092	0.913
0.4	0.8341	0.831
0.6	0.7711	0.769

The values K were calculated by Clausing and K' by Freeman and Searcy.

From the results obtained in his studies Balson²⁴ has mathematically computed what he terms the chance of out-flow W_o and compared his results with those derived by Whitman and Motzfeldt. Using a cylindrical effusion cell of radius 1 unit and length 2 units with a small axial effusion hole of radius r , his results for W_o are

Hole radius, r	0.1	0.2	0.3	0.5
W_o (Balson)	0.9953	0.9704	0.9348	0.8354
W_o (Whitman and Motzfeldt)	0.9906	0.9635	0.9215	0.8083

The mathematical analysis done by Adams et. al.²⁷ leads these authors to the conclusion that whereas at very low pressures, such that the Knudsen number (ratio of mean free path to orifice diameter) exceeds the limits for

molecular flow, the Clausing theory is expected to be valid, the Clausing angular number distribution is not quantitatively correct for either the long or short orifices at low angles. They observe that the Clausing theory predicts a greater probability of effusion in the forward direction than is found experimentally and recommend that, when using the Knudsen technique for the determination of low vapour pressures, the orifices should be as short as possible, when the angular number distributions agree with theory. Ward²⁸ has studied the case of effusion probabilities and related problems by Monte Carlo computer methods. In view of the fact that the Monte Carlo method requires no mathematical approximations or simplifying assumptions, results analogous to real cell behaviour are to be expected and therefore Ward concludes that a comparison of his results with the Montzfeldt treatment reveals that Montzfeldt's formula is applicable and quite accurate over a wide range of experimentally encountered conditions. Ward's work also shows that the upper limit of the Knudsen region is of the order of several tenths of torr, and then the gaseous collisions become important. Clausing's results are quite satisfactory if the length to radius ratio for the orifice is less than one.

Lozgachev²⁹ developed a general correlation giving the conductance of a vessel with respect to vapour species based on first principles. He then employs this formula to calculate conductance, or Clausing coefficient K , of a tube of circular cross section. The result he obtained is

$$K = 1 / (1 + l/2r) \quad (3)$$

where l is the length of the tube and r its radius. The validity of this result is confirmed by Kennard³⁰, who sets the limits of its application at $0 \leq l/r \leq 1.5$. The Clausing factors calculated in this work are based on this method.

What at first sight appears to be a simple and straight forward method for determination of absolute vapour pressures is now seen to be problematical. The next problem is posed by the evaporation co-efficient.

Burns ³¹ defines this factor as the ratio of the rate of evaporation per unit area of a simple vapour species from a surface to the equilibrium rate of flow of that species from the surface both by evaporation and reflection. Rosenblatt ³² is of the opinion that the vaporisation co-efficient is the ratio of the number of molecules actually evaporating from a plane surface in unit time to the number of molecules calculated to strike that surface in unit time when the surface is in equilibrium with its vapour. The condensation co-efficient is the fraction of molecules striking a plane surface which sticks to the surface and is closely related to the vaporisation co-efficient.

The vaporisation and condensation co-efficients are frequently assumed to be equal. Nesmeyanov ³³ is of the opinion that in the measurement of low vapor pressures condensation of the residual gases on the surface is insignificant, and the measured pressure can be even lower than the residual pressures. Hence the evaporation co-efficient will not be affected by the residual gases present in insignificant quantities within the apparatus. The physical state of the evaporating surface is also a vital factor for concern as vaporisation will undoubtedly occur in the interstices between small crystals and contribute to the measured flux, giving, according to Rosenblatt and Lee ³⁴, a higher vaporisation rate than that calculated from the exposed area, when the vaporisation co-efficient is less than unity. Vidale ³⁵ treats the vaporisation of a uniform porous powder sample by viewing the problem to be one of diffusion through the powder. His treatment leads to the equation

$$A' = 1.55 B (\epsilon/\alpha)^{\frac{1}{2}}$$

Where A' is the effective vaporising area of the powder, B is the cross-sectional area of the container, ϵ is the ratio of pore volume to total volume of powder and α is the vaporisation co efficient from a uniform plane surface which since

$$\alpha A' = \alpha_{\text{Powder}} B \quad \text{gives}$$

$$\alpha_{\text{Powder}} = 1.55 (\epsilon\alpha)^{\frac{1}{2}}$$

The effect of the vaporisation co-efficient on the equilibrium vapour pressure may be considered by the following treatment. Let S be the area of evaporation of the sample placed in the closed cell and α its evaporation (condensation) coefficient. Per unit time there will accumulate within the enclosure $n'\alpha S$ molecules, where n' is the number of molecules colliding with the surface (per unit time and surface area). This gives a true pressure P' . Now if the same enclosure is opened, then where there was previously equality of rate of evaporation and rate of condensation, there is now imbalance. If b is the area of the hole, the material balance may be written

$$\begin{array}{ccccc} nb & = & n'\alpha s & = & n\alpha s \\ (1) & & (11) & & (111) \end{array}$$

- (1) rate of flow out
- (11) amount of evaporation
- (111) amount of condensation

$$n/n' = \alpha/(b/s + \alpha)$$

That is $P/P' = \alpha/(b/s + \alpha)$ where P is the equilibrium vapour pressure. Thus when b/s is small with respect to α the measured pressure

is essentially equal to the equilibrium pressure. However, as will be seen later, when α is very small, as not infrequently occurs, this is far from being the case. Brewer and Kane³⁶ have discussed the size of the vaporisation coefficient. They conclude that all the materials that they investigated (mostly metal oxides) have unit vaporisation coefficient and all ionic salts, such as alkali halides, that vaporise predominantly as monomeric gaseous molecules, also have vaporisation coefficient close to unity. Their study also reveals clearly that substances have low vaporisation coefficients when the main molecular gaseous species does not exist as such in the condensed phase. "In general", these authors conclude "We would expect low vaporisation coefficients when the main gaseous species is a polyatomic molecule that does not exist as such in the condensed phase and, because of the rigidity of the lattice, cannot readily form within the lattice. Motzfeldt²³ attributes the low vaporisation coefficient of liquid sodium carbonate to the difficulty of bending the triangular carbonate ion to form the linear carbon dioxide molecule.

Estimation of the vaporisation coefficient usually begins with the equation by Motzfeldt²³,

$$P_m = P_{eq} - \left(\frac{1}{\alpha} + \frac{1}{W_A} - 2 \right) P_m^f \quad (2a)$$

The equilibrium vapour pressure, P_{eq} , may be estimated by plotting the observed steady state pressure, P_m , as a function of P_m^f for constant temperature and varying ratio f (i.e. different hole sizes), a straight line should result, with slope $-\left(\frac{1}{\alpha} + \frac{1}{W_A} - 2 \right)$ and with

intercept for $f = 0$ equal to P_{eq} . For a cell of about equal diameter and height (In this work, cell diameter (.7 cm) is more or less equal to its height (.8cm)). W_A is about 0.5, so that $\frac{1}{W_A}$ and 2 will tend to cancel each other. The expression for the slope may be simplified to $-\frac{1}{\alpha}$.

Some examples of compounds whose vaporisation coefficients differ from unity are given below, together with the source of information

Strontium Chloride	0.3 ³⁷
$Al_2O_3, Ga_2O_3, In_2O_3$	0.3 ³¹
Antimony	0.54 ³⁴
Graphite	0.15 ³⁸
Sodium hydrogen fluoride	0.006 ³⁹
Magnesium hydroxide	0.0018 ⁴⁰
Barium Fluoride	0.9 ⁴¹

Bolson²⁴ taking into account the evaporation co-efficient computes a new overall chance of outflow W_o , where $W_o, \alpha/W_o$ is given by

$$W_o, \alpha/W_o = \alpha/[1 - G(1 - \alpha)]$$

G is a dimension factor. $W_o, \alpha \rightarrow W_o$ as $G \rightarrow 1$ and becomes independent of α . With the effusion vessel filled completely up to the effusion hole the value of $W_o, \alpha/W_o$ becomes equal to α for G is zero, and the evaporation coefficient is exerting its maximum effect. Thus a Knudsen cell should not be filled to assist in the saturation of vapour inside. Balson's calculation of the influence of evaporation coefficient on the effusion rate from a cylindrical container with

a small effusion hole (container radius $R=1$, length $L=2$, effusion hole radius r) is given below

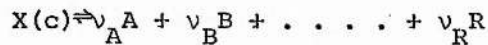
Evaporation coefficient	$W_o, \alpha / W_o$ $r/R = 0.1$		$W_o, \alpha / W_o$ $r/R = 0.2$	
	Balson	Motzfeldt	Balson	Motzfeldt
0.9	0.9996	0.9990	0.9948	0.9960
0.5	0.9968	0.9900	0.9552	0.9625
0.1	0.9720	0.9095	0.7031	0.7425
0.01	0.7463	0.5050	0.1767	0.2076

In calculating the vapour pressure from the Knudsen formula, it is absolutely essential that a value must be assumed for the molecular weight of the effusate. If the vapour species is identical with the condensed species no difficulty attaches to this; if, however the two states cannot be represented accurately by the molecular weight, as for instance is the case of complete or partial dissociation in the vapour phase, then an allowance must be made. Pashinkin^{42,43,44} has examined this question in detail in a series of papers. This author has formulated general equations for the calculation of equilibrium vapour pressures when the condensed material dissociates on evaporation. Pashinkin's argument is based on the assumption that the vapour in the cell retains the stoichiometric composition of the condensed phase during an effusion experiment. However, Knox and Wyatt⁴⁵ believe Pashinkin's assumptions to be false, and are of the opinion that at the steady state (when the condensed phase does not alter in composition) it is the effusing

vapour which retains the original composition of the condensed phase and the partial pressures within the cell must adjust to allow the species to satisfy the effusing equations. These authors then go on to formulate the ratios of the true equilibrium pressure of a dissociating substance to the pressure which actually exists within the cell during an effusion experiment, and to the nominal pressure which would be calculated from the rate of weight loss in ignorance of the presence of dissociation. In the equations given below, the various pressure terms are distinguished by the following notation:

- P* = Equilibrium vapour pressure of the substance in a closed container
- P = Actual pressure in the cell during an effusion experiment
- P' = Nominal pressure calculated from the rate of weight loss using the formula molecular weight
- P'' = Estimated pressure within the cell calculated from the simple effusion equations, as for P', but using a "mean 'molecular weight' of (known) dissociation products" instead of the formula weight.

For the condensed phase which evaporates with dissociation according to the equation



the equilibrium vapour pressure P* and the steady state pressure P (which is obtained directly by Torsion method) are related to each other by the following equation

$$\frac{P^*}{P} = \frac{\nu}{\sum_i \nu_i m_i} \left(M_A^{\nu_A/\nu} M_B^{\nu_B/\nu} \dots M_R^{\nu_R/\nu} \right)^{1/2} \quad (6)$$

M denotes the molecular weight. When specific cases are considered it transpires that P^*/P does not differ greatly from unity. The nominal pressure P' calculated from the rate of weight loss (assuming undissociated X is emerging from the cell) can be converted by the use of the following equation to give P^*

$$\frac{P^*}{P'} = (v/M_X)^{1/2} (M_A^{v_A/v} M_B^{v_B/v} \dots M_R^{v_R/v})^{1/2} \quad (7)$$

Since P' is measured by weight loss and P by the Torsion method, comparison of these two results should reveal the presence of dissociation and their ratio is given by

$$\frac{P'}{P} = M_X^{1/2} / \sum_i v_i M_i^{1/2} \quad (8)$$

Similarly the pressure P'' obtained by using the mean molecular weight along with the rate of weight loss in the effusion equation is related to the steady state pressure P by the expression

$$P''/P = v^{1/2} / \sum_i v_i (M_i/M_X)^{1/2} \quad (9)$$

These authors then conclude that, if the form of dissociation does not change over the temperature range under investigation, the factors on the right of (6), (7), (8), (9), remain constant and any of the quantities P^*, P, P' or P'' will therefore serve equally for obtaining the slope of a graph of $\log P^*$ against $1/T$ for enthalpy determinations.

This brief general discussion on the Knudsen method should not be concluded without a mention being made of the accuracy of the method in general terms. Rossman and Yarwood⁴⁶ derive the expression met with earlier that

$$b/S = \alpha(P/p - 1)$$

where b is the effusion orifice area, S is the evaporating surface area, p is the measured pressure and P the saturation vapour pressure. If $p = XP$, where X is very nearly equal to one, then

$$X = [1 + (b/S\alpha)]^{-1}$$

or putting $b/S = f$,

$$X = [1 + (f/\alpha)]^{-1} \quad (10)$$

With the orifice in the form of a short tube the resultant impedance to the flow of vapour will be equivalent to making the orifice area, b , smaller. The effective area of the actual surface can only be larger than S , the cross section area of the crucible. Hence the above equation (10) gives the maximum possible error with the vapour pressure determination, the error being zero when $x = 1$. The effective area of the condensate is fundamentally related to the pressure of the effusing gas, since Z is a function of b , S and α . Whitman⁴⁷ derives an expression similar to that of Rossman and Yarwood,

$$p/p = K = 1/[1 + f/W_A - f] (1 \geq W_A > 0). \quad (11)$$

for a cell with a very thin orifice. The condensation coefficient, α , is unity and p is determined by the measured effusion rate. It is evident from (11) that K will be greater than, equal to, or less than Yarwood's x , depending on the depth of the cell which determines W_A (see Motzfeldt's²³ notation). The effusion rate, is therefore

dependent on two factors, the effective area of condensate and its location relative to the orifice. This, Whitman concludes, would provide pertinent consideration for any experimental arrangement since, in general, the assumption of a steady state pressure is not justifiable. Rossman and Yarwood's Z would not therefore be a reliable estimate of the accuracy of an effusion measurement. Carlson¹⁴ finds, from mathematical consideration, that a cell having value $H = 2$ and $P = 0.1$ yields 99% of the equilibrium value for unit vaporisation co-efficient. H is the ratio of the length of the cylindrical Knudsen cell to its radius and P is the ratio of the radius of the orifice to that of the cell. In this work, the diameter and height of the Knudsen cell used is 0.7cm and 0.8cm respectively ($H = 2.1$). The orifices used were of three different sizes, 0.0725, 0.0490 and 0.0336cm diameter ($P = 0.1$).

During the course of this summary of the Knudsen method for the measurement of low vapour pressures an attempt has been made to introduce the concepts of Clausing factors and coefficients of evaporation and condensation. Mention has also been made of complications that may arise out of vapour phase dissociation and finally how to relate the vapour pressure determinations made by the Torsion and Weight Loss methods (considering both absence and presence of dissociation cases) to the equilibrium pressure.

Transpiration Method 48,49,50

The transpiration technique of measuring the vapour pressure is based on the following principle. A steady, measured, stream of inert gas is passed over the substance under investigation, which is maintained at a constant temperature. The gas removes the vapour or volatile component of the substance at a rate which is dependent upon their relative pressures and upon the rate of gas flow. The vapour is condensed or collected by absorption or chemical combination at a cooler portion of the apparatus. Under conditions where the inert gas is saturated with vapour, the following relationships hold

$$\frac{p}{n} = \frac{RT}{V} \quad \text{and} \quad \frac{P_1}{N} = \frac{RT}{V} \quad (11)$$

Where p is the vapour pressure of the substance being studied

p_1 is the pressure of the transporting gas

V is the volume of the inert gas, which is equal to the volume of the vapour in the absence of the gas flow

n is the number of moles of the sample and

N is the number of moles of inert gas

Hence,

$$P_1 = \frac{Np}{n} \quad (12)$$

Since, according to Dalton's law, the total pressure is

$$P = p + P_1$$

then
$$P = p \left(1 + \frac{N}{n}\right) \quad (13)$$

and
$$p = P \frac{n}{n+N} \quad (14)$$

This relationship holds good only under conditions when the inert gas is saturated with vapour, i.e., zero rate of gas flow or at a rate close to zero. However, when the rate of gas flow is changed, the final result changes. It is necessary, therefore, to make measurements at various rates of gas flow and extrapolate the results to zero rate. This introduces errors into the final results, since thermal diffusion enters as a factor at slow flow rates. Consequently, extrapolation to zero rate may give high results. Lumsden⁵¹ is of the opinion that the vapour pressure data should be represented as a function of $\frac{1}{v}$ and extrapolated to infinitesimally low flow rate assuming that saturation occurs at all rates of flow. Such an opinion is confirmed, however, only by a single study of Braune⁵² who measured the vapour pressure of cadmium and Zinc. Alcock and Hopper⁵³ in a study of vapour pressure of gold by this technique found that saturation could be achieved over a wider range of flow rates the more the evaporating surface could be made to fill the cross section of the reaction tube. In the apparatus used by Fischer and Rahlf⁵⁴ for the study of aluminium halides, the reaction and condensation chambers were connected by a heated tube. This allowed experiments to be done with a very slow gas flow which ensured complete saturation, without any loss of transported vapour by condensation elsewhere than in the collecting vessel.

Errors arising out of thermal diffusion at low flow rates, are usually made negligible by paying great attention to the apparatus design. Constrictions are made in the furnace tube on both sides of the sample to minimise counter diffusion of the vapour. Battat et. al.⁵⁵ have employed recently the transpiration method in a modified

form to evaluate the vapour pressures and equilibrium constants for heterogeneous reactions. The effect of thermal diffusion was minimised by causing turbulent mixing of the gas in the reaction zone or by blowing the gas stream fast to reduce the boundary layer over the solid or liquid. Barthel and Dode⁵⁶ have used radio-active indicators for determining the amount of substance carried off by the flowing inert gas.

The transpiration method discussed above is applicable to the measurement of low vapour pressures (below 1mm Hg). It doesn't yield highly precise results. Nevertheless it is free from serious errors. Results obtained by the flow method, when combined with data of other methods, can be satisfactory.

Identification of High Temperature Species.

In calculating the vapour pressure from the Knudsen formula, it is absolutely essential that a value must be assumed for the molecular weight of the effusate. If the vapour species is identical with the condensed species no difficulty attaches to this. If however the two states cannot be represented accurately by the molecular weight, as for instance is the case of complete dissociation or partial dissociation in the vapour phase, then identification of the high temperature species is highly desirable.

Margrave et. al.¹¹ have critically analysed the results obtained by various instrumental techniques, which are currently in use for identifying the high temperature species. These authors then list the

techniques in the following order, reflecting their decreasing relative importance and general applicability to high temperature species.

- (a) Infra red spectra of the matrix isolated species
- (b) High temperature Mass-spectrometry
- (c) Electron diffraction of molecular beams
- (d) Electric-dipole deflection in nonhomogeneous electric fields
- (e) Rotational analysis of electronic spectra
- (f) Micro Wave analysis of rotational structure.

Although the matrix isolation technique is the most highly sensitive analytical tool for determining structures and stabilities of high temperature species, mass-spectrometry is still widely used by research workers in this field on account of its comparative simplicity to the matrix technique and its ability to provide data for estimating the heats of reaction and dissociation energies with reasonable accuracy. A general analysis of the advantages and disadvantages of mass-spectrometry and a detailed description of the matrix isolation technique are presented below.

Mass -spectrometry:- The technique of high temperature Mass spectrometry has been well documented ^{57a,b,c} and an exhaustive critical review of the method and the results obtained has appeared more recently ¹¹. Heats of reaction and bond dissociation energies resulting from the gaseous equilibria of the type:



can be determined by this technique to a precision of about $\pm 8 \text{ kJ mol}^{-1}$,

although disagreement between various laboratories is often greater. However Margrave¹¹ is of the opinion that the recent renaissance of Photo-ionisation mass spectrometry,^{57,58} inspired mainly by the development of high intensity windowless photon sources and more efficient ion detection, provides a powerful new technique for stability determination of high temperature species^{59,60,61}. This author finally concludes that, even with the limiting effect^{60,62} of thermal excitation on the obtainment of a sharp photoionisation threshold, an order of magnitude reduction in the uncertainty of existing data is possible (e.g. $\pm 1 \text{ kJ mol}^{-1}$ error). Another advantage of photo ionisation technique is the ease with which step-wise dissociation energies of polyatomic species can be measured. One of the disadvantages of Knudsen effusion - Mass spectrometric technique is that errors may arise due to ambiguity in the assignment of ions as fragments or parents. For example, in the $(S)_n$ and $(Se)_n$ systems^{63,64} where polymers $n = 2 - 8$ were observed, fragment ions were treated sometimes as parents (e.g. S_4^+), leading to incorrect second law heats of vaporisation for the lower polymers. Also, contrary to the original interpretation, $Na_2BeF_3^+$ has been shown⁶⁵ to be a fragment of $(NaBeF_3)_2$ rather than Na_2BeF_4 . Another inadequacy of the mass-spectrometric technique is its inability to distinguish geometrical isomers, for example, $(LiF)_2$ ⁶⁶ and Li_2O_2 ⁶⁷ which have very different heats of vaporisation and formation. It can be concluded that while the present mass-spectral data are sufficiently accurate to permit a better understanding of the factors important to chemical bonding throughout most of the periodic table,

they are mostly unsuitable for an accurate free energy or partial pressure description of high temperature systems. The overall errors in ΔH and ΔS magnify in K as order of magnitude errors. Matrix isolation technique has overcome all these disadvantages associated with Mass-spectrometry, thus providing a new and essential technique to the high temperature field.

Matrix Isolation spectroscopy

Knudsen effusion techniques acquired new versatility when combined with matrix isolation spectroscopy for characterizing the vapour species. The first successful application of matrix isolation technique to the observation of infra red spectra of high temperature species was made by Linevsky⁶⁸ in 1960. Important later developments in this technique have been well reviewed^{69,70}.

Matrix isolation in its most commonly used form is the preparation of a rigid sample of effectively isolated molecules or reactive species in an inert matrix medium. Matrix isolation is achieved usually by the co-condensation of a gaseous material with a large excess (10^2 - 10^4 mole ratios) of inert material such as a rare gas. The trapped species do not undergo translational motion - i.e., diffusion - and usually are prevented from rotating, but may vibrate with frequencies that are within a few percent of the gas phase values. The spectra of the material in these matrices, therefore, are frequently much simpler than those obtained for any other state of matter, particularly if low temperatures are used.

(a) Isolation Technique:- The use of matrix isolation for spectroscopic studies of high temperature inorganic species at low temperatures requires the use of high temperature Knudsen cells for production of molecular species and cryogenically cooled surfaces for the trapping of these species in an inert-gas solid. The work of Becker and Pimentel⁷¹ demonstrated the isolation efficiencies of solids such as N₂, the rare gases, and other effectively inert materials such as CO₂ and CCl₄. It is evident from their studies that for efficient isolation the ratio of matrix to active molecules (M/A) can vary from several hundred to several thousand, and effective isolation, in the case of HN₃, with M/A = 325 - 340, improved from N₂ to Ar to Xe at 20 K. While ESR spectroscopy can detect radical concentrations of $\sim 10^{-8}$ molar, Raman and Infra-red spectroscopy can detect species of $\sim 10^{-5}$ and 10^{-7} molar concentration respectively.

Light scattering from the matrix surface is an important factor and has to be minimised by a study of the choice of matrix material, deposition rate, and trapping temperature. Glass-forming materials for visible spectroscopy and rare gases and alkali halides for the Infra-red region are suitable. A practical upper limit to trapping temperatures is determined by isolation effectiveness, which falls off with increasing temperature. Choice of trapping temperature is therefore often the result of a compromise between a gain in light level and loss in the degree of isolation. Matrix thickness t is usually determined from counting n interference fringes in the Infra-red, using the expression

$$t = \frac{n}{2(\Delta\nu)}$$

Where $\Delta\nu$ is the frequency interval. Thicknesses of 0.1 - 1 mm are common. Thicker matrices usually have a tendency to peel off the Cryogenic surface. Further light loss by scattering tends to increase with matrix thickness. The rate of deposition can vary widely - e.g., 10^{-3} - 10^{-6} mol h⁻². A suitable matrix can be obtained after several minutes of trapping or after several hours depending upon the nature of the molecules under investigation. Controlled pulse technique ⁷² can be employed to deposit matrices in a matter of seconds.

(b) Preparation of Matrix:- The apparatus required for matrix preparation depends largely on the degree of volatility of both the matrix material and the substance to be isolated. There are three possible cases -

- (1) Both matrix and inorganic material volatile
- (2) Matrix material volatile and inorganic material non volatile
- (3) Both matrix and inorganic material non volatile

Case two is potentially the most important, as the majority of known inorganic species like those involved in the present work are volatile only at elevated temperatures. The production of a molecular beam ¹⁴ of material with the use of Knudsen cells as well as the production of cold trapping surfaces ⁷³ is well documented. The only precaution to be taken is that the cold trapping surface be reasonably well shielded from the radiation of the high temperature source. A physical separation of approximately 12 cm is common; a schematic diagram of a typical system is given in Fig. 1. Details of the simplified model of the system used here, with its liquid nitrogen

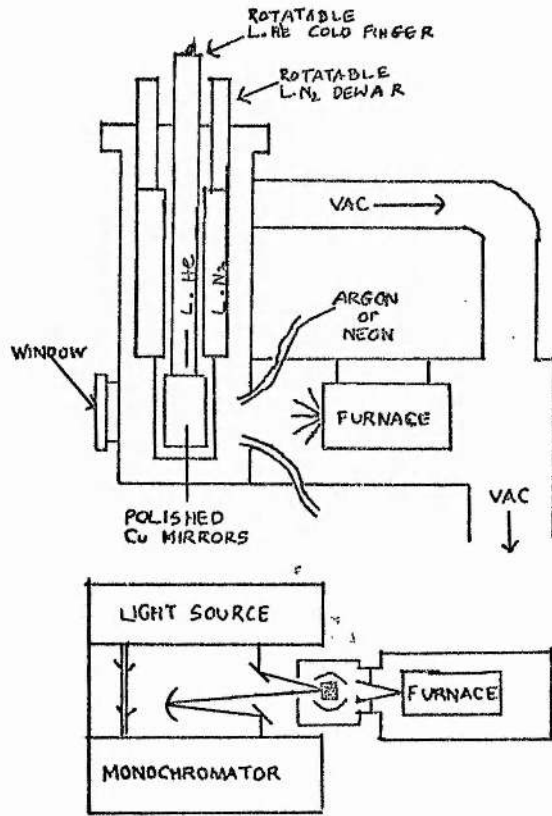


Fig. 1.

cooling system, are presented in the experimental section.

The matrix concentration is readily controlled by the rate of effusion $\frac{dw}{dt}$ from the Knudsen cell as given by the equation

$$\frac{dw}{dt} = BP \left(\frac{M}{2\pi RT}\right)^{1/2}$$

and also by the solid angle subtended by the trapping surface and the Knudsen orifice. B is the orifice area, P the pressure in the cell, R the gas constant, M the molecular weight, and T the cell temperature. Only a few percent of the effusate and the matrix gas molecules actually reach and are collected by the cold surface. Thus only an approximate calculation of the matrix concentration can be made.

(c) Cryogenic System

The most common Cryogenates in use are liquid Helium (bp=4.2 K), liquid hydrogen (bp=20.4 K), and liquid Nitrogen (bp=77.4 K). Pumping on the refrigerant can reduce these temperatures to 1.2 K and 15 K for helium and hydrogen respectively. Matrix formation requires the temperature to be maintained around 20 K \pm 5 K for Argon, Xenon, Krypton and Nitrogen, and 5 K for Helium. The trapping surface is cooled by a controlled leak of liquid or gaseous refrigerant to the cold block that is in good contact with the trapping surface. Cryotips based on the Joule-Thompson technique are also employed. Liquid Dewars with a reasonable capacity are most economical and sufficient for lengthy experiments that do not require repeated breaking of the vacuum for such purposes as cleaning of the trapping surface or loading a sample

in a Knudsen cell.

Crystalline forms of quartz (far - IR), CsI, KBr, NaCl (IR), quartz, LiF (1050A), CaF₂ (Visible, UV) and sapphire rod for ESR spectra are the most ideal trapping surfaces.

Interpretation of the matrix spectra of inorganic species requires a detailed understanding of the special perturbation effects caused by the matrix environment ⁷⁴. Such effects mostly show up as small frequency shifts, multiplet structure, and variation in absorption intensities ⁷⁵, and are often a complicating factor in the initial spectral interpretation. The most common and easily identifiable matrix effect is the frequency shift from the gas-phase values. This effect has been observed for rotational, vibrational and electronic transitions. The shift is to lower frequencies and by only a few percent of the gas-phase values. Analysis of the matrix spectra of inorganic species so far studied shows that only a few small molecules such as H₂O, HF, HCl, HBr, CH₄, NH₃ and CO have shown a tendency to rotate in rare gas matrices. Robinson and Von Holle ⁷⁶ have studied the effect of various matrices on the $J = 1 \leftrightarrow J = 0$ transition in HF and DF. The data are presented in Table 1.

Table 1

Gas phase	HF 41.9 cm ⁻¹	DF 22.0 cm ⁻¹
Ne matrix	39.8	22.8
Ar	44.0	27.3
Kr	45.0	30.0
Xe	50.5	32.8

It can be observed that the matrix shift varies linearly with the rare gas atomic polarizability. These authors believe that the blue shifts are due to the collapse of the lattice around the small HF molecule, an effect that should increase, as observed, with the larger rare-gas atoms ⁷⁷.

Molecular vibrations will also be affected by the matrix environment. This can be viewed initially as a dielectric effect and the red frequency shift is predicted by the Kirkwood - Bauer - Magat relation ⁷¹

$$\frac{\nu_0 - \nu}{\nu_0} = C \left[\frac{(D - 1)}{(2D + 2)} \right]$$

Where C is a constant characteristic of the molecule, D is the dielectric constant of the matrix, ν_0 is the gas-phase frequency, ν is the expected matrix frequency. The shifts observed for LiF, LiBr, and LiCl in argon, Krypton and Xenon matrices ⁷⁷ fit the above relationship. It is evident from the work of Linevsky ⁷⁰ that the two important factors leading to a red shift are the attractive-dipole-induced-dipole and the dispersive effects (induced-dipole-induced-dipole). Charles and Lee ⁷⁸ derive the following expression to calculate the attractive force experienced by the trapped species from the matrix. The first and second terms in the expression correspond to the dipole-induced-dipole and Induced-dipole-induced-dipole interactions.

$$- \frac{u_1^2 \alpha_1}{6 \gamma_{12}} - \frac{3}{2} \frac{\alpha_1 \alpha_2}{6 \gamma_{12}} \frac{I_1 I_2}{I_1 + I_2}$$

Where μ , α_1 , and I_1 , are the dipole moment, polarisability and ionisation potential, respectively, for the trapped species; α_2 and I_2 are the polarizability and ionisation potential respectively for the nearest-neighbour matrix molecule and γ_{12} is the distance between the trapped and nearest neighbour matrix species. Longuet-Higgins and Pople⁷⁹ are of the opinion that the red shift resulting from dispersive interactions can be expressed as

$$\text{red shift} \sim \frac{3\alpha_1\alpha_2 ZE}{8\gamma_{12}^6}$$

Where Z is the number of nearest-neighbour matrix molecules at a mean distance γ_{12} and E is the energy for transition. Margrave et. al.⁶⁸ have analysed and critically reviewed the matrix spectra of inorganic species studied up to 1972 and conclude that the following relations appear to hold for inorganic species:

- (a) The red vibrational shift increases with the expected charge separation along the vibrating bond, as given crudely by electro-negativity differences or, in the case of diatomic species, by dipole moments.
- (b) The red vibrational shift increases with increasing matrix polarisability - e.g. from Ne, Ar, Kr, to Xe. Shifts in N_2 are still greater.
- (c) The gas-phase vibrational frequency ν_g is to a good approximation ($\pm 6\text{cm}^{-1}$), related to the frequencies observed in neon and Argon matrices by the expression

$$\nu_g \sim \nu_{\text{Ne}} + (0.8 \pm 0.4) (\nu_{\text{Ne}} - \nu_{\text{Ar}})$$

The existing data for the lowest-frequency modes of polyatomic inorganic species suggest that larger matrix perturbations are likely for these cases. Pimentel and Charles⁷⁴ propose a "cage" model in which low-frequency vibrations feel the effect of a "tight cage" and could tend to show positive (blue) shifts, where as the higher frequencies should feel a "loose cage" and show negative (red) shifts.

Robinson⁸⁰ and McCarty⁸¹ have discussed the theoretical aspects of treating the matrix shifts for electronic as well as other spectra. In their theories, they treat the matrix as a solvent for the trapped species, and the interaction is described by a Lennard-Jones potential. However the theory does not appear to hold for Neon matrices. It is evident from the matrix spectra of the inorganic species, so far studied, that the blue shifts appear to be more common for electronic than vibrational spectra. As with vibrational transitions the spectra shift to lower energies with increasing matrix-atom polarizability - i.e., from Ne, Ar, Kr, to Xe. The largest blue shifts are observed for atomic species in Argon and the smallest for the most polarisable matrix⁸². Further, electronic spectra are found to be sensitive to matrix temperature and both blue and red shifts may be observed on warming the matrices.

Apart from the actual perturbation of rotational, vibrational and electronic states by the matrix, Multiplet structure will also be observed in the matrix spectra. This is believed, by the leading research workers in this field, to be due to the trapped species being located in several distinct sites, and therefore the phenomenon is strongly dependent on the relative dimensions of the isolated species

and the surrounding matrix atoms. The magnitude of site splitting is very small and by only a few wave numbers. Usually the splitting is either reduced or eliminated by a so-called annealing of the matrix, which is an irreversible process. A detailed account of the nature and properties of the rare gas solids is given by Boato⁸³, Cook⁸⁴, and Pollack⁸⁵. The structure of the rare gas solids is a major factor, apart from other parameters, in analysing and solving the matrix perturbations. The properties of rare-gas solids are given in Table II.

Small molecules may occupy both substitutional and interstitial sites, but substitutional sites are more likely for larger species. Bowers⁸⁶ suggested grain boundaries between micro crystals as possible matrix sites that are fairly insensitive to lattice environment. A high degree of consideration should be given to the molecular size of the inorganic species to be trapped in relation to that of the substitutional sites, while choosing a matrix material for isolation purposes. When the molecular size of the poly-atomic inorganic species exceeds the available space of a substitutional or interstitial site, the probability of the trapped species being located in a site where the cage also contains one molecule of the same species is increased. This cage will clearly perturb the trapped species by a different amount than a cage formed entirely by matrix molecules and thus will produce another effect known as the aggregation site effect. This is not to be confused with the formation of dimer species as actual chemical combination does not necessarily occur.

During the course of this discussion of the mass-spectrometry and matrix-isolation methods for identifying the high temperature inorganic species, the sensitivity and the limitations of mass-spectrometry

TABLE II

Mole- cule	Atomic Size (A)	δ (A)	α	Triple Point (K)	Density O K ₃ (8/cm ³)	Lattice Parameter O K(A)	Substitutional Site (A)	Interstitial diameter (A) octahedral
Ne	3.147	2.67	2.663	24.66	1.508	4.462	3.16	1.30
Ar	3.886	3.41	11.08	83.81	1.769	5.312	3.76	1.55
Kr	4.056	3.66	16.73	115.77	3.094	5.644	3.99	1.65
Xe	4.450	3.97	27.29	161.36	3.782	6.131	4.34	1.79

Substitutional and interstitial site diameters for N₂
correspond closely to those of Kr.

δ = Molecular diameter

α = Polarizability data

are presented, and the versatility of matrix isolation technique discussed in detail. This concludes the introduction to the methods that have been used in this work for the determination of vapour pressures of salts at high temperatures. As mentioned earlier in the introduction, the interest centred primarily upon sodium sulphate, but the other alkali metal sulphates were investigated for comparative purposes, together with calcium and magnesium sulphate. A review of the literature dealing with the vapour pressures of these compounds now follows.

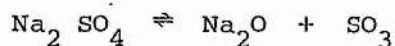
Sodium Sulphate:-

Mlle. Marchal⁸⁷ was the first to study the thermal decomposition of Sodium Sulphate quantitatively. Sodium Sulphate was treated in a platinum crucible and the progress of decomposition followed by recording the weight loss of the crucible at regular intervals. Decomposition rate was reported to be very slow at 1573 K. The heating time and weight loss figures are reproduced below.

<u>Temperature K</u>	<u>Heating Time</u>	<u>Wt. Loss %</u>
1573	1 h	0.87
	+ 1 h	2.61
	+ 63 Min	3.78
	+ 1 h	4.23

The author had recorded only weight loss measurements and there was no mention about vapour pressure or decomposition measurements which calls in question the results attributed to Marchal appearing in Kroger and Stratmann's paper, page 317, figure 9. Further Marchal reports that the addition of Silica and Aluminium oxide to the Sodium sulphate increased the rate of weight loss considerably. Terres⁸⁸ work does not provide any information on the experimental details but simply quotes the dissociation pressure over sodium sulphate as being 1.3×10^{-2} atmospheres at 1623 K and 0.7×10^{-2} atmospheres at 1473 K. Terres also observed and recorded an effect similar to that observed by Marchal. The results of Marchal and Terres clearly show that the partial pressure of Sulphur trioxide increases if silica is mixed with sodium sulphate. Although no explanation is offered by these authors, this rise in partial pressure of sulphur trioxide by the addition of silica might be due to a

reduction in the activity of sodium monoxide as it reacts with silica, resulting in a shift in the equilibrium



to the right. Terres reports⁸⁸ Quantitatively the effects. Thus $\frac{1}{2}$ mole % SiO_2 raises the partial pressure of SO_3 from 10 torr to 150 torr, 1 mole % SiO_2 gives 200 torr and 2 mole % SiO_2 raises the SO_3 pressure to 400 torr, all at 1623 K.

Liander and Olsson⁸⁹ measured the vapour pressure of sodium sulphate by the transpiration method using air as carrier gas. They worked in the temperature range between 1373 K and 1723 K and expressed their results by the following relation

$$\log_{10} (P/\text{torr}) = - \frac{7230 \text{ K}}{T} + 4.42$$

Eyber's⁹⁰ investigation gives values for the variation of vapour pressure, of sodium sulphate with temperature as well as the value of the equilibrium constant

$$K_p = \frac{p(\text{Na}_2\text{O}) p(\text{SO}_3)}{p(\text{Na}_2\text{SO}_4)}$$

The values quoted in his paper are presented on the next page.

I	II
<u>Temperature / K</u>	<u>Vapour pressure / atmospheres</u>
1273	0.02
1373	0.06
1473	0.17
1573	0.37
1673	0.80

III

log (K / atm)
P

- 14.3

- 12.6

- 11.1

- 10.0

- 8.8

- 7.4

Further Eyber gives the value for the heat of vaporisation as $168.9 \text{ kJ mol}^{-1}$.

The work of Kroger and Stratmann⁹¹, reported in 1961, provides full details about their experimental set-up employed for the vapour pressure determination of sodium sulphate over the temperature range 1025 K to 1124 K, by the Knudsen effusion technique. A Knudsen cell made of Nickel was used and an aluminium foil suspended over the cell from the arm of the micro balance collected

the condensate which was shown to be exclusively sodium sulphate.

The vapour pressure values quoted in their paper at various temperatures are given below

<u>Temperature / K</u>	<u>Vapour pressure / torr</u>
1025	0.103×10^{-3} , 0.145×10^{-3}
1056	0.425×10^{-3}
1087	1.25×10^{-3} , 0.62×10^{-3}
1109	1.9×10^{-3}
1114	2.7×10^{-3}
1124	3.85×10^{-3}

The heat of vaporisation was found to be $330.2 \text{ kJ mol}^{-1}$ and these authors represent the vapour pressure relationship by the equation

$$\log [p(\text{vap})/\text{torr}] = -1.73 \times 10^4 \text{ K/T} + 13.1$$

Extrapolation from this yields a boiling point of 1700 K. However, the vapour pressure values obtained by these authors for Potassium sulphate by the same technique were found to depend upon the crucible materials (Nickel and Platinum)

<u>Nickel</u>		<u>Platinum</u>	
Temperature/K	Vapour pressure/torr	Temperature/K	Vapour pressure/torr
1120	0.45×10^{-3}	1114	0.67×10^{-3}
1198	1.5×10^{-3}	1190	2.6×10^{-3}
1234	2.3×10^{-3}	1224	4.9×10^{-3}
1272	6.8×10^{-3}	1272	12.3×10^{-3}

Although these authors do not explain the reason for this difference in values obtained, it is probably due to the attack of the nickel cell by potassium sulphate. Hence it is reasonable to conclude that the true value for the vapour pressure of sodium sulphate could also be different from the one quoted in their paper. (The evidence produced later in this work will justify this conclusion). One should expect that the vapour pressure values to be higher if the material under investigation attacks the container as in the case of Nickel. However the data quoted shows that the vapour pressure values tabulated for Nickel cell to be lower than the values quoted for platinum cell. It is rather surprising and it might have been due to the formation of crust at the surface after the initial attack of nickel by the sulphate and thus affecting the final results.

Bruckner ⁹², while investigating the behaviour of glass melts with sodium sulphate at high temperatures, employed the dynamic method to determine the partial pressures resulting from the thermal decomposition of sodium sulphate. Nitrogen, air, oxygen, and an $\text{SO}_2 + \frac{1}{2}\text{O}_2$ mixture were used as carrier gas. The weight loss of the sodium sulphate sample was measured at different temperatures and at different carrier gas glow rates. Bruckner concludes that platinum has no effect upon the decomposition of sodium sulphate and "...from these measurements only the decomposition pressure and not the vapour pressure can be determined". However, the final column in his Table 5 shows the weight loss resulting from sodium sulphate being heated at various constant temperatures under an atmosphere of $\text{SO}_2 + \frac{1}{2}\text{O}_2$ gases. It is therefore evident that there should be a large enough

partial pressure of SO_3 to prevent decomposition of sodium sulphate. Further there are a few more anomalies in his analysis of the results. The weight loss was found too small to be detected at 1573 K, (see final column, Bruckner's Table 5) indicating a very low pressure. But using the values quoted in Bruckner's Table 5 at 1673 K and his equation 2 the following values for the vapour pressure of sodium sulphate are obtained,

$$15.97 \times 10^{-6} \text{ atm}$$

$$7.90 \times 10^{-6}$$

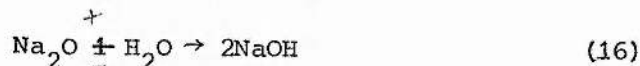
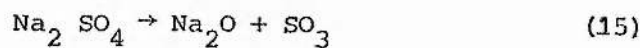
$$5.00 \times 10^{-6}$$

$$4.57 \times 10^{-6}$$

giving a mean value of 8.36×10^{-6} atm or 6.35×10^{-3} torr.

Bruckner then goes on to extrapolate his weight loss measurements to zero flow rate of the carrier gas to obtain the value for equilibrium pressure. If this is true, then the values in the nitrogen and air columns of Table 5 should give the values in the last column when extrapolated back to zero flow rate. However this does not seem to be the case, and the decomposition effect does not appear to be eliminated. Bruckner's extrapolation should yield the decomposition pressure of sulphur trioxide plus the vapour pressure of sodium sulphate and sodium monoxide. Further the curve in his figure 5 indicates that at a temperature of approximately 2123 K the decomposition pressure equals one atmosphere and, consistently with this, the author did not detect boiling up to a temperature of 2023 K. This author also studied the dependence of weight loss on the partial pressure of water vapour in damp nitrogen atmospheres. A close study of the values quoted in his Table 6 and

figure 4 reveals the linear dependence of weight loss on the square root of the water vapour partial pressure. This can be attributed to



The weight loss should naturally be expected to increase since the sodium hydroxide is more volatile than the sodium monoxide. The equilibrium constant for reaction (16) is

$$K = [\text{NaOH}]^2 / [\text{Na}_2\text{O}] [\text{H}_2\text{O}]$$

and $[\text{NaOH}]^2 \propto [\text{H}_2\text{O}]$, since $[\text{Na}_2\text{O}]$ will be constant due to the equilibrium set up in reaction (15). Hence, if the weight loss is proportional to the amount of sodium hydroxide present then $[\text{NaOH}] \propto (\text{pH}_2\text{O})^{1/2}$ 93.

The Russian workers Fotiev and Slobodin⁹⁴ have carried out a thermogravimetric study of sodium sulphate. These authors heated sodium sulphate in a platinum cell in a vacuum furnace at 1663 K and observed that even after five hours of heating at this temperature no sulphur dioxide or sulphur trioxide evolved from sodium sulphate and the residue when analysed at the end of the experiment indicated the absence of sodium monoxide in the solid phase. Further the volatilisation was found to be appreciable only above 1473 K in air -- they found that in one hour volatilisation in air from 1 cm² surface area of the sulphate melt measured in mole % Na₂ SO₄ was

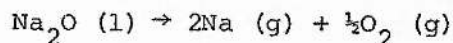
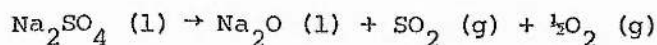
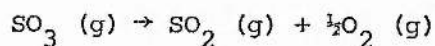
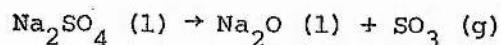
0.36×10^{-4} at 1373 K
 0.24×10^{-3} at 1473 K
 0.18×10^{-2} at 1593 K
 0.48×10^{-2} at 1663 K

In vacuum at 1323 K the volatilisation was considerable

12.3% in 15 min
49.0% in 40 min
80.8% in 70 min
86.1% in 80 min

The rate of weight loss was found to be linear with time and the apparent activation energy they calculated was 322 kJ mol^{-1} . Heating the sulphate in quartz, porcelain, corundum or alundum resulted in a considerable change in weight loss and liberation of sulphur trioxide was noticed. These authors therefore conclude that sodium sulphate does not dissociate at atmospheric pressure or in a vacuum until the temperature exceeds 1673 K, and sodium sulphate loses weight in a platinum vessel entirely due to volatilisation, but in other materials chemical reaction with them is possible.

Holmquist⁹⁵ considers only the following reactions to be of importance at high temperatures [above the melting point of the sulphate].



He derived the following expression for pure sodium sulphate of unit activity

$$K_3 = [\text{Na}_2\text{O}] \cdot p\text{SO}_2 \cdot p\text{O}_2^{1/2} = K_1 \cdot K_2 = [\text{Na}_2\text{O}] \cdot p\text{SO}_3 \cdot K_2 \quad (14)$$

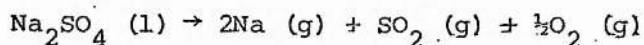
It is evident from the above expression that the activity of sodium oxide is inversely proportional to the partial pressure of sulphur trioxide and at zero activity of sodium oxide the decomposition pressure of the sulphate would approach infinity. The partial pressure of sodium oxide must be directly proportional to its activity in the sulphate melt, which in turn depends on the gas composition above the melt - if the sulphate melt is subjected to an atmosphere free of sulphur dioxide and oxygen, it is then highly probable that the activity of sodium oxide would become very high in the sulphate melt. However Holmquist considers this condition to prevail at the very surface only.

Holmquist tabulates values for $\log K_3$, which were obtained by extrapolating the data of Kellogg⁹⁶. These values can be plotted against temperature according to the equation

$$\log K = 11.9 - 3.38 \times \frac{10^4}{T} K$$

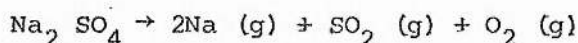
<u>T/K</u>	<u>log K₂</u>	<u>log K₁</u>	<u>log K₃</u>
1157	0.40	-17.73	-17.3
1200	0.56	-16.85	-16.3
1300	0.97	-14.90	-14.0
1400	1.13	-13.35	-12.2
1473			-11.0
1500	1.35	-12.00	-10.6
1600	1.54	-10.75	- 9.2
1700	1.71	- 9.67	- 8.0

ManYing et. al.⁹⁷ had suggested that sodium sulphate decomposes only according to the following reaction

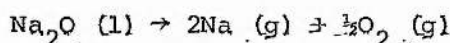


after taking into consideration the findings of Brewer and Margrave⁹⁸ who have shown that metal oxides do not exist in the vapour phase. ManYing had further indicated that the total pressure according to the above pattern of thermal decomposition would reach one atmosphere at 1698 K. Holmquist takes this suggestion and points out that, at this temperature, from equation (14) and using the values from the table above, $\log [\text{Na}_2\text{O}]$ would be equal to -7.1 when $p_{\text{SO}_2} = p_{\text{O}_2} = \frac{1}{4}$. The partial pressure of sodium oxide will therefore be negligible and the above reaction is the most significant with regard to material transport.

Wyatt⁹⁹ has shown that the calculation based on the reaction mechanism



will yield $\Delta G^{\circ}/T = 252.43 \text{ J deg}^{-1}$ at 1600 K and $104.08 \text{ J deg}^{-1}$ at 2000 K hence $p_{\text{Na}}^2 \cdot p_{\text{SO}_2} \cdot p_{\text{O}_2} \sim 5 \times 10^{-14} \text{ atm}^4$ at 1600 K and $\sim 3.5 \times 10^{-6} \text{ atm}^4$ at 2000 K with evaporation into a vacuum this would give a total vapour pressure of 10^{-3} atmospheres at 1600 K and $\sim 10^{-1}$ atmospheres at 2000 K. The same author also introduced the correlation between the stabilities of the alkali oxides towards formation of metal vapour and the relative stabilities of sodium and potassium sulphates. The following calculations were presented in support of the same.



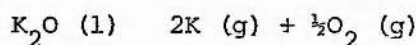
$$\Delta G^{\circ}/T = 83.6 \text{ J deg}^{-1} \text{ at } 1600 \text{ K}$$

$$= 14.84 \text{ J deg}^{-1} \text{ at } 2000 \text{ K}$$

$$p_{\text{Na}}^2 \cdot p_{\text{O}_2}^{1/2} = 4 \times 10^{-5} \text{ atm}^{5/2} \text{ at } 1600 \text{ K}$$

$$= 0.13 \text{ atm}^{5/2} \text{ at } 1200 \text{ K}$$

and

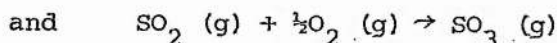
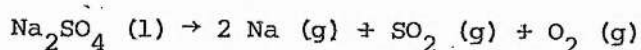


$$\Delta G^{\circ}/T = 21.99 \text{ J deg}^{-1} \text{ at } 1600 \text{ K with}$$

$$p_{\text{K}}^2 \cdot p_{\text{O}_2}^{1/2} = 0.07 \text{ atm}^{5/2} \text{ at } 1600 \text{ K.}$$

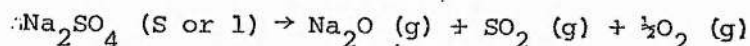
Ficalora et. al.¹⁰⁰ employed the high temperature mass-spectrometric technique to study and derive the high temperature thermodynamic properties and the vapour pressures of alkali metal sulphates. All the sulphates were heated in an alumina-lined Knudsen cell and the effusing molecular beam was analysed mass-spectrometrically. The ions observed in the mass-spectrum obtained from the sodium sulphate

melt were Na^+ , O_2^+ , SO_2^+ , SO_3^+ , SO^+ and S^+ , and the fragmentation pattern did not change even when the temperature was raised to 50 K above the melting point of sodium sulphate. Their ionisation efficiency curves showed Na^+ , SO_2^+ , O_2^+ , and SO_3^+ over solid sodium sulphate as the parent ions and SO^+ and S^+ to be the fragments. These authors therefore concluded that the thermal dissociation of sodium sulphate should be described by the following mechanisms



The heat of decomposition at 1087 K calculated for the above reaction by these workers from their results was 1316 kJ mol^{-1} , which is in fair agreement with the calculated value (Based on JANAF values) of 1325 kJ mol^{-1} .

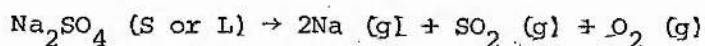
Another Mass-spectrometric investigation reported by Kosugi ¹⁰¹, being in Japanese, is intelligible to the present author only through the tables and figures and the abstract. Kosugi's mass-spectrum reveals the presence of the Na_2SO_4^+ ion with intensities ranging from 0.1 to 0.55 of the Na^+ ion. However Kosugi interprets his results to indicate that the following reaction represents the predominant vaporisation equilibrium



A Knudsen effusion study of the sodium sulphate was carried out earlier in this Laboratory by Powell and Wyatt ¹⁰². Spinel [$\text{Al}_2\text{O}_3 \cdot \text{MgO}$] Knudsen cells were used. These authors observed a change of slope in the $\ln p$ vs $1/T$ plot which has not yet been satisfactorily explained. However these authors suspected that the sodium sulphate melt must

must have attacked the spinel cell, thus affecting their final results.

In 1972 Daniel Cubbicciotti and Keneshea¹⁰³ studied the sodium sulphate system by the dynamic method, using Nitrogen as well as mixtures of SO₂ + O₂ gases as transporting gases, over the temperature range between 1400 and 1625 K. These authors rightly believed that the vapour pressure values obtained at different temperatures with the SO₂ + O₂ mixtures being used as carrier gas are essentially the equilibrium pressures of Na₂SO₄, since the SO₂ + O₂ atmosphere would prevent or almost completely suppress the dissociation of Na₂SO₄. Further these authors observed that adding the equilibrium pressure of Na₂SO₄, obtained in the above manner, to the theoretically calculated total pressure [based on values quoted in JANAF tables] based on the mechanism:



yielded vapour pressure values which were in very close agreement with the vapour pressure values obtained with nitrogen as the carrier gas. These authors therefore conclude that sodium sulphate decomposes through simple volatilisation as monomer as well as by the dissociation mechanism yielding Na, SO₂, and O₂. They derived the following expressions to represent the vapour pressure relationship determined in Nitrogen and SO₂ + O₂ atmospheres

For Nitrogen

$$\log_{10} p \text{ (Na, atm)} = 7.081 - 1.619 (10^4/T).$$

For SO₂ and O₂

$$\log_{10} p \text{ (Na}_2\text{SO}_4 \text{ atm)} = 5.858 \pm 0.15 - \frac{(15540 + 380)}{T}$$

Lithium, Rubidium and Caesium Sulphates

Jaeger¹⁰⁴ studied the thermal behaviour of Lithium, Rubidium, and Caesium sulphates and reports that while the Lithium sulphate decomposes at 1473 K, vaporisation of Rubidium and Caesium sulphates was noticeable only at 1598 K. A similar thermal study was reported by Hopkin¹⁰⁵. This author estimated from his results the comparative volatility of Potassium, Rubidium and Caesium sulphates. The ratio of their volatilities was reported to be 1 : 1.4 : 2.1. Hopkin also believes that volatility depends mainly on, and may be determined by, the changes of bonding which take place in the liquid state, rather than by the ionic bonding in the solid state. It appears that stronger bonding in the solid state is associated with weaker bonding in the liquid state.

Spitsyn and Shostak¹⁰⁶ investigated in detail the volatilities of all the normal sulphates of alkali metals. In their experiments the sulphates were heated over a temperature range between 1073 K and 1473 K in air, in a current of air, and in a current of steam. These authors conclude from their results that Potassium, Rubidium and Caesium vaporise predominantly as molecular sulphate but for Lithium and Sodium decomposition occur. The residue after heating Lithium sulphate showed alkalinity. Further Spitsyn and Shostak are of the opinion that the polarising action of the Lithium ion upon the sulphate ion and the consequent reduction of the ionic nature of the bond between them influences the volatility of the Lithium sulphate. Sodium sulphate was found to be the least volatile of the alkali metal sulphates, which these authors believe may be due to the considerably less polarising

action of the sodium ion (in comparison to the Lithium ion) upon the sulphate ion. Although some weight loss measurements were recorded by these authors, no conclusions were arrived at concerning the absolute values of the vapour pressures of the sulphates studied. The mass-spectral study of Fica-Lora et. al.¹⁰⁰, which has already been mentioned earlier in connection with sodium sulphate, reveals that only Li^+ , SO_2^+ , O_2^+ , and SO_3^+ ions were found to be present over the Lithium sulphate melt. No evidence was found for the presence of Lithium sulphate monomer or lithium monoxide. The heat of decomposition of solid lithium sulphate was reported to be 1354 kJ mol^{-1} at 1080 K. Brewer and Margrave are of the opinion that the probability of the existence of monoxide of alkali metals in the vapour phase is highly negligible except possibly in the case of lithium monoxide.

The Spitsyn and Shostak¹⁰⁶ studies reported earlier show that the residues of Rubidium and Caesium sulphate obtained after heating were neutral. Their results thus indicate that Rubidium and Caesium sulphate evaporate congruently, but the nature of the gaseous species is not elucidated. Spiridonov, Khodchenkov, and Akishin¹⁰⁷ studied the vapours of Caesium sulphate by electron diffraction and derived a structure for the Cs_2SO_4 molecule. Buckler, Stauffer, and Klemperez¹⁰⁸ studied the electric deflection of molecular beams of Cs_2SO_4 with a mass-spectrometer detector and concluded that the Cs_2O^+ and Cs^+ ions originated from the parent molecule Cs_2SO_4 . The mass spectral study of Ficalora et. al.¹⁰⁰ showed Rb_2SO_4^+ and Cs_2SO_4^+ to be the parent ions and Rb^+ and Cs^+ resulted from them. Thus these authors conclude Rb_2SO_4 and Cs_2SO_4 to be the major species over the respective sulphate

melts and report a value of 267 kJ mol^{-1} and $291.3 \text{ kJ mol}^{-1}$ for the enthalpy of sublimation of Caesium and Rubidium sulphates at 1200 K from their measurements. Daniel Cubicciotti¹⁰⁹ has recently reported results of his Knudsen effusion study of Caesium and Rubidium sulphates. A platinum effusion cell was used. This author reports that the residues in the cell after heating the respective sulphates were found to be neutral. Further taking into consideration the mass-spectral evidence reported by other workers Cubicciotti concludes that the predominant species that exist in the vapour phase over these sulphate melts are Cs_2SO_4 and Rb_2SO_4 . He then goes on to calculate the equilibrium vapour pressures of Cs_2SO_4 and Rb_2SO_4 from his weight loss measurements and represents the vapour pressure relationship by the following equations.

$$\log p(\text{Cs}_2\text{SO}_4)/\text{atm} = 32.857 - \frac{19084}{T} - 7.15 \log T$$

[1090 - 1260 K]

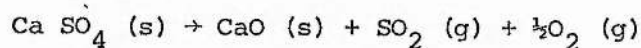
$$\log p(\text{Rb}_2\text{SO}_4)/\text{atm} = 32.876 - \frac{20468}{T} - 7.05 \log T$$

[1090 - 1300 K]

This author also reports the enthalpies and entropies of sublimation at 1200 K to be $295.26 \text{ kJ mol}^{-1}$ and $35.4 \text{ gibbs mol}^{-1}$ for Cs_2SO_4 , $322.56 \text{ kJ mol}^{-1}$ $36.0 \text{ gibbs mol}^{-1}$ for Rb_2SO_4 respectively.

Magnesium and Calcium Sulphates

Stern and Weise ¹¹⁰ have calculated and list the equilibrium pressures for the dissociation of calcium sulphate based on the following mechanism.



They report the equilibrium pressure to be of the order of 3.73×10^{-8} atmospheres at 1000 K and 2.29×10^{-5} atmospheres at 1200 K. Tschappat and Piece ¹¹¹ represent the vapour pressure relationship by the following expression derived on the belief that calcium sulphate decomposes to give SO_2 and O_2 at high temperatures.

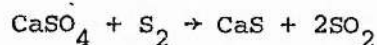
$$\log p/\text{torr} = -14024 \text{ k/T} + 10.280$$

The enthalpy change was found to be 404 kJ mol^{-1} . These authors found that their results obtained with both anhydrite and dehydrated gypsum fit the above relationship, and are in close agreement with the values reported by Zawadski ¹¹² for anhydrite. However Zawadski's results for dehydrated gypsum were found to be very close to those of Mlle. Marchal ¹¹³ and markedly different from those of Tschappat and Piece. Marchal quotes a ΔH value of 260 kJ mol^{-1} . Dewing and Richardson ¹¹⁴ investigated the calcium sulphate system by differential thermal analysis. They assumed that at high temperatures the decomposition products emanating from CaSO_4 are sulphur-dioxide and oxygen only. The sulphate was kept in a furnace and the temperature was raised slowly while a mixture of N_2 , SO_2 and O_2 at known partial

pressures was passed over the sample. When the decomposition commences at a particular temperature, that is when the vapour pressure of the sulphate equals the total pressure of SO₂ and O₂ surrounding it, a thermal effect (an absorption of heat) occurs and this was detected by a differential thermocouple. Their results are represented by the following equation

$$\Delta G^{\circ} [1483 \text{ K} - 1638 \text{ K}] = (111,000 - 56.62T) \text{ cal} \\ (463,980 - 236.67T) \text{ J}$$

These authors then take into account the available data on the equilibrium between CaO, CaS¹¹⁵ and SO₂¹¹⁶ and making use of these data together with the measurements made by Fykse¹¹⁷ on the equilibrium



at temperatures between 1303 K and 1373 K derive the following equation for the formation of CaSO₄ from CaO, SO₂, and O₂, which is in reasonable agreement with their values.

$$\Delta G^{\circ} [1303 \text{ K} - 1373 \text{ K}] = (108,700 - 55.96 T) \text{ cal.} \\ (451,440 - 233.91 T) \text{ J}$$

By further calculation, these authors find the values obtained for the formation of CaSO₄ by making use of the data of Schenck and Hammerschmidt¹¹⁸ on the sulphate + sulphide equilibrium to be in very close agreement with their value.

A study of the papers published so far reveals that the thermal decomposition of magnesium sulphate starts at 1168 K,¹¹⁹ 1013-1333 K¹²⁰ or 1393 K¹²¹ according to different authors. Kowalska¹²² studied the kinetics of thermal decomposition of magnesium sulphate and

reports a value of $206.5 \text{ kJ mol}^{-1}$ for energy of activation.

Pechkovsky¹²³ has carried out a detailed study of the rate of thermal decomposition of magnesium sulphate. The rate of thermal decomposition was investigated in relation to various factors such as temperature, time, oxygen concentrations in the gas passed over the sulphate, and the presence of various metal oxides in the sulphate. Both the solid and gaseous reaction products were analysed. This author reports the following observations:

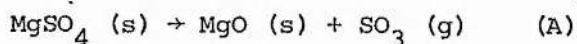
(a) Pure magnesium sulphate decomposes at an appreciable rate at temperatures above 1233 K and decomposition is very rapid at 1373 K and is accompanied by strong caking of the mass.

(b) The gaseous products resulting from the thermal decomposition of the sulphate were found to be sulphur dioxide and sulphur trioxide.

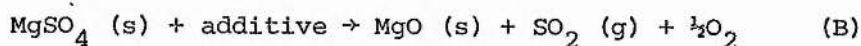
(c) The decomposition rate of the pure sulphate and the composition of the gaseous products depended mainly on the temperature and less on the concentration of oxygen in the gas passed over the sample. The overall rate of decomposition of pure MgSO_4 remained constant even when the oxygen concentration in the gas passed over the sample was changed. However the composition of the gaseous products changed depending upon the oxygen concentration.

(d) When metal oxides such as CuO and Fe_2O_3 were present in the magnesium sulphate the rate of decomposition was higher than the rate for pure magnesium sulphate, thereby indicating that the additives accelerate the rate of thermal decomposition. However the acceleration of the rate of decomposition in the presence of

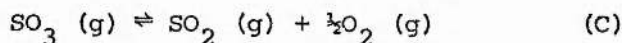
metal oxides was dependent on the concentration of oxygen in the gas passed over the sample. A decrease in oxygen concentration resulted in a higher rate of decomposition. As mentioned earlier this was not the case with pure magnesium sulphate, for which the overall rate remained constant irrespective of the oxygen concentration. Pechkovsky therefore concludes that pure magnesium sulphate decomposes according to the following mechanism



and in the presence of additives such as CuO or Fe₂O₃ by



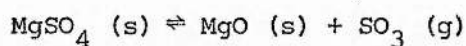
His conclusion is based on the following argument. In the case of pure magnesium sulphate the SO₃ formed by decomposition is continuously removed by the flowing oxygen gas and therefore there was no time for the following equilibrium to be established over the sulphate



This reasoning is the basis for the constancy of the general rate of decomposition observed in the experiments with pure magnesium sulphate, irrespective of the concentration of oxygen in the gas passing over the sample. This author contends that increase of SO₂ concentration found in the gas at the exit of the furnace is due to the approach of the gas phase composition to the equilibrium state not in the reaction zone itself, but while passing through the porcelain tube of the furnace. When additives such as CuO and Fe₂O₃ were present the composition of the gaseous products approached

the equilibrium state even while they were passing through the layer of material and this resulted in the higher decomposition rate of magnesium sulphate. In other words, the presence of additives helps the decomposition of SO_3 and leads to a closer approach to the equilibrium state indicated in equation (c) over the sample. This also in turn explains why the rate of thermal decomposition of magnesium sulphate (in the presence of additives) increases or decreases with the corresponding decrease or increase of the oxygen concentration in the gas flowing over the sample. It is fair to assume, from the observations and results of Pechkovsky, that the MgO layer which would be formed at the surface from the initial decomposition of magnesium sulphate does not have the catalytic effect to decompose SO_3 gas diffusing through it. Bnonnikov¹²¹ studied the rate of thermal decomposition of magnesium sulphate with a stream of air flowing over the sample in one set of experiments and a mixture of air plus water vapour in another set. He also investigated the influence of SiO_2 on the rate of decomposition of magnesium sulphate when it was added in different amounts to the sulphate. This author concludes that pure magnesium sulphate decomposes to give the solid oxide and sulphur trioxide. When SiO_2 was mixed with the sulphate the rate of decomposition was accelerated indicating that SiO_2 catalyses the dissociation of SO_3 as it passes through the oxide layer.

Knopf and Staude¹²² measured the decomposition equilibrium of magnesium sulphate by the transpiration technique and are of the opinion that decomposition proceeds as follows.



They express their vapour pressure measurements by the following equation

$$\log P/\text{torr} = -1.2487 \times 10^4 K/T + 11.3748$$

Dewing and Richardson¹¹⁴ however studied the magnesium sulphate system by the differential thermal analysis technique, as mentioned earlier in the case of calcium sulphate, and express their results by the following relation-ship

$$\Delta G^{\circ}[1173\text{K} - 1423\text{K}] = 87,180 - 60.2 T. \text{ cal}$$

$$364412 - 251.64 T. \text{ J}$$

EXPERIMENTAL

EXPERIMENTAL

1. Materials used

The material used for investigation in this work were all of 'Analar' quality. The percentage purity of the samples were checked and determined again before use by Atomic absorption for the metal content and by gravimetric estimation of the amount of sulphur. The purity of the samples were as follows.

Na_2SO_4 - 99.5%	$\text{MgSO}_4 \cdot 7\text{H}_2\text{O}$ - 99.5%
Li_2SO_4 - 99.3%	$\text{CaSO}_4 \cdot 2\text{H}_2\text{O}$ - 99.3%
Rb_2SO_4 - 99.0%	
Cs_2SO_4 - 99.0%	

2. Study of the action of Alkali metal sulphates on spinel cell ($\text{MgO} + \text{Al}_2\text{O}_3$)

The vapour pressure values obtained using spinel Knudsen cells for sodium and lithium sulphates by Powell and Wyatt in this Laboratory, which was mentioned earlier in the literature review section, were suspected to have been affected by the reaction of the molten sulphates with the spinel cell at high temperatures. The extent to which the alkali metal sulphates attacked the spinel material was studied as follows.

PROCEDURE:- About 0.5 grams of the alkali metal sulphate, previously dried in an oven, was taken in a thoroughly cleaned, washed, dried and accurately weighed spinel Knudsen cell and kept in a muffle furnace which was maintained at 1250 K for different periods (24, 15, 10, and 5 hours).

At the end of each experimental run the spinel cell was taken out, washed and cleaned thoroughly, then dried in an air oven and finally cooled and weighed. The experiments were carried out in similar manner with all the alkali metal sulphates.

3. Knudsen effusion method

(a) Apparatus:- The two principal constituent parts of the experimental assembly (a) vacuum system, furnace and balance, (b) Heating control system are diagrammatically represented in figures 2 and 3. The vacuum system was simple and consisted of an oil diffusion pump backed up by a rotary pump. Two pressure gauges were incorporated as indicated. While the Pirani gauge gave an indication of the backing pressure near the diffusion pump the Penning gauge showed the degree of vacuum or in other words the residual pressure inside the ceramic tube housing the Knudsen cell. Three liquid nitrogen traps as shown in the figure 2 were used only to protect the gauges from undesirable condensates. The rotary pump was joined to the oil diffusion pump by a 1cm bore glass tube and through rubber bellows and a metal to glass vacuum seal. Further, as shown in the diagram, the glass line carried a three way stopcock, a 5 litre glass bulb and the Pirani gauge. A 2.5cm bore copper tube connected this vacuum system to the left arm of the vacuum balance head through a screw-on metal cap¹O'ring seal and B 34/35 cone and socket. Similarly the right arm of the vacuum balance was attached to the ceramic tube housing the Knudsen cell through a screw-on metal cap¹O'Ring seal combination with aluminium socket and

1. ROTARY PUMP
2. RUBBER BELLOWS
3. THREE WAY STOP-COCK
4. GLASS BULB
5. PIRANI GAUGE
6. OIL DIFF. PUMP
7. N₂ TRAPS
8. COPPER TUBING
9. SCREW ON TYPE SEAL WITH O RINGS
10. MICRO BALANCE
11. PENNING GAUGE
12. CERAMIC TUBE
13. COOLING JACKET
14. Cr-Al THERMOCOUPLE
15. FURNACE
16. MOLYBDENUM WIRE
17. Pt-13% Rh THERMOCOUPLE.

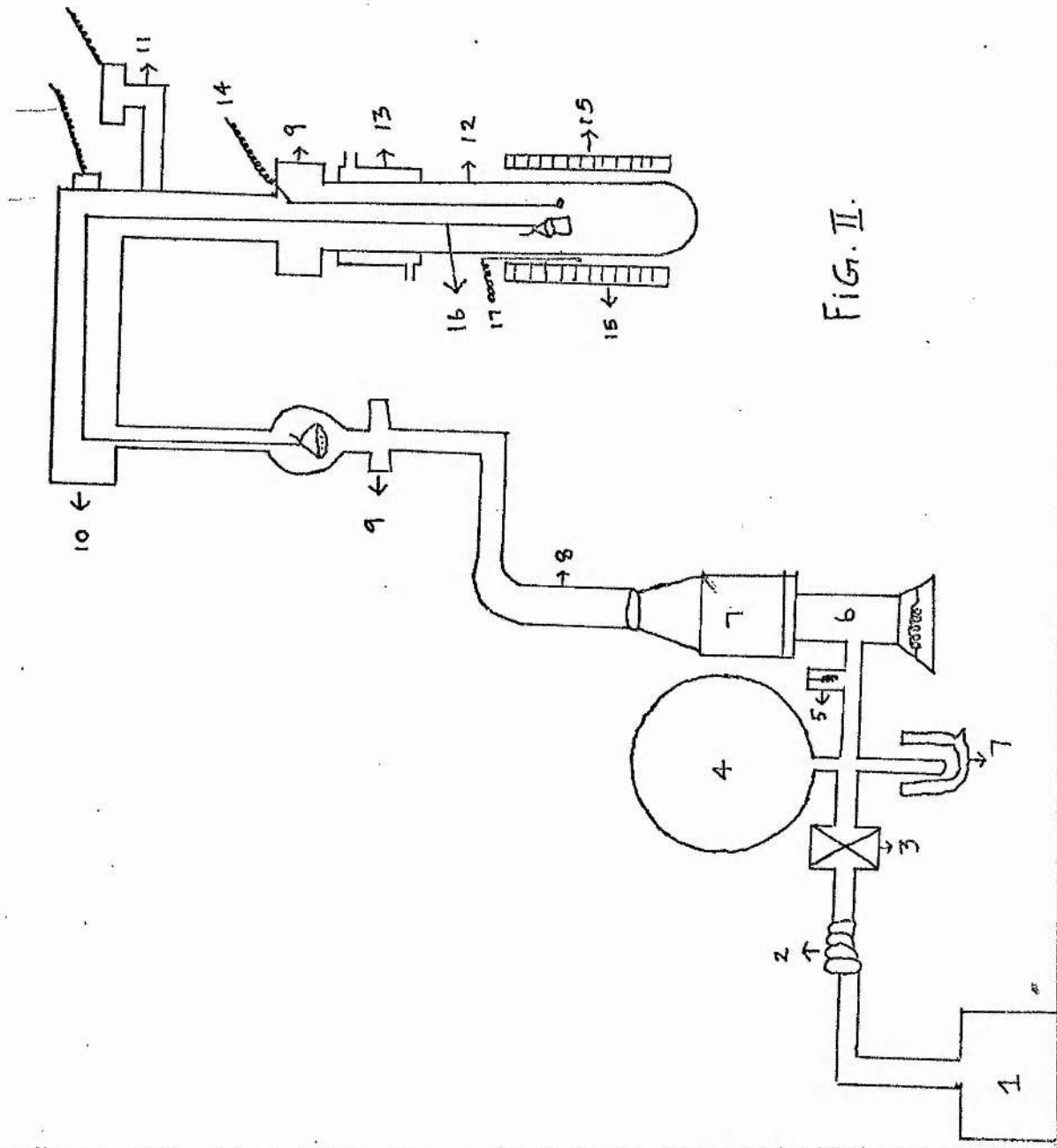


FIG. II.

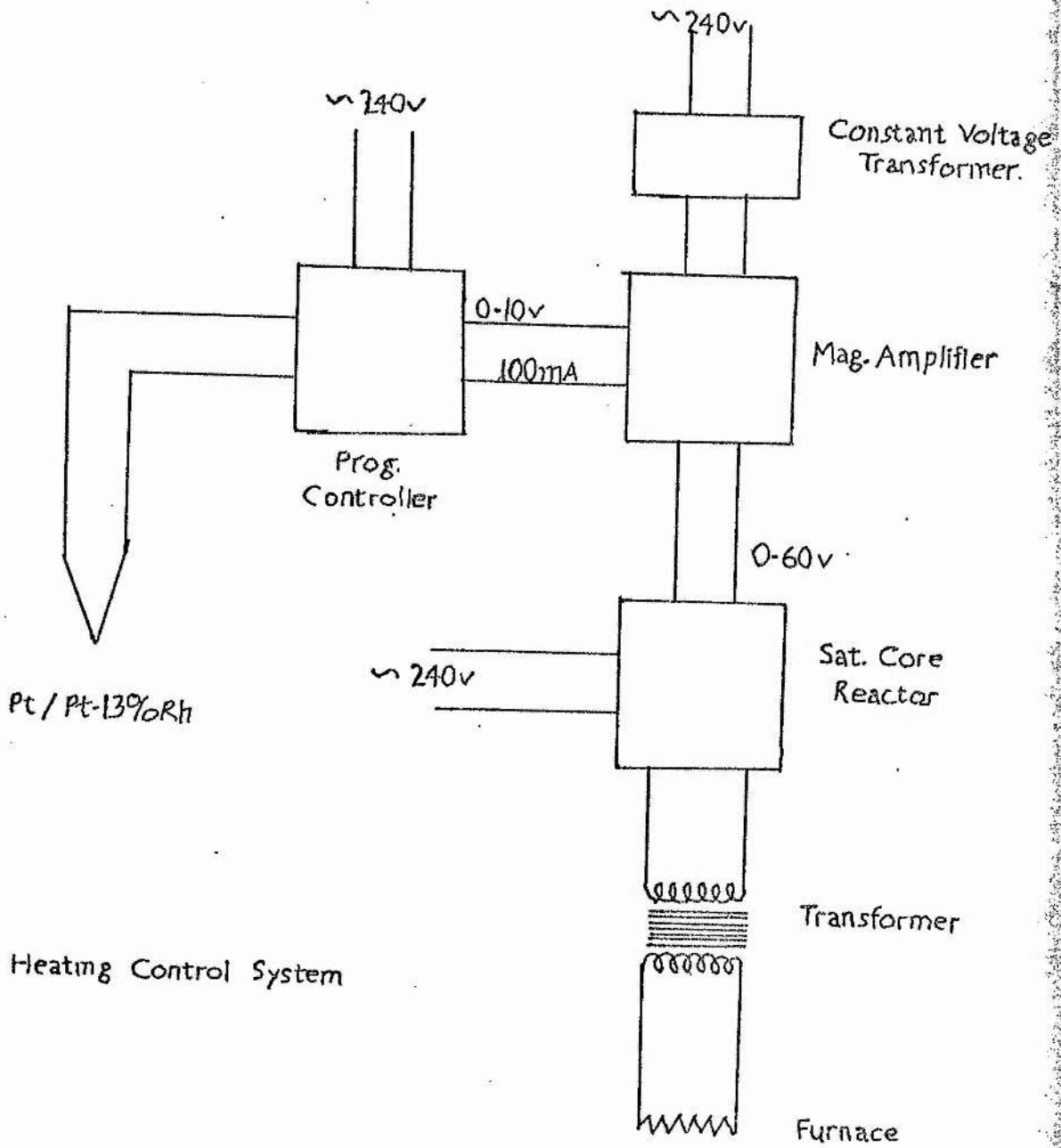


fig.3. Heating Control System

B 34/35 cone. The Chromel-Alumel thermocouple led into the ceramic tube through ceramic lead-throughs and, positioned very near to the Knudsen cell, measured the Knudsen cell temperature. The platinum - 13% Rhodium thermocouple placed outside the ceramic tube enabled the power supply and in turn the furnace temperature to be controlled. The heating control system enabled the temperature to be maintained ± 4 K in the experimental temperature range. The whole unit was fixed on a steel structure and supported on the ground by a wooden board on rubber mountings.

The tubular furnace consisted of three cylindrical tubes of increasing diameters. The innermost or the core of the furnace was a ceramic tube wound suitably with the heating element (Kanthal wire 'A') and carried on it a coating of fine clay. This was placed inside a metallic tube whose diameter was 1cm larger, and the space between them was filled with asbestos powder. This combination in turn was housed in another cylindrical metallic tube and the empty space was filled up with asbestos wool. The furnace was supported on a movable guide so that it could be moved up and down the ceramic tube housing the Knudsen cell.

The experimental weight losses were measured on a vacuum micro balance (Mark 2B) as supplied by C.I. Electronics. The instrument was in two parts, an evacuable weighing compartment containing the balance head and the electrical control cabinet. A multi-way cable connects the two parts. The balance could be operated in five ranges, as shown below.

Range 1	-	0	-	25	ug
2	-	0	-	250	ug
3	-	0	-	2.5	mg
4	-	0	-	10	mg
5	-	0	-	100	mg

However, in the present work it was found difficult to work in the highly sensitive ranges 1 and 2 due to vibrational problems, and therefore weight loss measurements were made in the ranges 3, 4 and 5 only. The Knudsen cell containing the sample sulphate was suspended by a 0.25 mm diameter molybdenum wire from the right arm of the balance. The weight loss was followed on the meter of the control box. The tip of the balance arm was more than fifty centimeters above the hot part of the furnace, sufficient distance to enable any effects of temperature to be neglected. Further, the cooling jacket fixed on the ceramic tube and the radiation shields completely eliminated the possible thermal effects on the sensitivity and operation of the micro balance.

The samples were all contained in Platinum and spinel ($MgO+Al_2O_3$) cells of $0.4cm^2$ cross section and depth 0.8cm. Earlier work ¹²³ has shown that spinel cells are both inert and non-porous to potassium sulphate and this condition was confirmed in the recent work for its salt, and also for rubidium and caesium sulphates, but not for sodium of lithium sulphate. Platinum foil of 0.025mm thick was used to cover the cell and was held to the walls of the cells by a series of individually tightened loops of 0.25mm diameter molybdenum wire. The relative co-efficients of linear expansion of the various components ensured that these bindings tightened further as the temperature increased.

The effusion orifices were made with hardened steel punches and were clean edged and circular under the microscope. Microscopic measurements were made to check the diameters of the orifices. The ratio of the cross-sectional area of the Knudsen cell to the orifice

area exceeded 100 to 1 in every case. The Knudsen orifices used were of three different sizes, 0.0725, 0.0490 and 0.0336cm diameter. Kennard's ¹⁷ method was adopted in calculating the Clausing factor for each orifice. The position of the Knudsen cell and the thermocouple were kept the same for all experimental runs and for the initial calibration procedure using potassium sulphate. The total loads on the balance were about 1.5 grams in the case of spinel cell and less than 1 gram whenever the platinum cell was used.

(b) PROCEDURE:- A sample of the sulphate under investigation was ground and dried in an oven for 24 hours at 383 K. About 0.1 grams of this dried material was then weighed into the Knudsen cell, covered with the platinum foil, already furnished with an effusion orifice of known size, and the lid was held tight and secure by bindings of molybdenum wire. The material taken in the Knudsen cell was enough to cover the bottom of the cell to the depth of 4mm. The molybdenum suspension wire was fixed, and it was ensured that the Knudsen cell was vertically below the point of suspension on the balance arm. The length of the suspension wire was kept the same for all the experimental runs.

With the Knudsen cell suspended in position, the unit was attached to the vacuum system and evacuation started. The vacuum pumps were left to pump down usually for 15-20 hours before the furnace was switched on. The furnace was then switched on and brought to the working temperature slowly and steadily over a period of 6-8 hours. Then it was allowed to stabilise over a period of up to half an hour and, when it was clear that

the relationship between the weight loss of the cell and the time of heating was linear, measurement commenced. During the course of any actual measurement, the rotary pump was isolated from the system by the use of the three-way stop-cock and switched off. This was done in order to avoid the balance and in turn the weight loss measurements being affected by the vibrations from the rotary pump. During any actual weight loss measurement therefore, the vacuum was maintained by the oil diffusion pump alone. The 5 litre glass bulb situated in between the three-way stop-cock (Fig. 2) and oil diffusion pump enabled the pressure difference to be maintained and at no time during a series of measurements was the pressure in the furnace allowed to increase beyond 2×10^{-5} torr. The time over which a weight loss was measured depended on the temperature and the nature of the substance under investigation. It usually varied from three to six hours. At the end of this period, the furnace was adjusted to the next desired temperature, the pause for equilibration was observed, and the procedure was repeated. Thus, a series of weight loss experiments were carried out on increasing the furnace temperature in steps. Measurements were also made at specific temperatures on cooling the furnace at the end of a run. The furnace was switched off between two separate sets of measurements when night intervened.

The vapour pressures were calculated from the Knudsen equation, mentioned earlier in the introduction, using these measured weight losses. A Clausing factor was used in each calculation to adjust for the channelling effect of the orifice upon the effusing molecules.

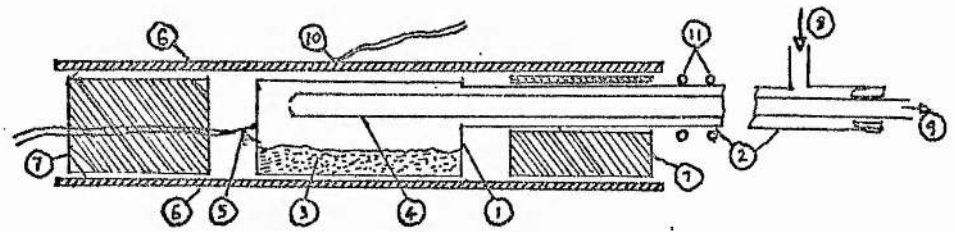


FIG. 4.

(4) TRANSPIRATION METHOD

(a) Apparatus

The apparatus used for the vapour pressure studies by the transpiration method is almost identical to the one employed by Daniel Cubbicciotti ¹⁰³ and is represented diagrammatically in figure 4. The heating control system was identical to those described in the previous section. The descriptions of various parts of the apparatus indicated by numbers in figure 4 are as follows.

- (1) cell, Platinum - 10% Rhodium, 2.5cm diam x 5cm long
- (2) Entrance tube to cell, 1cm diam x 27cm long
- (3) sample, molten sulphate
- (4) collector tube, platinum 0.5cm diam x 28cm long with a 1mm opening at the hot end
- (5) Thermo couple, Platinum - 13% Rhodium
- (6) Furnace, identical to the one used for Knudsen effusion studies
- (7) Fire brick insulation
- (8) Carrier Gases inlet
- (9) Gas outlet to the analyser and collector
- (10) Control Thermocouple, Platinum - 13% Rhodium
- (11) Cooling Jacket.

The cell and the furnace were tipped about 5° from horizontal so that the salt that diffused between the collector and the gas entrance tube drained back into the cell. The Carrier gas flow rate was maintained constant in the following manner. A constant pressure of gas (about 5 psi) was obtained from a commercial cylinder with a two-stage

diaphragm regulator. By passing it through a fritted glass disk a constant gas flow was obtained and measured accurately by a previously calibrated flow meter before delivery into the transpiration cell. Preliminary experiments showed that saturation was achieved in the range 15-25 per min of carrier gas flow rates. When the $\text{SO}_2 + \text{O}_2$ mixture was used as the carrier gas, about 12cc of each of these gases were delivered into the transpiration cell per minute.

(b) PROCEDURE: The samples of each sulphate used were from the same source as those used in the weight loss experiments and as before they were ground and dried at 383 K for about 24 hours prior to use. Sufficient quantity of the sample sulphate (about 1.5 grams) was introduced into the cell. The carrier gas, accurately measured, was then fed into the cell with the dummy collector tube in its place. The furnace was then switched on and brought to the operating temperature slowly and gradually over a period of 5-6 hours. After the system had been at this operating temperature for several hours, usually 3-4 hours, the dummy collector tube was replaced by a clean, dry, and weighed collector tube and a collection made, usually for a period of 19-25 hours in the case of nitrogen and 25-40 hours when the $\text{SO}_2 + \text{O}_2$ mixture was used as carrier gases. When nitrogen was used the exit gas was collected over water, but $\text{SO}_2 + \text{O}_2$ exit mixtures were just passed through absorber bottles containing standard Sodium hydroxide solution and then collected over water. At the end of the experiment the collector tube was removed, cooled, its end stoppered, and its outside washed. Then the collector tube was

washed thoroughly and the amount of sodium present in the washing was estimated by Atomic absorption. When an $\text{SO}_2 + \text{O}_2$ mixture was used as the carrier gas the solutions in the absorber bottles were titrated for residual base with standard acid and for reducing power with standard I_3^- . The two titrations permitted the calculation of the total amounts of SO_2 and SO_3 in the exit gas. These amounts, together with the residual oxygen gas collected over water were used to calculate the amount of SO_2 and O_2 that had passed over the sample. The vapour pressure was calculated from the measurements made by use of the following equation.

$$P_{\text{atm}} = \frac{n}{N+n}$$

n = No. of moles of substance collected

N = No. of moles of carrier gas that passed over the sample during the experimental run.

RESULTS AND DISCUSSION

TABLE III

Substance	Changes in the weight of the spinel cell At the end of the experiment				Mechanical Strength
	24h	15h	10h	5h	
$Rb_2 SO_4$	Nil	Nil	Nil	Nil	No change
$Cs_2 SO_4$	Nil	Nil	Nil	Nil	No change
$K_2 SO_4$	Nil	Nil	Nil	Nil	No change
$Na_2 SO_4$	28 μg	18 μg	10 μg	10 μg	Cracked into pieces on applying slight thumb pressure
$Li_2 SO_4$	31 μg	19 μg	8 μg	11 μg	Cracked into pieces on applying slight thumb pressure

Alkali metal sulphates

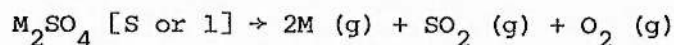
(a) Results and discussions of muffle furnace experiments

The results and observations for alkali metal sulphates are presented in Table III. In the case of Potassium, Rubidium and Caesium sulphates no change in the weight of the spinel cell nor in its mechanical properties was observed at the end of the experiments. However, in the case of sodium and lithium sulphates there was very small variation in the weight of the spinel cell. Further, the spinel cell at the end of each experimental run was found in these cases to have lost its mechanical strength completely. That is, on the application of slight thumb-pressure the cell broke into small pieces, indicating that the $MgO-Al_2O_3$ bonding in the spinel material had weakened due to the attack by the molten sodium and lithium sulphates. The vapour pressure values derived from effusion experiments, which will be presented in the next section, will show that the vapour pressure values obtained with both spinel and platinum cells for Rubidium and Caesium and Potassium sulphates closely agreed with each other, but for lithium and sodium sulphates the vapour pressure values obtained with spinel cell were markedly higher than the platinum cell values. One probable explanation for the very small variation in the weight of the spinel cell, at the end of the muffle furnace experiments, in spite of the attack by the molten lithium and sodium sulphates is that the molten sulphates while being cooled might have fused and bonded to the spinel cell in the places of attack.

The results and discussion of the Knudsen and transpiration experiments, which are presented in the following sections, although, initially several equations were tentatively presented to show the vapour pressure dependence on temperature, the equations representing the true relationship consistent with the final interpretation of the results are denoted by an asterisk mark.

(b) Results of Knudsen Effusion experiments

The results of weight loss experiments on the alkali metal sulphates are given in Tables IV, VI, VIII and IX and they are represented graphically in Figures V, VIII, X, and XI. In this figures $\log_{10} P/\text{torr}$ is plotted against $1/T$. P is the value of vapour pressure calculated by using a vapour phase molecular weight corresponding to the species $M_2SO_4(g)$ for Rubidium and Caesium sulphates. For Lithium and sodium sulphates P was calculated by using an average molecular weight value which was calculated on the basis of the following mode of decomposition for these two sulphates.



For all the sulphates the points may be represented by single straight lines within the experimental error. In the case of rubidium and Caesium sulphates the vapour pressure values obtained with both spinel and platinum cells agreed with each other very closely. However, in the case of Lithium and sodium sulphate, the spinel cell vapour pressure values were markedly higher than the platinum cell values. A linear relationship was observed for the rate of weight loss with time. The residues of all the alkali metal sulphates were extracted at the end of the experiment with water and were found to be neutral (to Phenolphthalein) except in the case of Lithium sulphate. The vapour pressure of all the alkali metal sulphates were found to be independent of the Knudsen orifice area. Thereby indicating that the alkali metal sulphates do not have low accommodation co-efficient.

SODIUM SULPHATE

The results of weight loss experiments on sodium sulphate are given in Table IV and represented graphically in Figure V and compared in Figure VII with those obtained by transpiration and mass-spectral methods by previous workers. The vapour pressure relationship with temperature can be represented by the following equations.

TABLE IV

SODIUM SULPHATE Na_2SO_4 (Molecular weight 142.04)PLATINUM CELL

T/K	Rate of weight loss /mg min ⁻¹	P/torr	orifice area/cm ²
1217	8.45×10^{-4}	1.71×10^{-3}	8.9×10^{-4}
1267	2.03×10^{-3}	4.21×10^{-3}	
1312	5.847×10^{-3}	1.15×10^{-2}	
1332	1.33×10^{-2}	2.81×10^{-2}	
1381	4.28×10^{-2}	9.20×10^{-2}	
1227	1.49×10^{-3}	1.383×10^{-3}	1.9×10^{-3}
1282	4.17×10^{-3}	3.90×10^{-3}	
1340	2.22×10^{-2}	2.16×10^{-2}	
1390	8.00×10^{-2}	7.62×10^{-2}	
1243	5.14×10^{-3}	2.192×10^{-3}	4.1×10^{-3}
1287	1.75×10^{-2}	7.60×10^{-3}	
1345	5.414×10^{-2}	2.40×10^{-2}	
1362	8.933×10^{-2}	3.99×10^{-2}	
1404	1.62×10^{-1}	7.35×10^{-2}	

SPINEL CELL

1167	2.00×10^{-2}	1.812×10^{-2}	<u>1.9×10^{-3}</u>
1231	1.09×10^{-1}	1.01×10^{-1}	
1272	2.50×10^{-1}	2.37×10^{-1}	
1321	4.00×10^{-1}	3.90×10^{-1}	
1377	5.00×10^{-1}	4.80×10^{-1}	
1181	5.33×10^{-2}	2.22×10^{-2}	<u>4.1×10^{-3}</u>
1226	1.66×10^{-1}	7.01×10^{-2}	
1275	2.50×10^{-1}	1.08×10^{-1}	
1325	5.00×10^{-1}	2.20×10^{-1}	
1375	6.15×10^{-1}	2.80×10^{-1}	

-77-
FIG. V

Na_2SO_4 KNUDSEN EFFUSION RESULTS

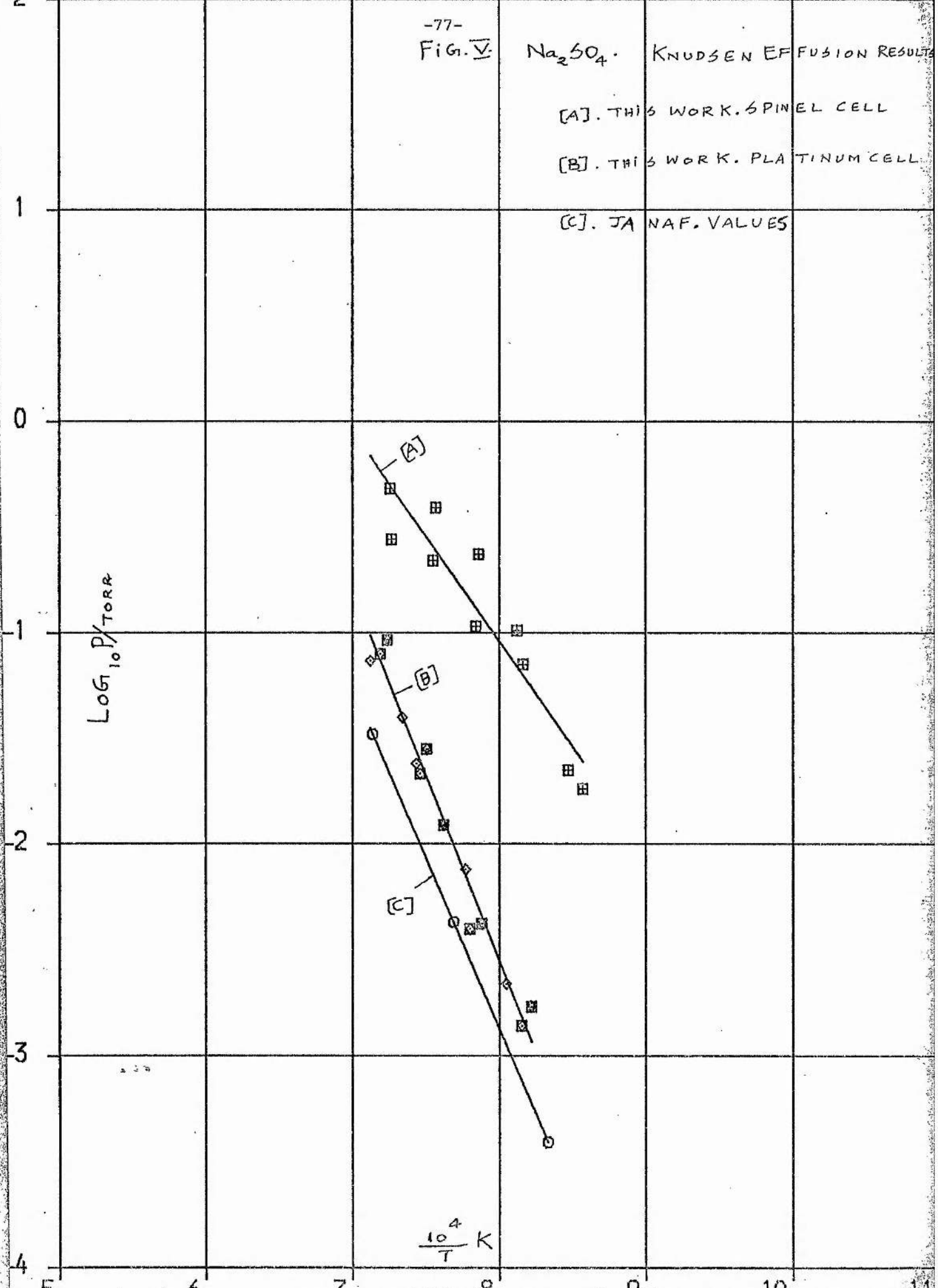
[A]. THIS WORK. SPINEL CELL

[B]. THIS WORK. PLATINUM CELL

[C]. JANAF. VALUES

$\text{LOG}_{10} P/\text{TORR}$

$\frac{10^4}{T} \text{ K}$



Spinel cell

$$\log_{10} [P/\text{torr}] (1200 - 1400 \text{ K}) = -0.996 \pm 0.13 \times 10^4 \text{ K/T} + 1.95 \pm 1.01$$

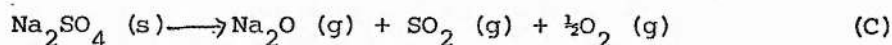
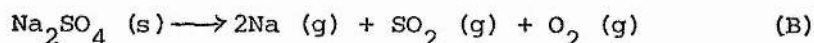
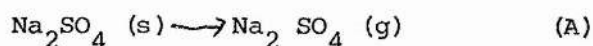
Platinum cell

$$*\log_{10} [P/\text{torr}] (1200 - 1400 \text{ K}) = -1.75 \pm 0.86 \times 10^4 \text{ K/T} + 2.71 \pm 0.66$$

As can be seen from figure V, the vapour pressure values obtained with the spinel cell are much higher than those obtained with the platinum cell. In view of the fact that the spinel cell was attacked by the sodium sulphate during the muffle furnace experiments, the results obtained with this cell are therefore discarded for discussion purposes. Powell and Wyatt's¹⁰² values, obtained earlier in this laboratory, using spinel cell should therefore be treated with reservation. Hence the values obtained with the platinum cells are only being taken into consideration in the following discussion.

DISCUSSION

The vaporisation of sodium sulphate might occur in the following possible ways :



The mass-spectral evidence of Ficalora et al¹⁰⁰ seems to indicate that vaporisation of sodium sulphate occurs predominantly by the mechanism (B). However, Kosingi,¹⁰¹ in spite of observing Na_2SO_4^+ ion in his mass-spectrum interprets his results on the basis of mechanism (C). The recently published mass-spectral study of Kohl et al¹²⁵ reveal that Na_2SO_4^+ , Na^+ , SO_2^+ and O_2^+ ions are the principal species. These workers have therefore calculated and reported the pressures of $\text{Na}_2\text{SO}_4 (\text{g})$ over molten sodium sulphate from

ion intensity measurements. They also conclude that sodium sulphate decomposes by both the mechanisms (A) and (B). The present results are as mentioned earlier, calculated and represented graphically on the basis of mechanism (B). With the values of the free energy functions quoted in the JANAF thermochemical tables,¹³⁵ calculations performed for reaction (B) showed that the expected total pressures are about 3.0×10^{-4} atmospheres at 1500 K and 5.15×10^{-7} atmospheres at 1200 K. The decomposition of Na_2SO_4 (s) at 1300 K to form 2Na (g), SO_2 (g) and O_2 (g) according to the tables should be accompanied by a ΔH value of 310 kJ mol^{-1} . The total pressures observed in this work are two times greater than the JANAF values. The enthalpy of the decomposition reaction calculated from the slope of the $\log 10 P$ vs $1/T$ plot is 331 kJ mol^{-1} . Since the thermochemical values used to derive the thermodynamic functions in the JANAF tables were well established experimentally, the slightly higher vapour pressure found in this work suggests the presence of an additional vapour species in the vapour phase. Before ultimately ascribing the difference to the species Na_2SO_4 (g), some alternative vapour molecules must first be eliminated. The equilibrium pressure of Na_2 can be considered with the help of the JANAF table.



The following expression for the equilibrium constant K_p holds if the degree of dissociation is represented by α

$$K_p = (1 - \alpha) (1 + \alpha) / 4\alpha^2 P$$

or more conveniently

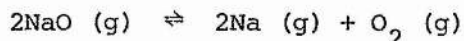
$$1/K_p = 4\alpha^2 P / (1 - \alpha)^2$$

At 1200 K, K_p is about 1 (atmosphere)⁻¹, or $1/K_p$ about 1 atmosphere.

Substituting the experimental vapour pressure of 10^{-6} atmospheres in the above equation yields a value of 0.02 for $(1 - \alpha)$, (very close to 1), and

therefore the presence of sodium dimer in the vapour phase can be ruled out.

The possibility of the vapour phase reaction

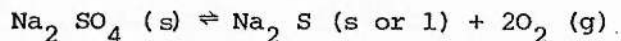


making a contribution to the higher vapour pressure can be examined in a similar way. Assuming if the degree of dissociation is again expressed as α , K_p for the above reaction can be expressed by

$$K_p = \alpha^3 P / [2(1-\alpha)^2 (1 + \alpha/2)].$$

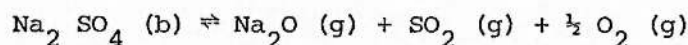
Calculation made using the values quoted in the JANAF tables yields a K_p value of 5.25×10^{-3} atmosphere at 1200 K. If the total pressure is again taken as 10^{-6} atmospheres, $(1 - \alpha)$ becomes 0.01 and it can be seen that NaO is completely dissociated at 1200 K.

Calculations performed on the equilibrium



reveal that at 1000 K the equilibrium constant for the reaction is of the order of 10^{-35} (atmospheres)². In other words this means that for pressures of the order of 10^{-6} atmospheres formation of Na_2S is completely negligible. The situation is even clearer at 1200 K.

The possibility of Sodium sulphate vaporising as shown in the mechanism (C)



is worth examining. Combining the data for $\text{Na}_2\text{O (g)}$ obtained from the results of Hildenbrand and Murad,¹²⁶ with those of JANAF, the calculated vapour pressure is several orders of magnitude lesser than observed here. Further, as observed by Spitsyn and Shostak, the residue in the cell extracted with water at the end of the effusion experiment was found to be neutral. It is also important that Na_2O^+ ion has not been observed in the mass-spectral experiments. Hence it can be assumed that vaporisation

of sodium sulphate does not proceed by the mechanism (C).

The possibility of Na_2SO_4 (g) being present in the vapour phase, as observed in Kosugi's ¹⁰¹ as well as Kohl et al ¹²⁵ mass-spectral studies can be examined in the following way. Assuming a cuprite type crystal lattice for both sulphates then a Madelung constant of about 4.12 may be applied to Sodium sulphate in the solid state. Approximate value for the corresponding constant for the vapour phase monomer may be estimated using the simplified model of two positive ions each a distance r from the sulphate ion. This system gives rise to two attractive forces of $2e^2/r$ units each, and one repulsive force of $e^2/2r$ (assuming an intercationic distance of $2r$). The net-force produced is then $7e^2/2r$ units. The heat of aggregation of 2Na^+ (g) and SO_4^{2-} (g) to Na_2SO_4 (s) is in the ratio of 4.12 to 3.5 to the heat of aggregation of Na_2SO_4 (g) monomer. A rough value for the heat of sublimation from crystal lattice to gaseous monomer may therefore be obtained from $0.62 u/4.12$ where u is the relevant lattice energy. The lattice energy for Na_2SO_4 is 1948 kJ mol^{-1} which give heats of sublimation of 293 kJ mol^{-1} . This value is not far from the enthalpy of 331 kJ mol^{-1} found in this work and elsewhere. Hence it is possible that Na_2SO_4 (g) might be present in the vapour phase.

The partial pressure of Na_2SO_4 (g) over the solid sulphate was measured by the transpiration method which is discussed in the next section. As can be seen from figure VII the Cubicciotti's ¹⁰³ transpiration vapour pressure results obtained in an atmosphere of nitrogen agree very closely with those of the present effusion and transpiration work. The Knudsen vapour pressures of Kroger and Stratmann ⁹¹ obtained with a nickel cell are about two and one-half orders of magnitude higher than the present results. As contended by Cubicciotti, the presence of carbon as an impurity in the nickel cell could have generated larger pressures, and hence there is no basis for comparison with the present

results. The mass spectrometric results of Ficalora et al.¹⁰⁰ can be discarded likewise since they do not observe the Na_2SO_4^+ ion in their spectrum and their results might have been affected by the reaction of molten sulphate with the Alumina Container.

(C) Results of Transpiration experiments

The results of transpiration experiments obtained either in a dry nitrogen atmosphere or in mixtures of SO_2 and oxygen are given in table V and represented graphically in figure VI and compared with those of previous workers and the Knudsen effusion results of the present work in figure VII. The vapour pressure values obtained in a nitrogen atmosphere and calculated on the basis of mechanism (B) are related to the temperature by the following equation

$$\begin{aligned} \text{Log}_{10} [\text{P/torr}] [1200 - 1400 \text{ K}] = & -1.76 \pm 0.59 \times 10^4 \text{ K/T} \\ & + 2.69 \pm 0.43 \end{aligned}$$

The vapour pressures measured in an atmosphere of sufficient SO_2 (g) + O_2 (g) should be essentially those of Na_2SO_4 (g) since the SO_2 and O_2 would suppress the decomposition of sodium sulphate. The pressure of Na_2SO_4 (g) according to the present results can therefore be represented as follows

$$\text{Log}_{10} (\text{P/torr}) \quad 1300 - 1400 \text{ K} = -1.53 \pm 0.04 \times 10^4 \text{ K/T} + 1.56 \pm 0.30$$

DISCUSSION

As can be seen from the table V and figure VI and VII vapour pressure values obtained in an atmosphere of nitrogen agree closely with those of the Knudsen effusion technique. The ΔH calculated from the N_2 -transpiration slope is 337 kJ mol^{-1} , that is only about 6 kJ mol^{-1} higher than the Knudsen value. The pressures of Na_2SO_4 (g) are also presented in figure VI and the slope of the $\text{log}_{10} P$ vs $1/T$ plot for Na_2SO_4 (g) yields a ΔH value of $293.0 \text{ kJ mol}^{-1}$ for the reaction

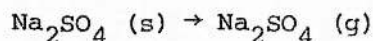


TABLE V

(B) SO₂ (g) + O₂ (g) as carrier gas

Temp K	Time min	O ₂ gas collected No. of moles	Total Acid equivalent moles	Total reducing power moles	Na ₂ SO ₄ collected mg	Log of pressure/ TORR
1289	1151	0.52	0.86	0.64	0.39	-2.68
1311	2185	0.87	1.42	0.92	1.16	-2.44
1342	1824	0.62	1.10	0.84	1.43	-2.21
1366	1200	0.54	0.96	0.60	2.29	-1.96
1395	1393	0.47	0.86	0.56	3.12	-1.77
1412	1449	0.58	0.74	0.48	4.48	-1.63

moles of SO₂ = $\frac{1}{2}$ value in column 4

moles of O₂ = value in column 3 + $\frac{1}{2}$ value in column 4 - $\frac{1}{2}$ value in column 5

TABLE V

SODIUM SULPHATE MOLECULAR WEIGHT (142.05)

(A) Nitrogen as Carrier Gas

Temp K	Time Min	No of moles of N ₂ collected	Na ₂ SO ₄ collected mg	Log ₁₀ P/torr
1301	1160	0.929	0.411	-202
1350	1245.5	0.958	1.19	-1.58
1408	1159	0.928	4.41	-0.99
1426	2060	1.650	11.26	-0.84

FIG. VI. NO_2SO_4 . TRANSPIRATION RESULTS.

- [A]. THIS WORK. N_2 AS CARRIER GAS.
- [B]. THIS WORK. $\text{SO}_2 + \text{O}_2$ AS CARRIER GAS.
- [C]. JANAF. VALUES.

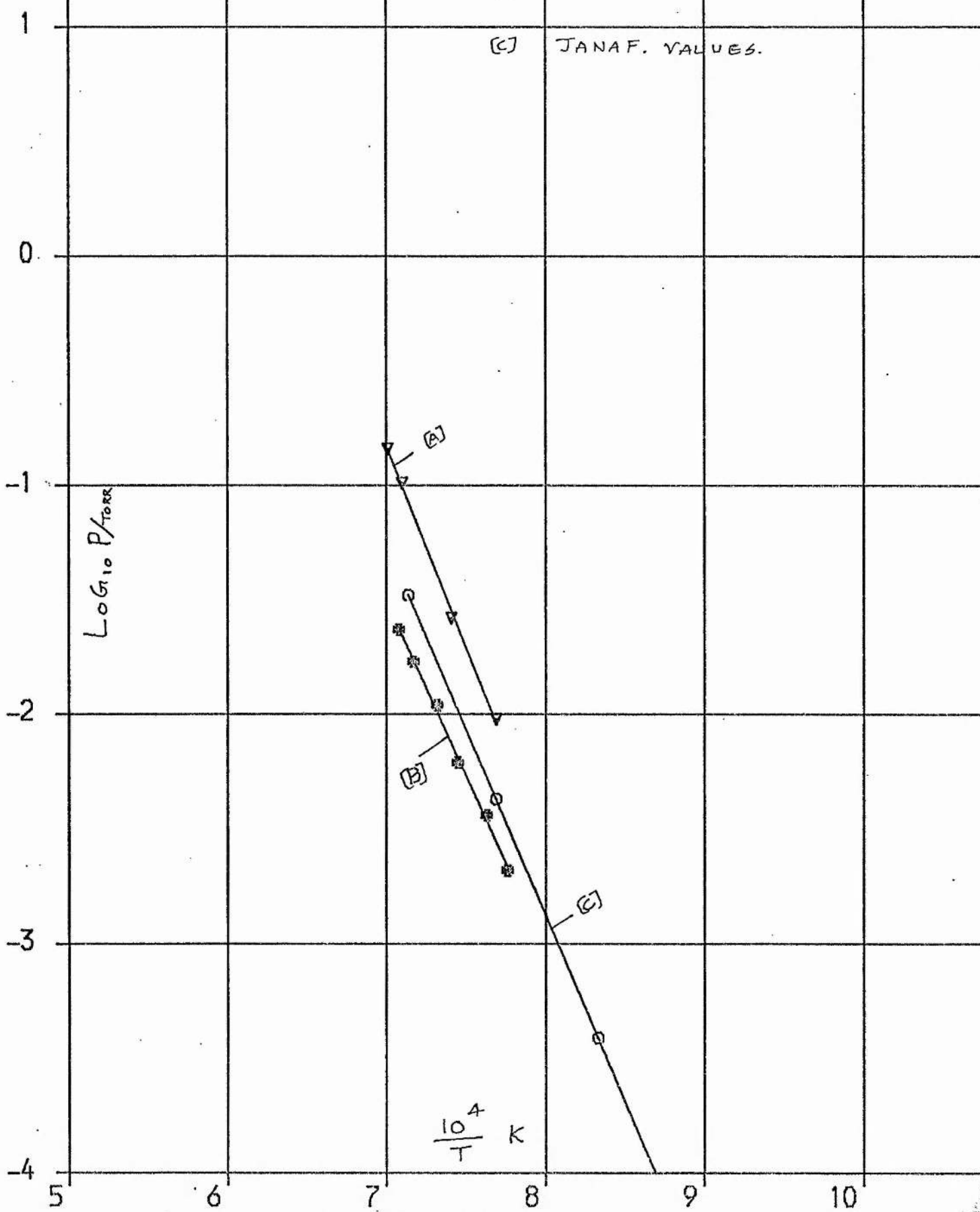
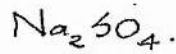
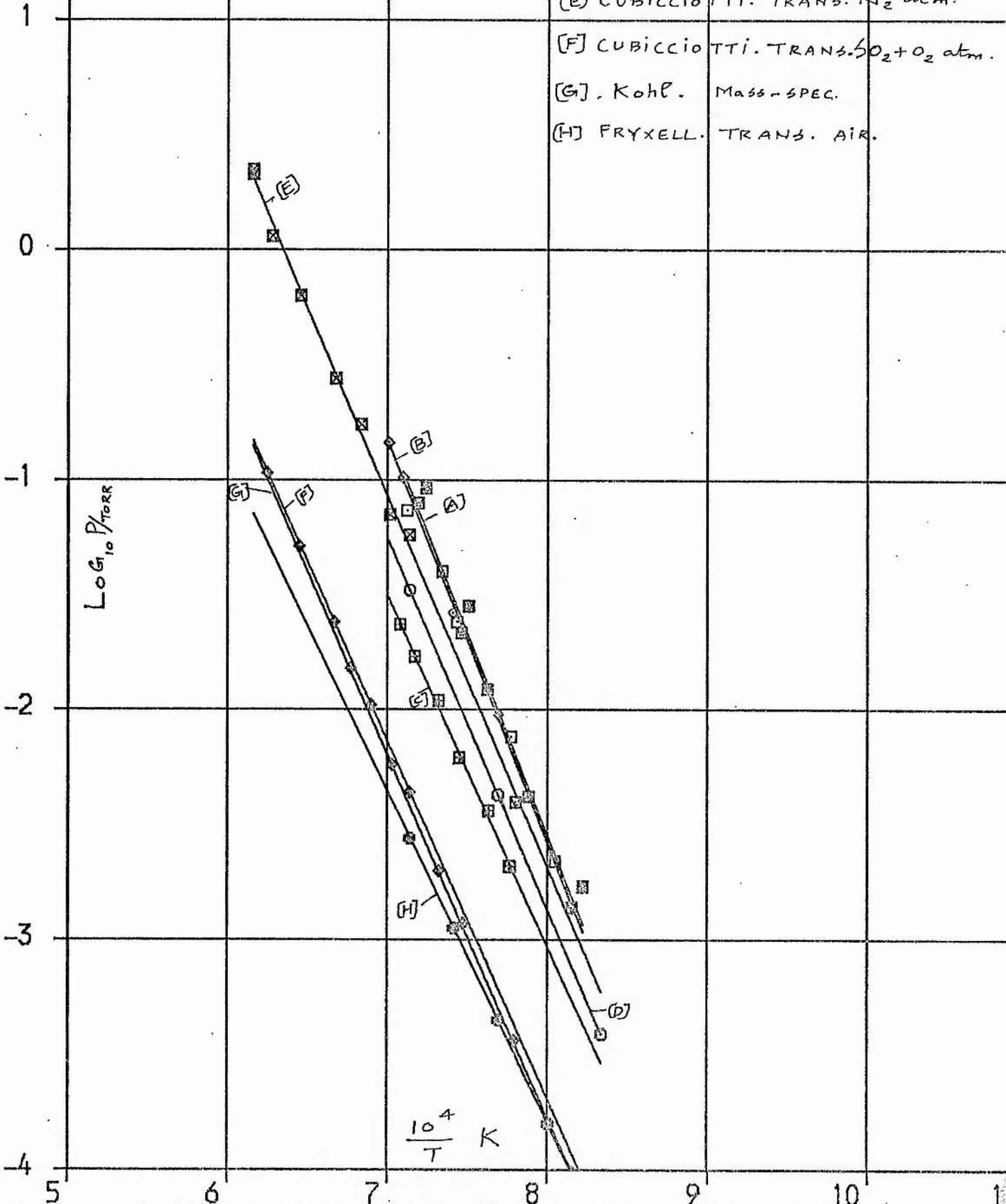


FIG. VII.

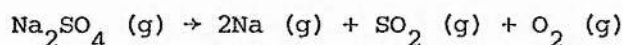


- [A]. THIS WORK. EFFUSION.
- [B]. THIS WORK. TRANS. N2 atm.
- [C] THIS WORK. TRANS. SO2 + O2 atm.
- [D] JANAF. VALUES
- [E] CUBICCIOTTI. TRANS. N2 atm.
- [F] CUBICCIOTTI. TRANS. SO2 + O2 atm.
- [G]. Kohl. MASS-SPEC.
- [H] FRYXELL. TRANS. AIR.

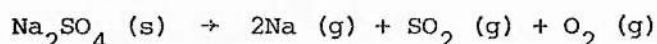
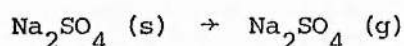


in excellent confirmation of the former lattice energy calculation.

But the strength of this agreement is somewhat weakened by the fact that there is no complete accord with the quoted values of the other workers, as shown below. If the pressures of Na_2SO_4 (g) obtained in an atmosphere of SO_2 (g) + O_2 (g) mixture are added to the total pressures calculated from JANAF values for the reaction



one obtains the value of pressure nearly equal to the pressures obtained in the Nitrogen transpiration and Knudsen effusion experiments. It is therefore consistent to conclude that the higher pressures of Knudsen effusion and transpiration results in N_2 atmospheres compared with the JANAF values are due to the presence of Na_2SO_4 (g) in the vapour phase. While the ΔH of the reaction to form Na_2SO_4 (g) estimated from the results of the present work, namely 292 kJ mol^{-1} , agrees well with the theoretically calculated value of 293 kJ mol^{-1} (from the lattice energy), the values reported by Cubicciotti,¹⁰³ Fryxell et al¹²⁷ and Kohl et al¹²⁵, 297 kJ mol^{-1} , 304 kJ mol^{-1} and 276 kJ mol^{-1} respectively are also in good agreement. Despite this concordance in ΔH however, the Na_2SO_4 vapour pressure values of all these workers agreed with each other closely, while the present results are about 3 to 4 times higher than theirs. However, the overall agreement of the present results with the previous worker's within the experimental error, lends strong support to the argument that decomposition of sodium sulphate proceeds by the following mechanisms

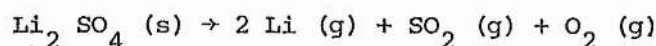


The enthalpy and standard entropy of sublimation at 1350 K, being the mid point of the experimental range, calculated from the slope and intercept of the present results are 292 kJ mol^{-1} and $120.9 \text{ J K}^{-1} \text{ mol}^{-1}$.

The values for the free energy functions of Na_2SO_4 (g) calculated and reported by Cubicciotti ¹⁰³ from molecular constant data and his experimental entropy of sublimation are presented in Appendix I.

(d) Lithium sulphate

The results of weight loss experiments on lithium sulphate are given in table VI and represented graphically in figure VIII. As in the case of sodium sulphate the vapour pressures were calculated in the first instance using an average molecular weight based on the following mode of decomposition



The vapour pressure relationship with temperature can be represented by the following equations.

Platinum cell

$$\text{Log}_{10} \text{ P/torr [1200 - 1400]K} = -1.45 \pm 0.08 \times 10^4 \text{ K/T} + 1.47 \pm 0.67$$

Spinel cell

$$\text{Log}_{10} \text{ P/torr [1200 - 1400 K]} = -1.42 \pm 0.13 \times 10^4 \text{ K/T} + 3.33 \pm 0.99$$

As can be seen from figure VIII the vapour pressure values obtained with the spinel cell are markedly higher to those obtained with the platinum cell.

In view of the fact that the spinel cell was attacked during the muffle furnace experiments, the results obtained with this cell in the present work as well as those of Powell and Wyatt¹⁰² obtained earlier in this laboratory are discarded and only the values obtained with platinum cells are taken into consideration for discussion purposes.

DISCUSSION

The JANAF thermochemical table does not list values of free energy functions for the solid sulphate. However, Denielou et al¹²⁸ have recently reported the high temperature heat capacity measurements for the solid lithium sulphate. The National Bureau of Standards¹²⁹ recommends a value of $-342.8 \text{ kcal mol}^{-1}$ ($1434.3 \text{ kJ mol}^{-1}$) for ΔH_{298}° . The absolute entropy

TABLE VI

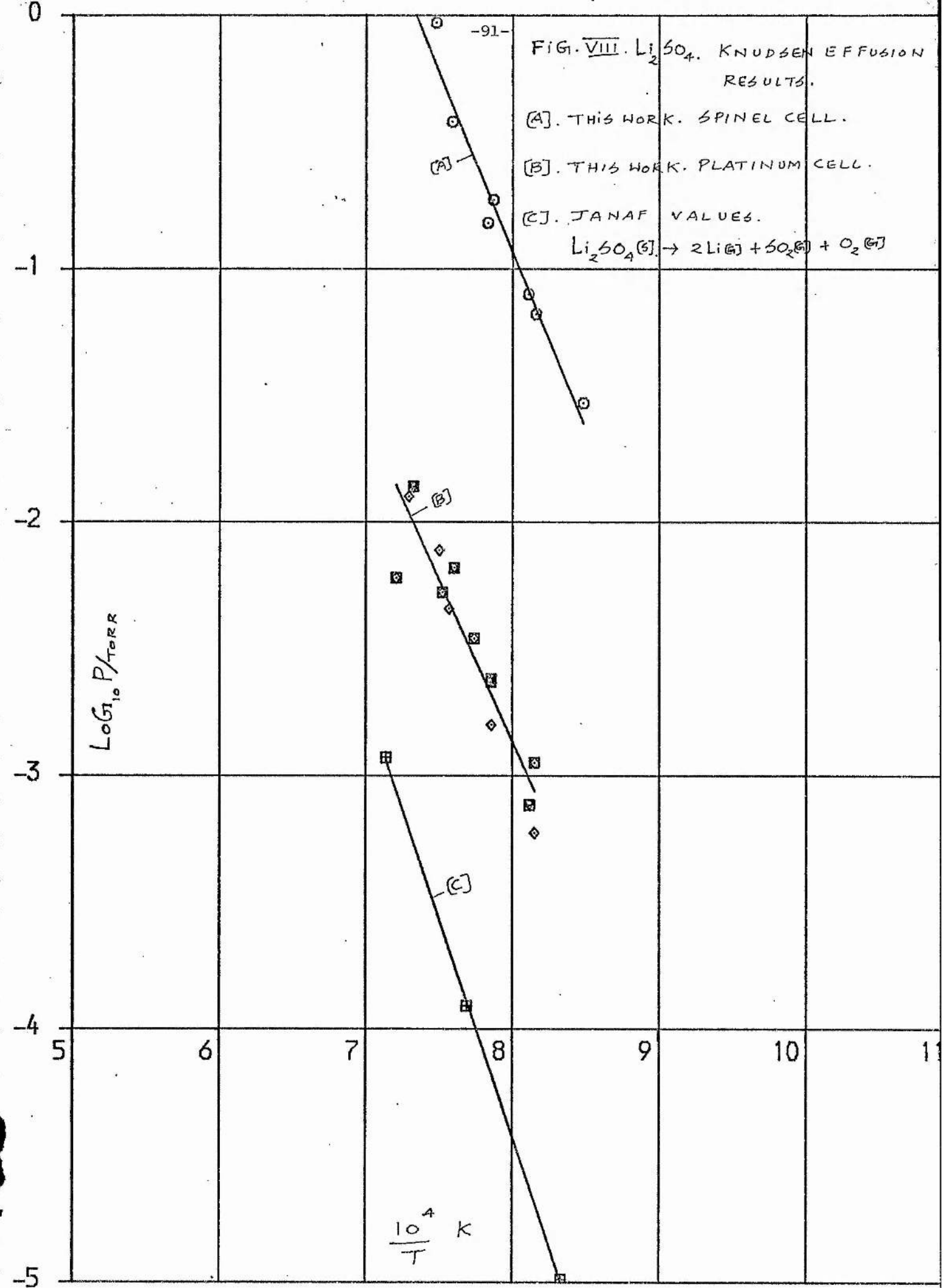
LITHIUM SULPHATE Li_2SO_4 (molecular weight 110)

Platinum cell

T/K	Rate of weight loss /mg min ⁻¹	P/torr	orifice area/cm ²
1227	1.23×10^{-3}	5.94×10^{-4}	<u>4.1×10^{-3}</u>
1273	3.23×10^{-3}	1.58×10^{-3}	
1321	9.12×10^{-3}	4.58×10^{-3}	
1333	1.54×10^{-2}	7.60×10^{-3}	
1371	2.48×10^{-2}	1.26×10^{-2}	
			<u>1.9×10^{-3}</u>
1228	1.06×10^{-3}	1.12×10^{-3}	
1273	2.17×10^{-3}	2.337×10^{-3}	
1292	3.20×10^{-3}	3.474×10^{-3}	
1329	5.88×10^{-3}	6.46×10^{-3}	
1351	6.29×10^{-3}	7.57×10^{-3}	
			<u>8.9×10^{-4}</u>
1232	3.308×10^{-4}	7.64×10^{-4}	
1273	1.02×10^{-3}	2.396×10^{-3}	
1315	2.76×10^{-3}	6.58×10^{-3}	
1365	5.69×10^{-3}	1.383×10^{-2}	

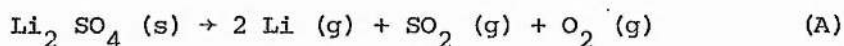
Spinel Cell

1226	2.884×10^{-2}	6.64×10^{-2}	<u>8.9×10^{-4}</u>
1271	8.00×10^{-2}	1.876×10^{-1}	
1317	1.60×10^{-1}	3.82×10^{-1}	
1337	3.80×10^{-1}	9.27×10^{-1}	
			<u>1.9×10^{-3}</u>
1179	2.86×10^{-2}	2.96×10^{-2}	
1233	7.5×10^{-2}	7.90×10^{-2}	
1277	1.41×10^{-1}	1.52×10^{-1}	

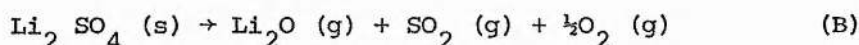


S_{298}° , calculated from the data provided by Latimer¹³⁰, is $29 \text{ cal K}^{-1} \text{ mol}^{-1}$ ($121.3 \text{ kJ mol}^{-1} \text{ K}^{-1}$). Combining these figures with heat capacity data, values for the various free energy functions were calculated and are presented in the Appendix II.

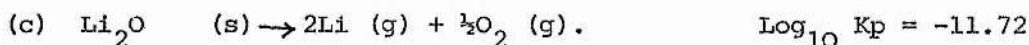
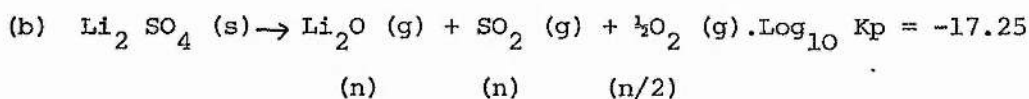
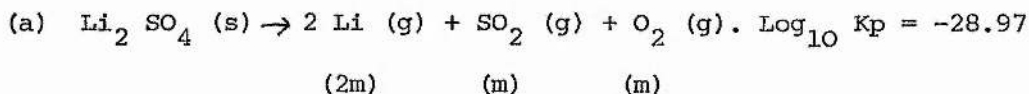
Calculations performed making use of the values quoted in Appendix II for Li_2SO_4 (s) and those of Li (g), SO_2 (g), and O_2 (g) from JANAF tables show that the total expected pressure at 1300 K for the following mode of decomposition



should be of the order of 1.63×10^{-7} atmospheres. However, the total pressure found in the present work is 5.01×10^{-6} atm, that is higher by more than an order of magnitude. This difference suggests that other modes of decomposition should be considered or that some other species are present in the gas phase. In view of the small ionic size of the lithium cation and its strong affinity for the oxygen ion, and also since the residue extracted with water at the end of the effusion experiment showed alkalinity, the following mode of decomposition was considered



calculations for vaporisation according to this reaction reveal that the total pressure should be of the order of 4.87×10^{-7} atmospheres, that is of the same order and in fact slightly higher than the total pressure expected from the decomposition scheme (A). This gives rise to the speculation that lithium sulphate solid might decompose by both the mechanisms (A) and (B). If this assumption is correct, then the expected values of the total pressure and the equilibrium partial pressures of the various species in the gas phase over solid lithium sulphate can be estimated by making use of the following equations and the respective K_p values at 1300 K:



then

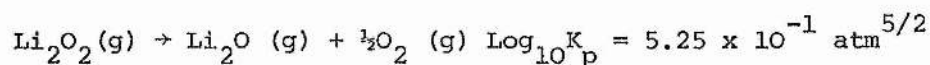
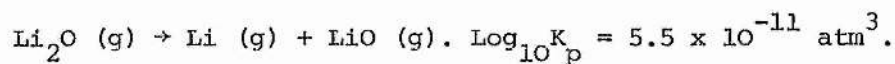
$$(a) p^2_{\text{Li}} \cdot p_{\text{SO}_2} \cdot p_{\text{O}_2} = 1.07 \times 10^{-29} \text{ atm}^4 = 4m^2 \times (n+m) \times (n/2+m) \text{ atm}^4.$$

$$(b) p_{\text{Li}_2\text{O}} \cdot p_{\text{SO}_2} \cdot p_{\text{O}_2}^{1/2} = 5.62 \times 10^{-18} \text{ atm}^{5/2} = n \times (n+m) \times (n/2+m)^{1/2} \text{ atm}^{5/2}.$$

$$(c) p^2_{\text{Li}} \cdot p_{\text{O}_2}^{1/2} / p_{\text{Li}_2\text{O}} = 1.91 \times 10^{-12} \text{ atm}^{3/2} = (4m^2 \times (n/2 + m)^{1/2} / n) \text{ atm}^{3/2}$$

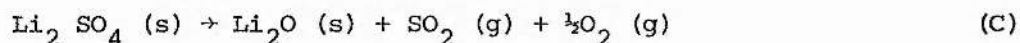
The symbols n and m stand for the number of moles of gaseous products formed by the first two reactions. By successive approximation, e.g. by assuming initially that $n/2 \approx m$ or $n/2 \gg m$, the values for n and m calculated were 13×10^{-8} and 1.5×10^{-8} respectively.

Substituting these values in the above equations yields a total pressure of 3.89×10^{-7} atm., which is again far below the observed Knudsen pressure. Further, if Lithium oxide is present as a solid phase, the equilibrium pressure of $\text{Li}_2\text{O} (g)$ at 1300 K calculated from the JANAF data should be 1.26×10^{-8} atm. Since the experimental pressure is higher than this value by an order of magnitude, if the JANAF $\text{Li}_2\text{O} (g)$ figures are reliable, it follows that $\text{Li}_2\text{O} (s)$ must be present in the system and that the species $\text{Li}_2\text{O} (g)$ can only be present to a very small and calculable extent (e.g.) 0.01×10^{-6} atm at 1300 K. These calculations also rule out the possibility of the presence of appreciable Li (g) in the gas phase. The pressure of both $\text{Li}_2\text{O} (g)$ and Li (g) can of course be calculated as minor corrections if required. Similarly calculations performed for the following reactions at 1300 K.



rule out the possibility of the presence of LiO (g) and Li₂O₂ (g) in the gas phase.

In view of the fact that the residue in the Knudsen cell when extracted with water at the end of the experiment showed alkalinity, the most favoured mode of decomposition according to the forgoing calculations is as follows



The total pressure at 1300 K would be 1.1×10^{-6} atm according to the calculations. This is only lower by a factor of 3 than the experimental Knudsen pressure when calculated using an approximate average molecule weight of 53.3. In view of the good agreement obtained between the Knudsen and other techniques in the case of sodium sulphate, it is most likely that the remaining difference is real and therefore requires explanation. As indicated earlier, the possibility of LiO (g), Li₂O (g), Li (g) being present in the gas phase have been ruled out. There still remains the possibility of Li₂SO₄ (g) however, i.e. monomer in the gas phase, which is now regarded as a prominent species in the cases of K₂SO₄, Rb₂SO₄, Cs₂SO₄ and which is now presented in this thesis as of greater importance in the case of Na₂SO₄ than was formally thought. In the transpiration experiments, which will be discussed later, the presence of lithium was observed in the vapour and estimated by the atomic absorption spectroscopy to be of the order of magnitude expected for congruent evaporation in the Knudsen technique. In view of this conclusion that the mode (C) takes place to some extent, while (A) and (B) are of very minor importance, the presence of lithium in the amount estimated by atomic absorption spectroscopy drives us to the conclusion that Li₂SO₄ (g) is not only an significant species

but must be the dominant species in our system. Mode (D) must therefore be very important :



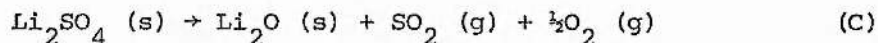
An approximate calculation performed, as in the case of Sodium sulphate, yields a value of 310 kJ mol^{-1} for the heat of sublimation into $\text{Li}_2\text{SO}_4 \text{ (g)}$. The ΔH calculated from the Knudsen slope yields a value of 277 kJ mol^{-1} which may be regarded as in satisfactory agreement in view of the uncertainties in the theoretical estimate, and gives additional support for the presence of $\text{Li}_2\text{SO}_4 \text{ (g)}$ monomer in the gas phase.

(E) Results of Transpiration experiments

The discussion of the results of Knudsen weight loss experiment rules out the possibility of most of the lithium containing species in the gas phase except $\text{Li}_2\text{SO}_4 \text{ (g)}$ monomer. Hence the transpiration data were used to calculate the equilibrium pressures of $\text{Li}_2\text{SO}_4 \text{ (g)}$ at various temperatures over the solid sulphate and presented in table VII and represented graphically along with the Knudsen effusion pressures in figure IX. The vapour pressure dependence on temperature can be expressed by the following equation.

$$*\text{Log}_{10} P/\text{torr} (1200 - 1300 \text{ K}) = -0.955 \pm 0.06 \times 10^4 \text{ K/T} + 0.12 \pm 0.46$$

As can be seen from the figure IX the equilibrium vapour pressure of $\text{Li}_2\text{SO}_4 \text{ (g)}$ is in fair agreement with the Knudsen effusion pressure calculated on the basis of a molecular weight appropriate to mode (C). If the pressure of $\text{Li}_2\text{SO}_4 \text{ (g)}$ is added to the total pressure expected (calculated from JANAF data) from the following mode of decomposition



the agreement is slightly worse. However, the Knudsen pressures were calculated using an average molecular weight based on the mechanism (C). Since $\text{Li}_2\text{SO}_4 \text{ (g)}$ is now assumed to be present as a major constituent in the

TABLE VII

Lithium sulphate molecular weight (110)

NITROGEN AS CARRIER GAS

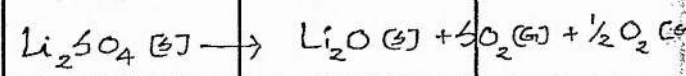
Temp K	Time min	No. of moles of N ₂ collected	Li ₂ SO ₄ collected mg	Log ₁₀ P/torr Li ₂ SO ₄ (g)
1333	1154	0.88	0.693	-2.26
1286	1362	1.20	0.466	-2.57
1258	1785	1.50	0.465	-2.67
1211	1475	1.30	0.188	-3.00

FIG. IX. Li_2SO_4 .

(A). THIS WORK. TRANS. N_2 atm.

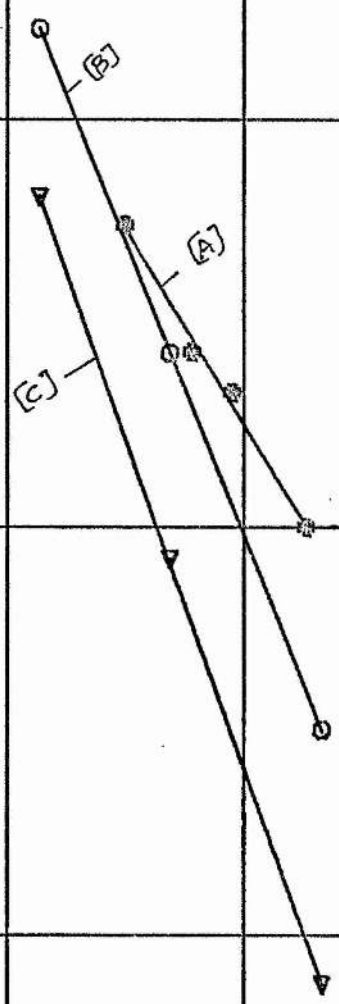
(B). THIS WORK. EFFUSION.

(C) JANAF. VALUES.

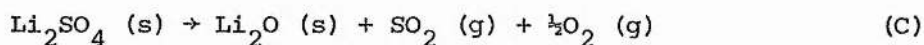


$\text{LOG}_{10} P/\text{TORR}$

$\frac{10^4}{T} \text{ K}$



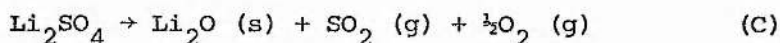
gas phase, the Knudsen equation needs modification in the molecular weight term. In fact the Knudsen pressures will be made more negative by a factor of about $-0.3 \log$ units. In other words, the recalculated Knudsen pressures would tend to be smaller than the transpiration values. The agreement between the Knudsen and transpiration results is therefore not good in detail, but a glance at figure IX shows that a much greater consistency has been introduced by the inclusion of the Li_2SO_4 (g) species, which brings the transpiration values down by a factor of 4 and makes the agreement much closer. In the present work the results obtained therefore seem to indicate that the lithium sulphate may be decomposing by the following routes:



However, a more realistic and quantitative treatment can be applied to the experimental data of the present work if authentic proof is obtained about the vapour phase composition over the solid lithium sulphate. The mass-spectral data of Ficalora et al ¹⁰⁰ cannot be considered very seriously, as pointed out by Cubicciotti, due to the fact that in the case of Na_2SO_4 no Na_2SO_4^+ ion was observed in their experiments, while the recent mass-spectral studies of Kohl et al have provided evidence for this. Further, the molten sulphate might have reacted with the Alumina container in a similar way to that found here in the spinel cell ($\text{MgO} + \text{Al}_2\text{O}_3$) experiments and led to erroneous results. Matrix isolation studies would very much help in clearing up the doubts about the vapour phase composition. In the present work, the transpiration technique indicates the Li_2SO_4 (g) pressure to be of the same order of magnitude as the Knudsen pressure but on close inspection, the transpiration results are still in fact slightly higher. Errors in the final results can arise in the transpiration method due to various reasons such as insufficient flow rate of the carrier gas, temperature

differences over the sample area which in turn can give rise to upsetting the equilibrium condition, etc. Although in the present work the transpiration technique gave satisfactory results with respect to Na_2SO_4 , in view of the disagreement in the case of Li_2SO_4 the transpiration results obtained for Li_2SO_4 are here regarded as only a qualitative proof for the presence of Li_2SO_4 (g) of the right magnitude in the gas phase over solid lithium sulphate. In the following paragraph, an attempt is made to calculate the equilibrium partial pressure of Li_2SO_4 (g) by making use of the Knudsen effusion data, which the author feels more reliable.

As mentioned earlier, the Knudsen effusion pressures calculated using on average molecular weight of 53.3 on the basis of the following mode of decomposition:



are higher by a factor of 3.45 times than the expected total pressures calculated, for the same mode of decomposition, on the basis of data listed in JANAF tables. The difference between the Knudsen and JANAF pressures at specific temperatures can then be regarded roughly to be the equilibrium partial pressure of Li_2SO_4 (g). However, the Knudsen pressure which should be considered now as the total pressure obtained due to some of the Li_2SO_4 (g) and mode (C) pressures was actually calculated in the first instance neglecting the Li_2SO_4 (g) contribution to the total pressure. Hence the Knudsen equation needs modification in the molecular weight term. A new approximate average molecular weight (i.e. better than the initial 53.3) was first calculated by taking into consideration the rough Li_2SO_4 (g) pressure obtained as described above, at a specific temperature and the fixed (JANAF) pressures due to SO_2 (g) and O_2 (g) over Li_2O (s) + Li_2SO_4 (s). This approximate average molecular weight was then substituted in the Knudsen equation and the total pressure recalculated. The fixed pressure expected from mode (C) at this temperature is now again deducted from

the recalculated Knudsen total pressure to yield a better equilibrium pressure of Li_2SO_4 (g). This better Li_2SO_4 (g) pressure is now again used in conjunction with the JANAF pressures of SO_2 (g) and O_2 (g) at the same temperature to calculate once more the average molecular weight and this to check whether the average molecular weight which we assumed earlier was the same. This approximation procedure was repeated until the average molecular weight changed no further. The Li_2SO_4 (g) equilibrium pressures obtained in this way over the experimental temperature range, along with the recalculated Knudsen total pressures, are plotted in figure IXa. The dependence of the Li_2SO_4 (g) pressure and the total pressure on temperature can be represented by the following equations:

$$\begin{aligned} * \log_{10} P \text{ Li}_2\text{SO}_4 \text{ (g) / torr} &= -1.364 \pm 0.003 \times 10^4 \text{ K/T} + 0.76 \pm 0.02 \\ &\text{(1200-1400 K)} \end{aligned}$$

$$\begin{aligned} * \log_{10} P \text{ total / torr} &= -1.466 \pm 0.001 \times 10^4 \text{ K/T} + 1.26 \pm 0.007 \\ &\text{(1200-1400 K)} \end{aligned}$$

The (1200-1400) slope of -1.36 from the first equation yields a value of 260 kJ mol^{-1} for the heat of sublimation of Li_2SO_4 (g) monomer at 1300 K. The standard entropy of sublimation (over the experimental temperature range) obtained from the intercept of the $\log_{10} P \text{ vs } 1/T$ plot and is $8.36 \text{ cal K}^{-1} \text{ mol}^{-1}$. If we now add the absolute entropy of the Li_2SO_4 (l) at 1300 K, which is $99.52 \text{ cal K}^{-1} \text{ deg}^{-1} \text{ mol}^{-1}$, to the above value, the resulting value $107.88 \text{ cal K}^{-1} \text{ mol}^{-1}$ is the absolute entropy of Li_2SO_4 (g) at 1300 K.

Molecular structure and thermodynamic functions for Li_2SO_4 (g)

It is necessary to generate a complete table of thermodynamic functions for a substance if calculations are to be made at temperatures outside

FIG. IXa.

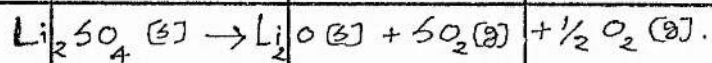
-101-
 Li_2SO_4 .

[A] THIS WORK. TRANS. N_2 atm. Li_2SO_4 (s)

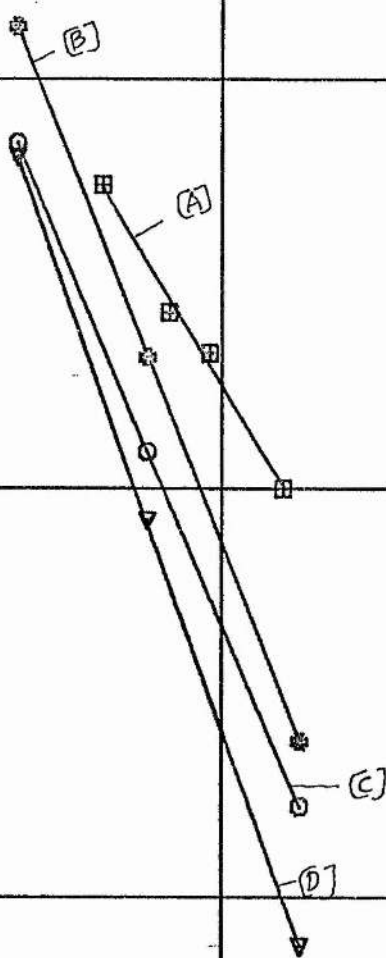
[B] THIS WORK. EFFUSION. TOTAL PRESSURE.

[C] THIS WORK. EFFUSION. Li_2SO_4 (s)

[D] JANAF. VALUES.



$\text{LOG}_{10} P/\text{TORR}$



$\frac{10^4}{T}$ K

the range of the experimental determination of the thermodynamic properties. The methods of statistical mechanics which are used to generate such a table for a gaseous molecule require the molecular geometry and other molecular constants to be specified.

However, an attempt was made to calculate the free energy functions for the Li_2SO_4 (g) in the following manner. The ΔH calculated from the slope of the $\text{Log}_{10} P$ torr Vs $1/T$ plot is constant over the entire experimental temperature range. Combining this value with the $-\left[\frac{\Delta G^{\circ}}{T}\right]$ values, calculated from the experimental vapour pressure at specific temperatures, one obtains the value for the standard entropy of sublimation of the Li_2SO_4 (g) at each temperature. If the standard entropy of the Li_2SO_4 (l) is now added to this standard entropy of sublimation at the respective temperature, the resulting value is the absolute entropy of the Li_2SO_4 (g). Since $\int_{T_1}^{T_2} \frac{C_p}{T} (g) dT$ gives the change in $S^{\circ} (g)$ between T_1 and T_2 , and if the $S_{T_1}^{\circ}$ is known at several temperatures then it should be possible to calculate the C_p of the gas from the expression, and hence to obtain an idea of the temperature dependence of the entropy.

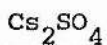
$$\text{If } C_p \text{ is constant, } C_p \int_{T_1}^{T_2} \frac{dT}{T} = S_2 - S_1 = C_p \ln \frac{T_2}{T_1}$$

However, the standard entropies of sublimation calculated from the experimental data were $21.04 \text{ J K}^{-1} \text{ mol}^{-1}$, $21.537 \text{ J K}^{-1} \text{ mol}^{-1}$, and $21.54 \text{ J K}^{-1} \text{ mol}^{-1}$ respectively at 1200 K, 1300 K and 1400 K. In other words the entropies of sublimation remain almost constant. This cannot be valid and evidently the data are not sufficiently precise for estimating the thermal properties of Li_2SO_4 (g) in this way. However, approximate values for the entropy of the gas can be calculated and they are presented below.

T/K	$S_T^{\circ} / \text{J K}^{-1} \text{ mol}^{-1}$
1200	116.596
1300	121.057
1400	124.74

(F) Caesium and Rubidium Sulphates

The weight loss results obtained for Caesium and Rubidium sulphates are given in tables VIII and IX, represented graphically in figures X and XI and compared with those of Cubbicciotti in figures XII and XIII. The vapour pressures of Caesium and Rubidium sulphates are related to the temperature by the following equations



Platinum cell

$$\log P/\text{torr} [1100 - 1270 \text{ K}] = -1.76 \pm 0.08 \times 10^4 \text{ K/T} + 3.60 \pm 0.475$$

Spinel cell

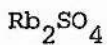
$$\log P/\text{torr} [1100 - 1270 \text{ K}] = -1.60 \pm 0.15 \times 10^4 \text{ K/T} + 3.36 \pm 1.26$$

In view of the fact, that the vapour pressure values obtained with platinum and spinel cell (see Figure X) agrees closely with each other within the experimental error, they have been treated as one set of data and represented by the following equation.

Platinum and spinel cell

*

$$\log P/\text{torr} [1150 - 1330 \text{ K}] = -1.70 \pm 0.06 \times 10^4 \text{ K/T} + 3.64 \pm 0.52$$



Platinum cell

$$\log P/\text{torr} [1150 - 1330 \text{ K}] = -1.59 \pm 0.05 \times 10^4 \text{ K/T} + 2.47 \pm 0.43$$

Spinel cell

$$\log P/\text{torr} [1150 - 1330 \text{ K}] = -1.593 \pm 0.08 \times 10^4 \text{ K/T} + 2.39 \pm 0.64$$

As in the case of Caesium sulphate the spinel and platinum cell vapour pressure values agreed with each other very closely (see figure XI) and therefore treated as one set of data and is represented by the following equation.

TABLE VIII

Caesium Sulphate Cs_2SO_4 (Molecular weight 361.87)Platinum cell

T/K	Rate of weight loss /mg min ⁻¹	P/torr	orifice area/cm ²
1110	4.25×10^{-3}	5.37×10^{-4}	<u>4.1×10^{-3}</u>
1146	1.33×10^{-2}	1.71×10^{-3}	
1193	4.60×10^{-2}	6.02×10^{-3}	
1239	1.43×10^{-1}	1.90×10^{-2}	
1265	3.47×10^{-1}	4.68×10^{-2}	
			<u>1.9×10^{-3}</u>
1108	1.81×10^{-3}	5.07×10^{-4}	
1153	6.90×10^{-3}	1.95×10^{-3}	
1201	2.50×10^{-2}	7.20×10^{-3}	
1246	7.27×10^{-2}	2.13×10^{-2}	
1270	1.86×10^{-1}	5.50×10^{-2}	
			<u>8.9×10^{-4}</u>
1102	6.93×10^{-4}	4.17×10^{-4}	
1141	3.33×10^{-3}	2.04×10^{-3}	
1191	1.17×10^{-2}	7.32×10^{-3}	
1233	3.64×10^{-2}	2.31×10^{-2}	
1269	1.77×10^{-1}	5.25×10^{-2}	

Spinel Cell

1112	3.37×10^{-3}	9.33×10^{-4}	<u>4.9×10^{-3}</u>
1151	8.92×10^{-3}	2.51×10^{-3}	
1195	5.00×10^{-2}	1.44×10^{-2}	
1243	6.66×10^{-2}	1.95×10^{-2}	
1266	3.26×10^{-1}	9.70×10^{-2}	
			<u>4.1×10^{-3}</u>
1103	5.50×10^{-3}	6.92×10^{-4}	
1143	1.80×10^{-2}	2.31×10^{-3}	
1195	6.45×10^{-2}	8.45×10^{-3}	
1237	1.90×10^{-1}	2.53×10^{-2}	

TABLE IX

Rubidium Sulphate Rb_2SO_4 (Molecular weight 267.03)

Platinum Cell

T/K	Rate of weight loss /mg min ⁻¹	P/torr	orifice area/cm ²
1159	9.259×10^{-4}	6.654×10^{-4}	<u>8.9×10^{-4}</u>
1203	2.44×10^{-3}	1.79×10^{-3}	
1237	6.25×10^{-3}	4.64×10^{-3}	
1286	1.90×10^{-2}	1.44×10^{-2}	
1337	5.71×10^{-2}	4.40×10^{-2}	
			<u>1.9×10^{-3}</u>
1165	1.78×10^{-3}	5.89×10^{-4}	
1217	5.55×10^{-3}	1.87×10^{-3}	
1268	1.94×10^{-2}	6.66×10^{-3}	
1311	5.45×10^{-2}	1.72×10^{-2}	
1332	7.76×10^{-2}	2.74×10^{-2}	
			<u>4.1×10^{-3}</u>
1161	3.23×10^{-3}	4.85×10^{-4}	
1207	8.82×10^{-3}	1.35×10^{-3}	
1251	2.70×10^{-2}	4.22×10^{-3}	
1299	9.19×10^{-2}	1.46×10^{-2}	
1329	1.61×10^{-1}	2.59×10^{-2}	

Spinel Cell

1177	4.17×10^{-3}	6.31×10^{-4}	<u>4.1×10^{-3}</u>
1223	1.62×10^{-3}	2.51×10^{-3}	
1275	3.81×10^{-2}	8.00×10^{-3}	
1315	1.14×10^{-1}	1.83×10^{-2}	
1330	1.53×10^{-1}	2.455×10^{-2}	

-106-
FIG. X. Cs_2SO_4

KNUDSEN EFFUSION RESULTS.

(A) SPINEL CELL

(B) PLATINUM CELL

$\text{LOG}_{10} P/\text{TORR}$

$\frac{10^4}{T} \text{ K}$

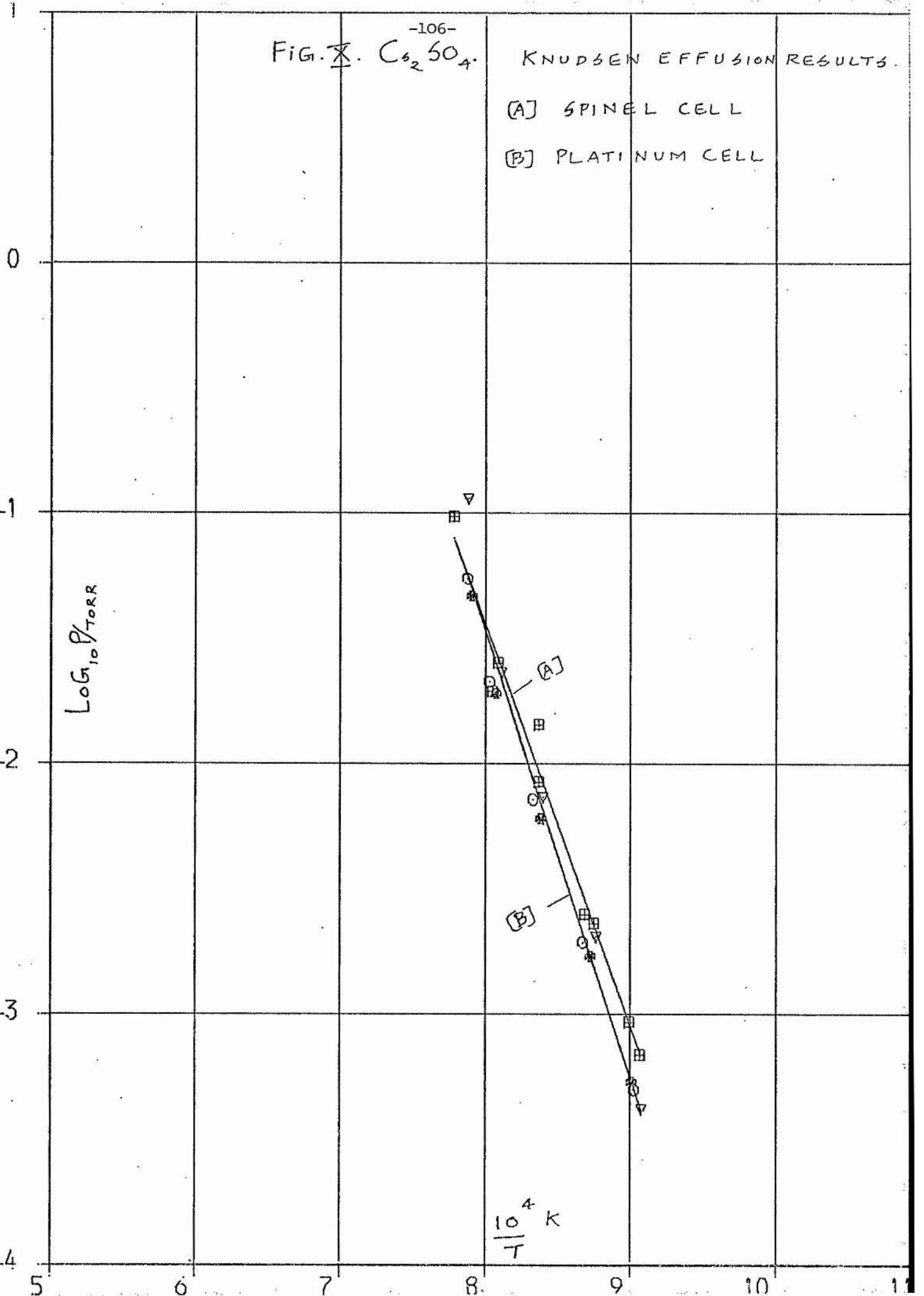


FIG. XI. Rb_2SO_4 . KNUDSEN EFFUSION RESULTS.

- (A) PLATINUM CELL.
- (B) SPINEL CELL.

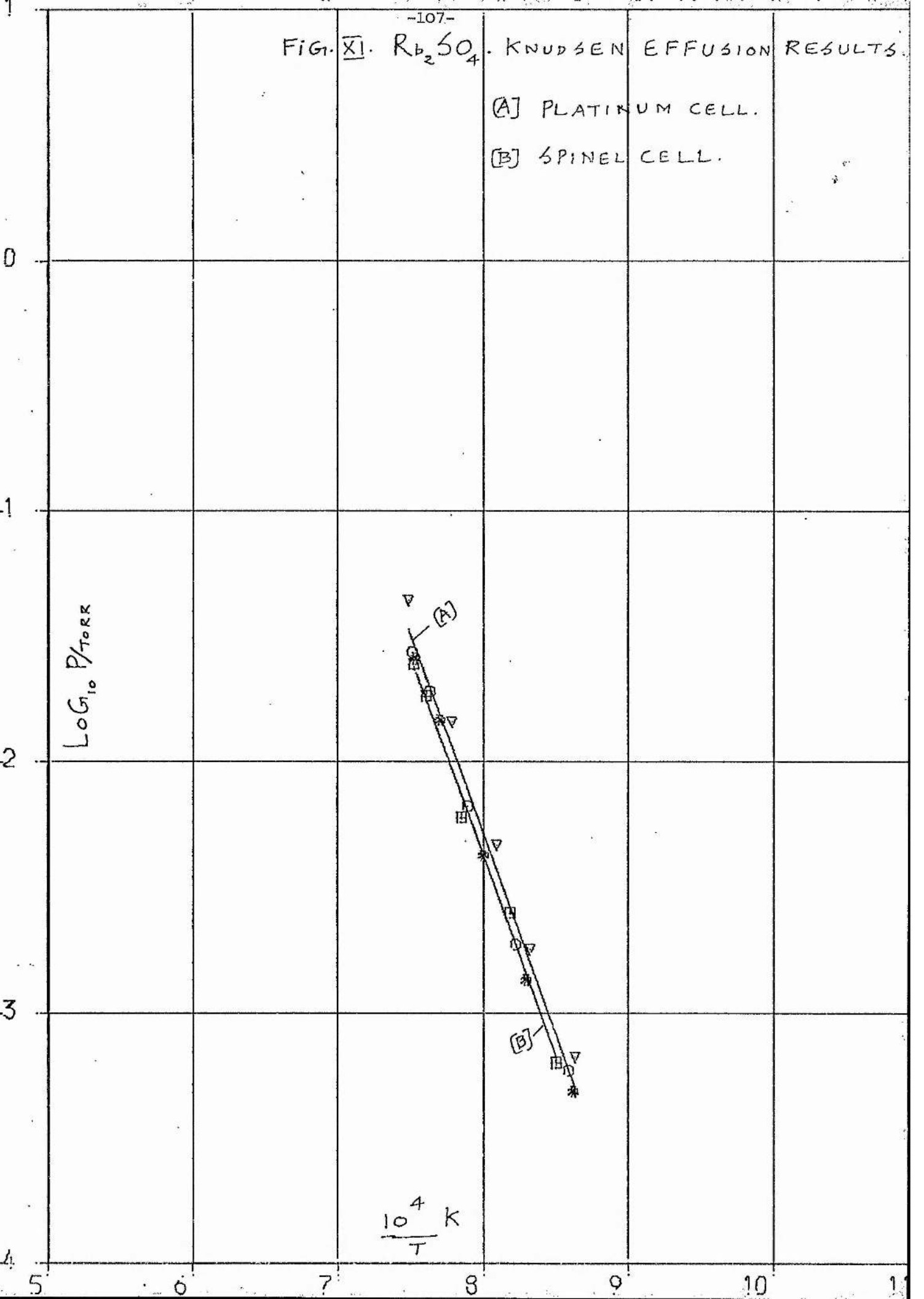


FIG. XII. Cs_2SO_4 .

(A). THIS WORK.

(B). CUBICCIOTTI.

$\log_{10} P/Torr$

$\frac{10^4}{T} K$

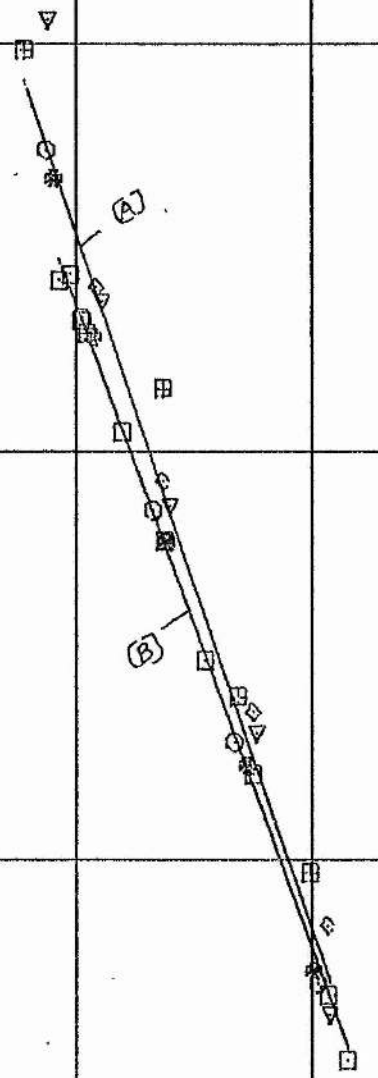


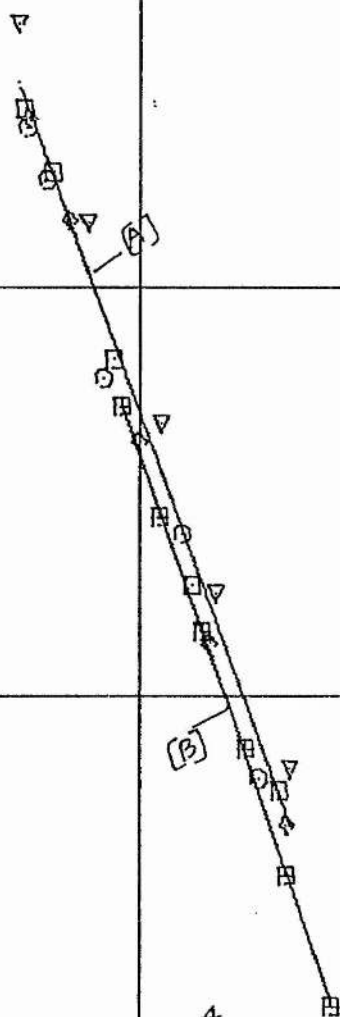
FIG. XIII.

-109-
 Rb_2SO_4 .

(A). THIS WORK

(B). CUBICCIOTTI

$\log_{10} P/Torr$



$1/T$

* Platinum and spinel cell

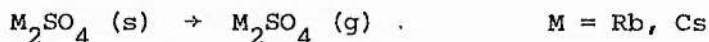
$$\log P/\text{torr} [1150 - 1330 \text{ K}] = -1.58 \pm 0.05 \times 10^4 \text{ K/T} + 2.42 \pm 0.39$$

DISCUSSION

The JANAF thermochemical table does not list the values of the free energy functions for the solid and monomeric gaseous species of Rubidium and Caesium sulphates. However, the absolute entropies of these salts at 298 K, the high temperature heat capacities, and the heat of formation of these salts at 298 K have been determined by Paukov et al¹³¹, Denielow et al¹³² and Skuratov et al¹³³ respectively. Cubicciotti¹⁰⁹ combining these data has calculated values for the free energy functions for the solid sulphates, and using the molecular constant data in conjunction with his experimental data estimated the values for the free energy functions for the gases. These values are given in Appendix 3 and 4.

The present vapour pressure results for Caesium and Rubidium sulphates obtained with Platinum and spinel cells are of the same order of magnitude and agree well with those of Cubicciotti¹⁰⁹ (see Figures XII and XIII).

The enthalpy of the decomposition reaction



per mole of the gaseous species calculated from the slopes of the $\log_{10} P/\text{torr}$ vs $1/T$ plot are 325.1 ± 11.5 kJ and 304.0 ± 9.6 kJ for Caesium and Rubidium respectively. However, Cubicciotti reports a value of 302.8 kJ and 326.4 kJ respectively. The enthalpy of the above decomposition reaction calculated theoretically by taking into consideration the thermodynamic data of the solid and gaseous sulphates (see appendix 3 and 4) and that of the gaseous alkali atoms, SO_2 and O_2 should be 313.8 kJ and 315.1 kJ for Caesium and Rubidium sulphates. The values obtained in this work agrees closely with these values within the experimental error.

Cubicciotti¹³⁴ has adopted the following Σ plot method to obtain the value of ΔH_{298}° and ΔS_{298}° for Na_2SO_4 (g).

$$\frac{\Delta G_T^{\circ}}{T} = -R \ln K = \frac{\Delta H_T^{\circ}}{T} - \Delta S_T^{\circ}$$

$$\frac{\Delta G_T^{\circ}}{T} = \frac{\Delta H_{298}^{\circ}}{T} + \Delta \left(\frac{\Delta H_T^{\circ} - H_{298}^{\circ}}{T} \right) - \Delta S_{298}^{\circ} - \Delta (S_T^{\circ} - S_{298}^{\circ})$$

Define

$$\Sigma' = R \ln K - \Delta \left(\frac{H_T^{\circ} - H_{298}^{\circ}}{T} \right) + \Delta (S_T^{\circ} - S_{298}^{\circ})$$

Therefore also

$$\Sigma' = \frac{\Delta H_{298}^{\circ}}{T} - \Delta S_{298}^{\circ}$$

A plot of Σ' vs $1/T$ should be a straight line whose slope gives ΔH_{298}° directly and whose intercept is ΔS_{298}° . In practice, one adds to a measured value of $R \ln K$, at a given temperature, the quantity $\Delta (S_T^{\circ} - S_{298}^{\circ}) - \Delta \left(\frac{H_T^{\circ} - H_{298}^{\circ}}{T} \right)$ obtained by interpolation from tabular data. The free energy functions for gaseous sulphates calculated from molecular constant data and reported by Cubicciotti are given in Appendix III and IV. Combining these values with the experimental pressures of Cubicciotti yields the following values for the enthalpies and entropies of sublimation at 298 K.

$$\text{Cs}_2\text{SO}_4, \Delta H_{298} = 340.2 \text{ kJ mol}^{-1}, \Delta S_{295}^{\circ} = 209.2 \text{ J K}^{-1} \text{ mol}^{-1}$$

$$\text{Rb}_2\text{SO}_4, \Delta H_{298} = 366.9 \text{ kJ mol}^{-1}, \Delta S_{298}^{\circ} = 217.2 \text{ J K}^{-1} \text{ mol}^{-1}$$

A similar treatment of the present data gives

$$\text{Cs}_2\text{SO}_4, \Delta H_{298} = 355.6 \text{ kJ mol}^{-1}, \Delta S_{298}^{\circ} = 224.7 \text{ J K}^{-1} \text{ mol}^{-1}$$

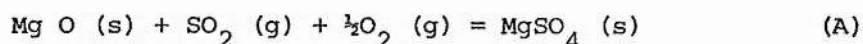
$$\text{Rb}_2\text{SO}_4, \Delta H_{298} = 341.0 \text{ kJ mol}^{-1}, \Delta S_{298}^{\circ} = 199.8 \text{ J K}^{-1} \text{ mol}^{-1}$$

Cubicciotti,¹⁰⁹ neglecting the influence of entropy term, contends from his results that the smaller enthalpy of sublimation of Caesium sulphate compared to that of Rubidium sulphate is responsible for its greater vapour pressure. In contrast to the findings of Cubicciotti,¹⁰⁹ the present results require that the higher entropy factor of Caesium sulphate compared to that of Rubidium sulphate is responsible for the higher vapour pressure of the former and not the lower enthalpy of sublimation as contended by Cubicciotti.¹⁰⁹ The present results are somewhat different from those of Ficalora et al¹⁰⁰. At 1200 K the present values are about eight times as great and at 1100 K about 5.5 times greater than their values. The enthalpies of sublimation are about 20 KJ mol⁻¹ and 50.21 kJ mol⁻¹ higher than their values for Rubidium and Caesium sulphates. One possible explanation for this substantial difference in the results may according to Cubicciotti,¹⁰⁹ be sought in the temperature measurements of their mass-spectrometer results. The difference would be explained if the temperature of the coolest part of the cell was from 60 to 80 K lower than the temperature measured and the difference increased with temperature. Finally it can be concluded that the present results agrees fairly closely with those of Cubicciotti and the theoretical values within the experimental error.

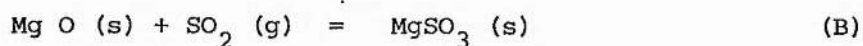
SUMMARY

The avowed intention of this study was to attempt to assess the relative merits of existing data on the vaporisation properties of the alkali metal sulphates. However, during the time this work was carried out, results from other laboratories were reported for Rubidium and caesium sulphate by the Knudsen effusion method and for sodium sulphate by the mass-spectral and transpiration methods. It can be said there has been more or less complete accord between the results published by other workers and this work regarding Caesium and Rubidium sulphates. With regard to sodium sulphate the effusion pressures of the present work were found to agree closely with the transpiration results obtained in a nitrogen atmosphere by Cubicciotti et al.¹⁰³. However, while the ΔH for the heat of sublimation of Na_2SO_4 (g) obtained in the present work is in close agreement with the values of Cubicciotti¹⁰³ and Kohl et al.¹²⁵, the actual vapour pressures are higher by a factor of 3. If the present results for Na_2SO_4 are examined in their own right, independently of the recent work of Cubicciotti et al, it can be seen that they are in complete harmony with the JANAF values and internally consistent with the present interpretation. They also agree with those of the other workers satisfactorily within the experimental error. It can also be said that Knudsen effusion method is capable of giving at least as reliable information as the transpiration, mass-spectral, and other methods. The situation with respect to lithium sulphate is not quite clear. Since no other laboratory has so far reported any information about the vaporisation properties of lithium sulphate, external comparison with the present results was not possible. However, a reasonably self-consistent interpretation has been advanced in the present work, and a more elaborate treatment will require more experimental information about the vapour phase composition.

As mentioned in the introduction this research arose out of the consideration currently being given to the corrosion suffered by magnesia bricks in the regenerator towers attached to glass making furnaces. In this concluding section this problem will be examined to see if the results of this work can help towards finding a consistent explanation of the observed effects. The worst corrosion takes place at about 1200 K and for this reason the calculations below have been carried out for 1000 K and 1200 K. (For the calculations of equilibrium constants which follow, all the free energy functions were taken from the JANAF thermochemical tables). Since it was initially believed that sulphur dioxide gas (formed by decomposition of Na_2SO_4 (s)) was responsible for the corrosion, the following mechanisms can be considered.



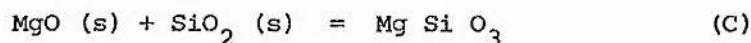
This reaction has a ΔH_{298}° of $-363.4 \text{ kJ mol}^{-1}$ and values of K_p of 2.3×10^4 (atmospheres) $^{-3/2}$ at 1000 K and 20.9 (atmospheres) $^{-3/2}$ at 1200 K.



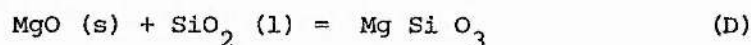
Free energy data are not available for Mg O (s) and $\text{Mg SO}_3 \text{ (s)}$. However ΔH_{298}° for this reaction is -110 kJ mol^{-1} which gives an idea that the ΔG_{298}° is also negative. Both these reactions show that attack of MgO by $\text{SO}_2 \text{ (g)}$ is possible. However, in the Knudsen effusion studies of calcium and magnesium sulphates, where $\text{SO}_2 \text{ (g)}$, $\text{O}_2 \text{ (g)}$ and $\text{SO}_3 \text{ (g)}$ were the decomposition products the results obtained with both the spinel and platinum cells were the same. If the spinel cell had been attacked by the sulphur oxide gases then the results obtained with this cell should be markedly different from those with the Platinum cell. Hence it can be concluded that corrosion of magnesia bricks in the glass-making furnace is not primarily due to the sulphur oxides. Further the Mg O in the furnace bricks is firmly bonded to the Al_2O_3 and hence is not completely free to be attacked by the sulphur oxides.

In this work it has been clearly shown that the magnesia or the spinel cell is attacked quite severely by the molten sodium sulphate (and also by Li_2SO_4). It is not quite clear whether the hot sodium metal atom, which is one of the decomposition products, or the molten sulphate, or the Na_2SO_4 (g) is chiefly responsible for the corrosion of the magnesia bricks. It is also not quite clear how Na (g) reacts with the magnesia brick. One possible route is that the sodium atom or the sodium-containing species would first break the strong bonding between MgO and Al_2O_3 in the "magnesia" brick and thereby expose the freed MgO for further attack by the sulphur oxides.

Once the MgO - Al_2O_3 bonding is broken and MgO is made free for attack, severe corrosion of the furnace walls can take place due to the strong reactivity of SiO_2 (which is present in the glass batch) towards MgO.



$\Delta H_{298}^{\circ} = -37.6 \text{ kJ mol}^{-1}$ $-\frac{\Delta G^{\circ}}{T}$ is about $35.11 \text{ J mol}^{-1} \text{ K}^{-1}$ at 1000 K and $28.42 \text{ J deg}^{-1} \text{ mol}^{-1}$ at 1200 K.



$\Delta H_{298}^{\circ} = -45.1 \text{ kJ mol}^{-1}$. $-\frac{\Delta G^{\circ}}{T}$ is about $37.58 \text{ J K}^{-1} \text{ mol}^{-1}$ at 1000 K and $29.97 \text{ J K}^{-1} \text{ mol}^{-1}$ at 1200 K.



$\Delta H_{298}^{\circ} -64.4 \text{ kJ mol}^{-1}$. $-\frac{\Delta G^{\circ}}{T}$ is about $62.78 \text{ J mol}^{-1} \text{ K}^{-1}$ at 1000 K and $51.75 \text{ J K}^{-1} \text{ mol}^{-1}$ at 1200 K.



$\Delta H_{298}^{\circ} -71.9 \text{ kJ mol}^{-1}$. $-\frac{\Delta G^{\circ}}{T}$ is about $65.25 \text{ J mol}^{-1} \text{ K}^{-1}$ at 1000 K and $53.29 \text{ J mol}^{-1} \text{ K}^{-1}$ at 1200 K. Reactions (C) - (F) represent pathways by which Mg SiO_3 and Mg_2SiO_4 could be formed by hot SiO_2 from the furnace coming into contact with "magnesia" bricks. It can be seen that all these

reactions are feasible. It is therefore reasonable to conclude that the Na (g) from sodium sulphate or Na_2SO_4 (l or s) itself rather than oxides of sulphur, is mainly responsible for the initial attack on the "magnesia" bricks which could subsequently be attacked further vigorously by both the sulphur oxides and the silicate.

This work has also proved that sodium sulphate vaporises by both simple volatilisation and dissociative mechanisms. The amount of Na_2SO_4 (g) that could be present at the glass making furnace temperatures can also be calculated from the present results.

II CALCIUM AND MAGNESIUM SULPHATE

The results of Knudsen weight loss experiments, obtained with platinum and spinel cells, are given in tables X and XI and represented graphically in figures XIV - XVII. As can be seen from the figures and tables the vapour pressure values obtained with spinel and platinum cells were in close agreement with each other. Both calcium and magnesium sulphate vapour pressures were dependent on the Knudsen orifice area, thereby indicating that these substances have low accommodation co-efficient. The equilibrium vapour pressures of both calcium and magnesium sulphates were calculated using the values obtained with a platinum cell and making use of the Whitman and Motzfeld²³ equation mentioned in the introduction,

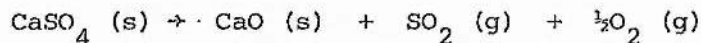
$$P_m = P_{eq} - \left(\frac{1}{\alpha} + \frac{1}{W_A} - 2 \right) P_m f$$

Plotting P_m versus $P_m f$ for constant temperature and varying ratio of f (that is different hole sizes) a straight line results, with the slope $-\left(\frac{1}{\alpha} + \frac{1}{W_A} - 2 \right)$ and intercept for $f = 0$ equal to P_{eq} . For a cell of about equal diameter and height, which is the same in the present work, W_A is about 0.5 so that $\frac{1}{W_A}$ and 2 cancel each other. The expression for the slope therefore simplifies to yield $-\frac{1}{\alpha}$

(a) CALCIUM SULPHATE

The weight loss results for calcium sulphate obtained with both spinel and platinum cells are presented in table X. The spinel cell vapour pressure values are plotted against $\frac{1}{T}$ and presented graphically along with the values of Dewing and Richardson¹¹⁴ in figure XIV. The platinum cell vapour pressure values, along with the equilibrium pressures obtained by extrapolation of these values together with those of Dewing and Richardson¹¹⁴ are presented graphically in figure XV. The vapour pressures were calculated using an average molecular weight of 53.3 in the Knudsen equation. This value for the molecular weight was a mean

value based on the following mode of decomposition



The apparent vapour pressure relationship with temperature can be represented by the following equations corresponding to the different orifices employed.

Spinel Cell

Log (P_{10}/torr) [1200 - 1445 K] :

orifice area

$$8.9 \times 10^{-4} \text{ cm}^2 \text{ --: } -2.14 \pm 0.03 \times 10^4 \text{ K/T} + 4.28 \pm 0.2$$

$$1.9 \times 10^{-3} \text{ cm}^2 \text{ --: } -2.13 \pm 0.02 \times 10^4 \text{ K/T} + 4.02 \pm 0.14$$

$$4.1 \times 10^{-3} \text{ cm}^2 \text{ --: } -2.21 \pm 0.05 \times 10^4 \text{ K/T} + 3.94 \pm 0.41$$

Platinum cell

Log $_{10} [P/\text{torr}]$ [1200 - 1445 K]

orifice area

$$8.9 \times 10^{-4} \text{ cm}^2 \text{ --: } -2.06 \pm 0.02 \times 10^4 \text{ K/T} + 3.92 \pm 0.17$$

$$1.9 \times 10^{-3} \text{ cm}^2 \text{ --: } -2.08 \pm 0.02 \times 10^4 \text{ K/T} + 3.71 \pm 0.13$$

$$4.1 \times 10^{-3} \text{ cm}^2 \text{ --: } -2.12 \pm 0.06 \times 10^4 \text{ K/T} + 3.56 \pm 0.43$$

The true equilibrium pressures estimated by extrapolation of the platinum cell values can be represented by the following equation

$$^* \text{Log}_{10} [P/\text{torr}] [1200 - 1445 \text{ K}] = -1.78 \pm 0.02 \times 10^4 \text{ K/T} + 3.82 \pm 0.06$$

TABLE X

Calcium Sulphate CaSO₄ (Molecular weight 136.2)

Platinum Cell

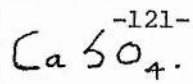
T/K	Rate of weight loss /mg min ⁻¹	P/torr	Orifice area/cm ²
			8.9 x 10 ⁻⁴
1241	2.66 x 10 ⁻³	4.43 x 10 ⁻³	
1263	4.73 x 10 ⁻³	7.94 x 10 ⁻³	
1281	8.33 x 10 ⁻³	1.41 x 10 ⁻²	
1335	3.33 x 10 ⁻²	5.75 x 10 ⁻²	
1386	1.33 x 10 ⁻¹	2.34 x 10 ⁻¹	
1437	4.43 x 10 ⁻¹	7.94 x 10 ⁻¹	
			<u>1.9 x 10⁻³</u>
1238	2.77 x 10 ⁻³	2.11 x 10 ⁻³	
1256	4.90 x 10 ⁻³	3.76 x 10 ⁻³	
1299	1.60 x 10 ⁻²	1.25 x 10 ⁻²	
1347	5.71 x 10 ⁻²	4.54 x 10 ⁻²	
1391	1.90 x 10 ⁻¹	1.53 x 10 ⁻¹	
1445	6.45 x 10 ⁻¹	5.31 x 10 ⁻¹	
			<u>4.1 x 10⁻³</u>
1247	4.70 x 10 ⁻³	1.64 x 10 ⁻³	
1279	8.95 x 10 ⁻³	3.16 x 10 ⁻³	
1297	1.74 x 10 ⁻²	6.19 x 10 ⁻³	
1347	6.67 x 10 ⁻²	2.42 x 10 ⁻²	
1392	2.42 x 10 ⁻¹	8.92 x 10 ⁻²	
1449	8.91 x 10 ⁻¹	3.35 x 10 ⁻¹	

Spinel Cell

T/K	Rate of weight loss /mg min ⁻¹	P/torr	Orifice area/cm ²
			<u>8.9 x 10⁻⁴</u>
1231	2.46 x 10 ⁻³	4.08 x 10 ⁻³	
1259	5.62 x 10 ⁻³	9.44 x 10 ⁻³	
1293	1.43 x 10 ⁻²	2.43 x 10 ⁻²	
1340	5.71 x 10 ⁻²	9.88 x 10 ⁻²	
1396	2.67 x 10 ⁻¹	4.71 x 10 ⁻¹	
1420	4.47 x 10 ⁻¹	7.94 x 10 ⁻¹	

1244	4.65×10^{-3}	3.55×10^{-3}	<u>1.9×10^{-3}</u>
1266	9.19×10^{-3}	7.08×10^{-3}	
1293	1.90×10^{-2}	1.48×10^{-2}	
1332	6.15×10^{-2}	4.86×10^{-2}	
1385	2.50×10^{-1}	2.01×10^{-1}	
1412	4.62×10^{-1}	3.76×10^{-1}	
			<u>4.1×10^{-3}</u>
1234	3.57×10^{-3}	1.24×10^{-3}	
1253	6.40×10^{-3}	2.24×10^{-3}	
1289	1.82×10^{-2}	6.39×10^{-3}	
1330	6.67×10^{-2}	2.40×10^{-2}	
1390	4.00×10^{-1}	1.47×10^{-1}	
1425	7.13×10^{-1}	2.66×10^{-1}	

FIG. XIV.



EFFUSION

RESULTS.

SPINEL CELL

[A] ORIFICE

AREA. $8.9 \times 10^{-4} \text{ cm}^2$

[B] " "

" . $1.9 \times 10^{-3} \text{ cm}^2$

[C] " "

" . $4.1 \times 10^{-3} \text{ cm}^2$

[D] DEWING AND RICHARDSON.
[DTA] RESULTS.

$\text{LOG}_{10} P_{\text{TORR}}$

$\frac{10^4}{T} \text{ K}$

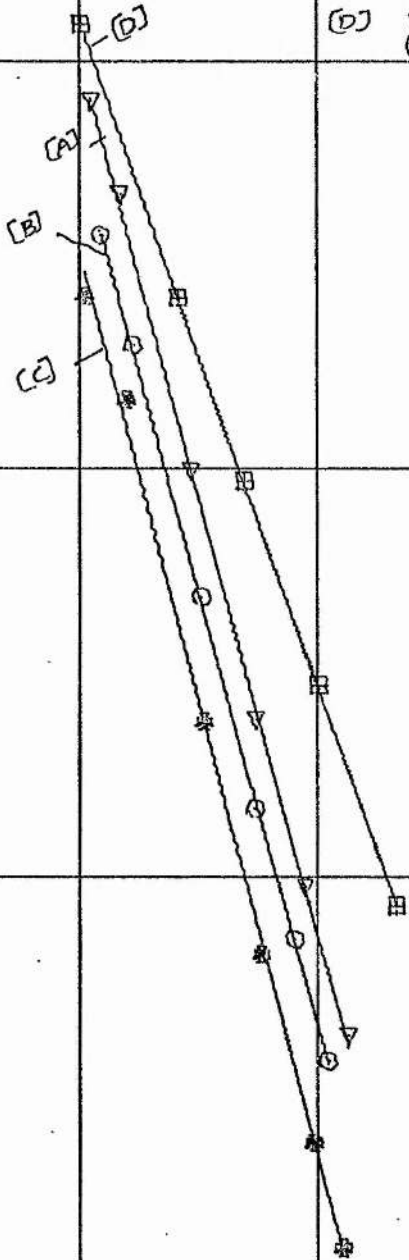


FIG. XV. CaSO_4 . EFFUSION RESULTS. PLATINUM CELL.

ORIFICE AREA.

(A) $8.9 \times 10^{-4} \text{ cm}^2$

(B) $4.1 \times 10^{-3} \text{ cm}^2$

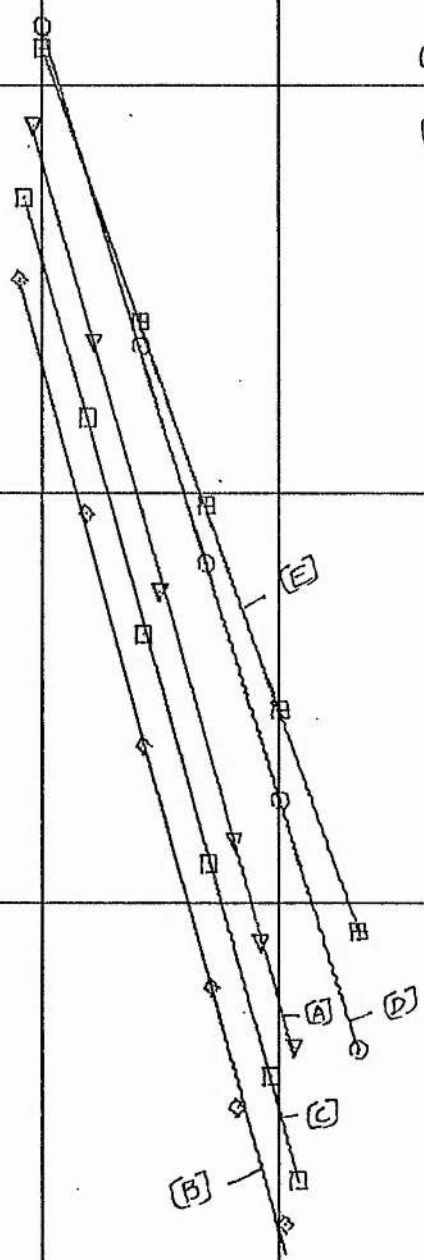
(C) $1.9 \times 10^{-3} \text{ cm}^2$

(D) 'PT' CELL EXTRAPOLATED VALUES

(E) DEWING AND RICHARDSON [DTA] VALUES.

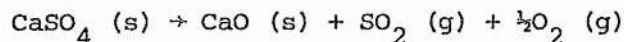
$\text{LOG}_{10} P/P_{\text{TORR}}$

$\frac{10^4}{T} \text{ K}$



DISCUSSION

The most favoured mode of decomposition is



Kurt and Stern¹¹⁰ report that the expected total pressure at 1200 K for decomposition in this way should be 2.29×10^{-5} atmospheres and should be accompanied by a ΔH value of 492 kJ mol^{-1} . The pressure found in this work at 1200 K is 1.02×10^{-5} atmospheres, which is in fairly close agreement with the value quoted. The experimental ΔH calculated from the slope yields a value of 510 kJ mol^{-1} . Combining the experimental enthalpy with the heat capacity terms gives a value at ΔH_{298}° 514 kJ mol^{-1} as against the value of 500 kJ mol^{-1} quoted in the Kurt and Stern's report NBS-7. This close agreement with the values quoted in the literature gives strong support to the conclusion that the vaporisation of calcium sulphate proceeds according to the mechanism indicated earlier. As can be seen from the figures the pressures quoted by Dewing and Richardson¹¹⁴ are of the same order of magnitude and agree fairly well with the values reported in this work. However the enthalpy value of the above reaction quoted by Dewing and Richardson¹¹⁴ was about 28 kJ mol^{-1} lower than that calculated from the report NBS-7¹¹⁰ and about 46 kJ mol^{-1} lower than the values obtained in the present work. The results obtained by the static method by Marchal,¹¹³ and Zawadski¹¹² for dehydrated gypsum, and anhydride and by the dynamic method by Tschappat and Piece¹¹¹ require the enthalpy of the decomposition reaction as 260 kJ mol^{-1} and 404 kJ mol^{-1} respectively. The static and dynamic methods are not as sensitive as the Knudsen effusion method and hence the differences in the values obtained by these methods are quite understandable.

The only anomaly requiring explanation is the dependence of the vapour pressure on the area of the Knudsen effusion orifice. It might

help to clarify the situation if each measured pressure is to be regarded as a pseudo-equilibrium vapour pressure which approaches the true equilibrium vapour pressure as the area of the orifice approaches zero. Thus the equilibrium vapour pressure, as mentioned earlier, was estimated by using the platinum cell values in combination with the Motzfeld²³ equation

$$P_m = P_{eq} - \left(\frac{1}{\alpha} + \frac{1}{W_A} - 2 \right) P_m f$$

The relation, due to Motzfeld,

$$\frac{P_{eq}}{P_m} = 1 + f/\alpha$$

where f is the ratio of the orifice area to cell cross section area may now be used to determine a value for α , the accommodation or vaporiation co-efficient. This was done for 1300 K, being the mid-point of the experimental range and yielded an average value of 2.1×10^{-1} for the vaporisation co-efficient.

(b) Magnesium Sulphate

The weight loss results for magnesium sulphate obtained with spinel and platinum cells are presented in table XI. The spinel cell vapour pressure values are plotted against $1/T$ and presented graphically in figure XVI. The platinum cell vapour pressure values, along with the equilibrium pressures obtained by extrapolation of these values, together with those of Dewing and Richardson¹¹⁴ are presented graphically in figure XVII. As in the case of calcium sulphate the vapour pressure values of the present work were calculated by using the average molecular weight of 53.3. The apparent vapour pressure dependence on temperature can be represented by the following expressions for the three different orifices employed.

Spinel Cell

$\text{Log}_{10} [P/\text{torr}][950 - 1150 \text{ K}]$:

orifice area

$$8.9 \times 10^{-4} \text{ cm}^2 \text{ --: } -1.09 \pm 0.01 \times 10^4 \text{ K/T} + 3.75 \pm 0.14$$

$$1.9 \times 10^{-3} \text{ cm}^2 \text{ --: } -1.08 \pm 0.06 \times 10^4 \text{ K/T} + 3.54 \pm 0.63$$

$$4.1 \times 10^{-3} \text{ cm}^2 \text{ --: } -1.08 \pm 0.05 \times 10^4 \text{ K/T} + 3.11 \pm 0.47$$

Platinum cell

$$8.9 \times 10^{-4} \text{ cm}^2 \text{ --: } -1.03 \pm 0.05 \times 10^4 \text{ K/T} + 3.56 \pm 0.44$$

$$1.9 \times 10^{-3} \text{ cm}^2 \text{ --: } -1.08 \pm 0.02 \times 10^4 \text{ K/T} + 3.63 \pm 0.24$$

$$4.1 \times 10^{-3} \text{ cm}^2 \text{ --: } -1.14 \pm 0.06 \times 10^4 \text{ K/T} + 3.48 \pm 0.58$$

Equilibrium pressures obtained by extrapolation of the platinum cell values can be represented by the following equation

$$* \text{Log}_{10} (P/\text{torr}) [950 - 1150 \text{ K}] = -1.06 \pm 0.01 \times 10^4 \text{ K/T} + 3.45 \pm 0.09$$

For extrapolation purposes the values obtained with the two smallest orifices having cross-section areas $8.9 \times 10^{-4} \text{ cm}^2$ and $1.9 \times 10^{-4} \text{ cm}^2$ were only used, since making use of the values obtained with the highest orifice area $4.1 \times 10^{-3} \text{ cm}^2$ for extrapolation purposes results in a marked departure from linearity. This was not the same in the case of calcium sulphate. Although no specific explanation could be given at this stage for this observation, an attempt is made at the end of the next section. Despite the fact that only two points were available for the Motzfeld orifice area plot the extrapolated results obtained are probably fairly reliable (or at least consistent) since they give rise to a satisfactory plot of $\log P$ against $1/T$. As a matter of fact that it is not unusual to use only two orifices for an extrapolation of this kind¹³⁶.

TABLE XI

Magnesium Sulphate MgSo₄ (Molecular weight 120.4)Platinum Cell

T/K	Rate of weight loss /mg min ⁻¹	P/torr	orifice area/cm ²
			<u>8.9 x 10⁻⁴</u>
954	5.44 x 10 ⁻³	7.94 x 10 ⁻³	
1009	2.11 x 10 ⁻²	3.16 x 10 ⁻²	
1054	5.33 x 10 ⁻²	8.18 x 10 ⁻²	
1107	2.00 x 10 ⁻²	3.14 x 10 ⁻¹	
1155	3.33 x 10 ⁻¹	5.35 x 10 ⁻¹	
			<u>1.9 x 10⁻³</u>
953	7.95 x 10 ⁻³	5.31 x 10 ⁻³	
1001	2.86 x 10 ⁻²	1.96 x 10 ⁻²	
1031	4.71 x 10 ⁻²	3.27 x 10 ⁻²	
1059	1.08 x 10 ⁻¹	7.61 x 10 ⁻²	
1107	2.67 x 10 ⁻¹	1.92 x 10 ⁻¹	
1153	6.66 x 10 ⁻¹	4.90 x 10 ⁻¹	
			<u>4.1 x 10⁻³</u>
1002	1.90 x 10 ⁻²	5.90 x 10 ⁻³	
1031	3.97 x 10 ⁻²	1.26 x 10 ⁻²	
1057	8.89 x 10 ⁻²	2.85 x 10 ⁻²	
1109	2.67 x 10 ⁻¹	8.71 x 10 ⁻²	
1136	3.64 x 10 ⁻¹	1.21 x 10 ⁻¹	

Spinel Cell

T/K	Rate of weight loss /mg min ⁻¹	P/torr	orifice area/cm ²
			<u>8.9 x 10⁻⁴</u>
957	4.59 x 10 ⁻³	6.71 x 10 ⁻³	
986	8.96 x 10 ⁻³	1.33 x 10 ⁻²	
1007	1.67 x 10 ⁻²	2.50 x 10 ⁻²	
1055	5.33 x 10 ⁻²	8.18 x 10 ⁻²	
1078	8.12 x 10 ⁻²	1.26 x 10 ⁻¹	
1103	1.33 x 10 ⁻¹	2.14 x 10 ⁻¹	
1151	3.33 x 10 ⁻¹	5.34 x 10 ⁻¹	

953	6.33×10^{-3}	4.23×10^{-3}	<u>1.9×10^{-3}</u>
1004	1.82×10^{-2}	1.25×10^{-2}	
1044	6.67×10^{-2}	4.67×10^{-2}	
1094	2.00×10^{-1}	1.43×10^{-1}	
1148	4.00×10^{-1}	2.93×10^{-1}	
			<u>4.1×10^{-3}</u>
959	5.75×10^{-3}	1.76×10^{-3}	
1004	1.56×10^{-2}	4.88×10^{-3}	
1055	6.66×10^{-2}	2.14×10^{-2}	
1104	1.82×10^{-1}	5.98×10^{-2}	
1149	3.33×10^{-1}	1.11×10^{-1}	

FIG. XVI. $MgSO_4$. EFFUSION RESULTS.
SPINEL CELL

ORIFICE AREA.

(A) $8.9 \times 10^{-4} \text{ cm}^2$

(B) $1.9 \times 10^{-4} \text{ cm}^2$

(C) $4.1 \times 10^{-3} \text{ cm}^2$

(D) DEWING AND RICHARDSON
(DTA) VALUES.

$\text{LOG}_{10} P/\text{TORR}$

$\frac{10^4}{T} \text{ K}$

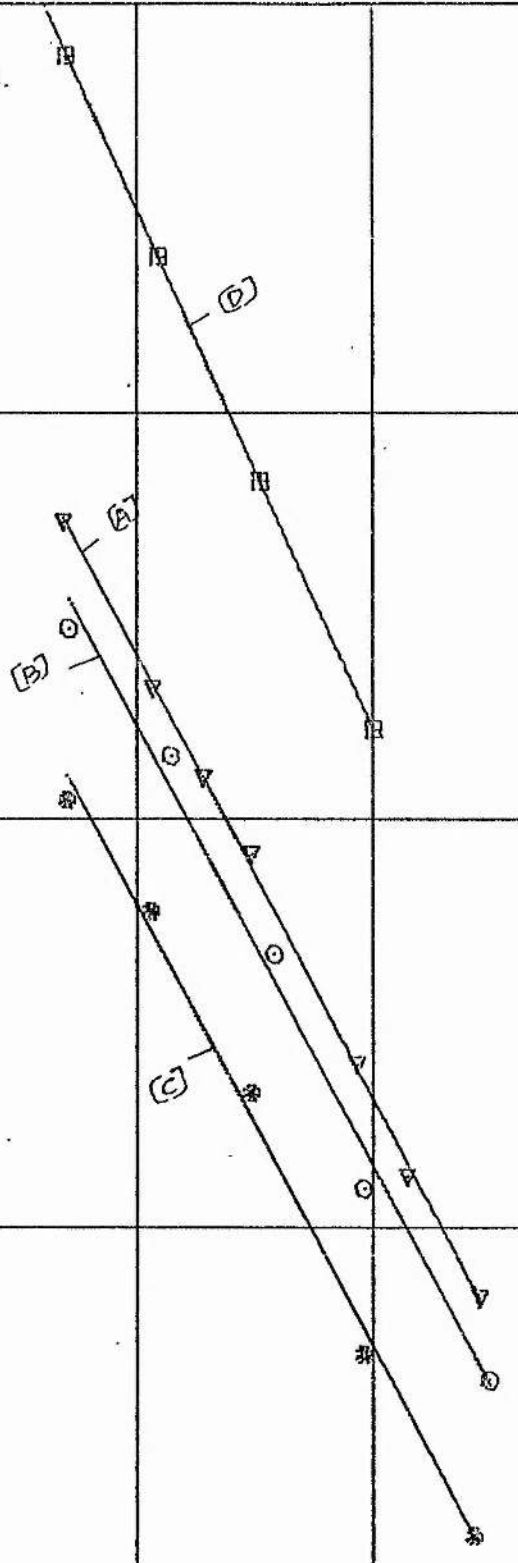


FIG. XVII. $MgSO_4$. EFFUSION RESULTS.
PLATINUM CELL.

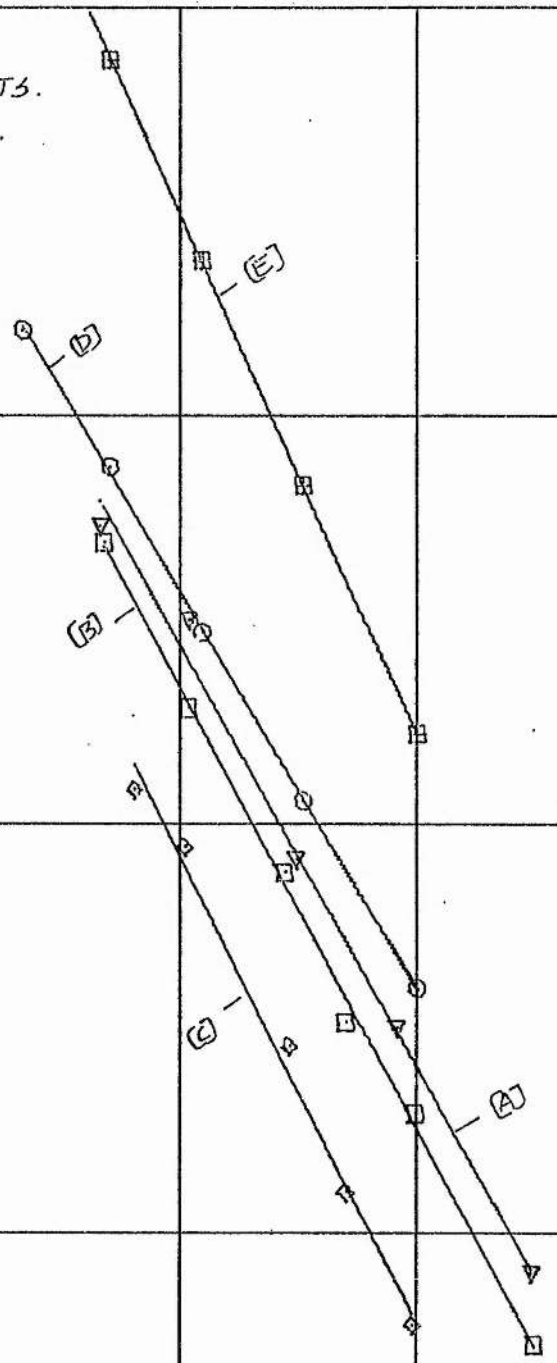
ORIFICE AREA

- (A) $8.9 \times 10^{-4} \text{ cm}^2$
- (B) $1.9 \times 10^{-3} \text{ cm}^2$
- (C) $4.1 \times 10^{-3} \text{ cm}^2$

- (D) 'PT' CELL EXTRAPOLATED VALUES
- (E) DEWING AND RICHARDSON (DTA) VALUES.

$\text{LOG}_{10} P/\text{TORR}$

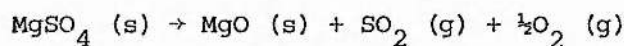
$\frac{10^4}{T} \text{ K}$



DISCUSSION

The values of various thermodynamic functions for magnesium sulphate listed in the JANAF thermochemical tables are based on the combination of the experimental results of Knopf and Staude¹²⁴ and the ΔC_p values for the corresponding CaSO_4 decomposition, there being no suitable heat capacity for MgSO_4 . There are various objections to the way in which Knopf and Staude¹²⁴ have handled their results, which will be dealt with in detail in the latter part of this section.

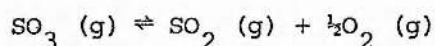
Assuming the values quoted in the JANAF thermochemical tables to be right, the following mode of decomposition,



should according to the calculations give a total pressure of 6×10^{-4} atmospheres at 1000 K and 4.7×10^{-2} atmospheres at 1200 K. It also should be accompanied by a ΔH value of $363.2 \text{ kJ mol}^{-1}$ at 1200 K. The pressure observed in this work at 1200 K is 4.0×10^{-3} atmospheres, that is lower than by an order of magnitude. The ΔH value calculated from the slope of the graph is found to be 304 kJ mol^{-1} which is again substantially lower than the JANAF value. However, it can be seen from the figure XVII, Dewing and Richardson's¹¹⁴ pressure at 1200 K is 3.0×10^{-2} atmospheres (again higher) but the ΔH value quoted by them, which is 364 kJ mol^{-1} is in very close agreement with the JANAF values. This close agreement is rather surprising in spite of the uncertainty in the ΔC_p values and the heat of α - β transition which has again been neglected.

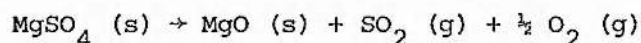
Pechkovsky's observation, which was mentioned in the introduction, clearly indicates that the primary decomposition product of magnesium sulphate in the experimental temperature range concerned is $\text{SO}_3 \text{ (g)}$. Then it can be argued that the pressures observed in this work correspond

mainly to SO_3 (g) as the sole decomposition product, while in the case of Dewing and Richardson's ¹¹⁴ experiments it can be assumed that kinetic equilibrium existed between SO_2 (g), O_2 (g) and SO_3 (g). The decomposition of the magnesium sulphate sample was detected by them only when the SO_3 (g) pressure of the sample equalled that of the SO_3 (g) pressure surrounding it. The SO_3 (g) pressures, calculated by using the SO_2 (g) and O_2 (g) pressures reported by Dewing and Richardson ¹¹⁴ and the K_p values for the following reaction, taken from the JANAF tables

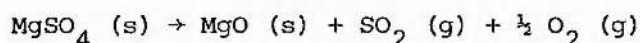


are 2.24×10^{-6} atmospheres ^{v/v} and 4.23×10^{-5} atmospheres ^{v/v} at 1000 K and 1100 K respectively. Upon substitution of a value of 80 for the molecular weight M in the Knudsen equation and combination with the weight loss values obtained with orifice area $8.9 \times 10^{-4} \text{ cm}^2$ the SO_3 (g) pressures calculated were 3.39×10^{-5} and 3.38×10^{-4} atmospheres at 1000 K and 1100 K respectively. The SO_3 pressures of this work, obtained with the highest orifice area, are thus an order of magnitude higher than Dewing and Richardson's ¹¹⁴ values. A similar treatment of the weight loss data obtained with the largest orifice area in the present work, namely $4.1 \times 10^{-3} \text{ cm}^2$, yields SO_3 (g) pressures of 7.08×10^{-6} and 7.7×10^{-5} atmospheres respectively at 1000 K and 1100 K. These values are only about 2.8 to 2.2 times higher than the SO_3 (g) pressures of Dewing and Richardson. This anomaly can be explained if SO_3 (g) tends to decompose to some extent depending upon such factors as the residence time of an SO_3 (g) molecule within the Knudsen cell, frequency of collision with the walls of the cell and the temperature. If the orifice were large enough, presumably Langmuir's ²⁰ free evaporation condition would be approached. It was therefore of interest to see if the largest orifice area in the present work was sufficiently large for this condition to have been attained.

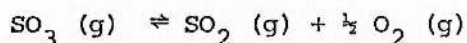
The results of a Langmuir's²⁰ experiment, from a sample surface area of $3.9 \times 10^{-1} \text{ cm}^2$, is listed in table XII and represented graphically in figure XVIII, will strengthen the above argument. The vapour pressures measured by Langmuir's method are lower than that of the Knudsen effusion pressures for the largest orifice area, thereby proving our earlier findings that the magnesium sulphate has a low accommodation co-efficient and that physical equilibrium is approached for the SO_3 decomposition even at the highest orifice area. If the mechanism of decomposition remains the same, that is,



then irrespective of the difference in the total pressures measured by the Langmuir's free evaporation and Knudsen effusion methods, both the methods should yield the same value for the ΔH of the above reaction when calculated from their slopes. However, the ΔH value calculated from Langmuir's slope is 221 kJ mol^{-1} as against the Knudsen ΔH value of 304 kJ mol^{-1} . This clearly indicates that the primary mode of decomposition cannot be represented by the following reaction



If the primary decomposition product is assumed to be $\text{SO}_3 (\text{g})$, on the basis of Pechkovsky's observations, and it decomposes completely in the Knudsen cell then the difference between enthalpies measured by the Langmuir and Knudsen method should correspond to the enthalpy of the reaction



The difference between the Langmuir and Knudsen enthalpies measured in this work is 83 kJ mol^{-1} which more or less corresponds to the enthalpy of the above reaction which is namely 96 kJ mol^{-1} . This small difference can be attributed to the incomplete dissociation of $\text{SO}_3 (\text{g})$. This whole

TABLE XII

MAGNESIUM SULPHATE (Molecular weight - 120.4)
Langmuir Results

T/K	Rate of weight loss /mg min ⁻¹	P/torr
1025	8.696 x 10 ⁻²	2.83 x 10 ⁻⁴
1070	1.80 x 10 ⁻¹	5.99 x 10 ⁻⁴
1113	3.50 x 10 ⁻¹	1.17 x 10 ⁻³
1155	5.70 x 10 ⁻¹	1.97 x 10 ⁻³

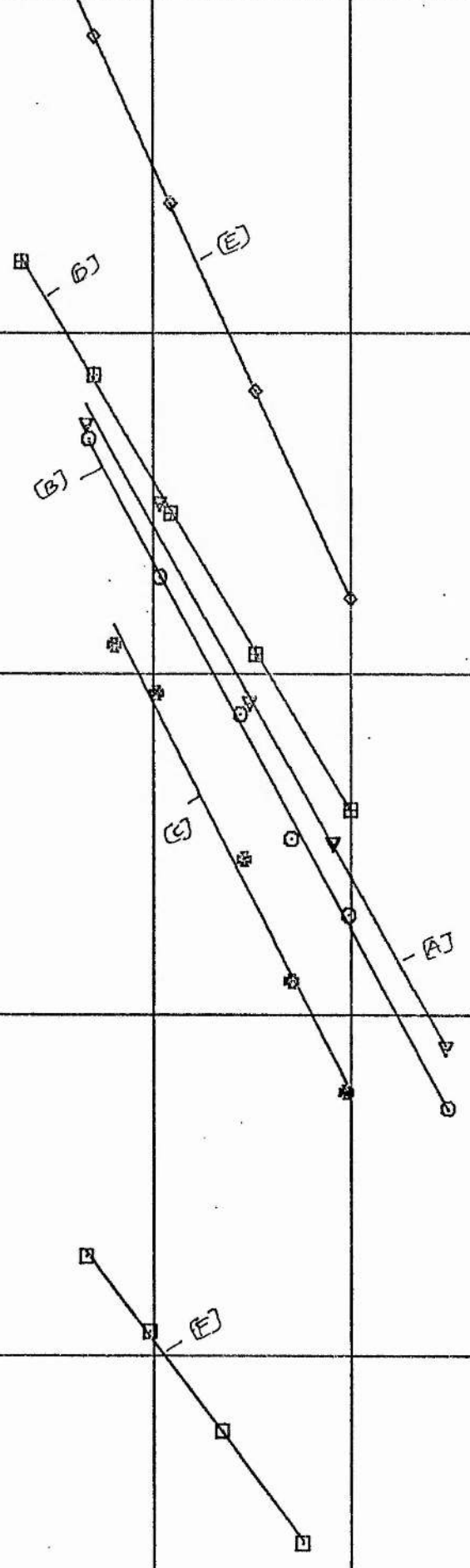
FIG. XVIII. $MgSO_4$.

ORIFICE AREA

- (A) $8.9 \times 10^{-4} \text{ cm}^2$
- (B) $1.9 \times 10^{-3} \text{ cm}^2$
- (C) $4.1 \times 10^{-3} \text{ cm}^2$
- (D) 'PE' CELL EXTRAPOLATED VALUES
- (E) DEWING AND RICHARDSON [DTA] VALUES
- (F) LANGMUIR RESULTS.

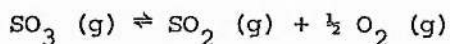
$\text{LOG}_{10} P/T_{\text{TORR}}$

$\frac{10^4}{T} \text{ K}$



argument also now explains the small positive difference in the SO_3 (g) equilibrium pressures calculated from Dewing and Richardson's¹¹⁴ and the present work for the largest orifice area.

Torsion effusion results of Cubicciotti¹³⁷ lends additional weight to the above argument. Cubicciotti finds that with the largest orifice areas the value for the molecular weight of the effusing species is 80, while with the smallest orifices, the molecular weight of the effusing species varies from 55 to 65. This is a clear proof that the SO_3 (g) in the primary product and dissociates in an approach to the following equilibrium within the Knudsen cell



to an extent depending on the residence time, temperature and the orifice area.

The Knudsen SO_3 (g) pressures (calculated for the largest orifice area $4.1 \times 10^{-3} \text{ cm}^2$) along with those of Dewing and Richardson are presented graphically in figure XIX. It can be seen from the figure that the SO_3 (g) pressures of the present work agree with those of Dewing and Richardson closely when extrapolated to high temperatures, while, the pressures are slightly higher at low temperatures. This is because the experimental temperature range of the Dewing and Richardsons' work (1200 - 1450 K) is much higher than ours (900 - 1150 K) and consequently when their SO_2 and O_2 pressures are extrapolated to lower temperatures for calculating SO_3 (g) pressures, the changes in heat capacity due to the phase changes have to be taken into account. However, as mentioned at the start of the discussion of this section, heat capacity values for MgSO_4 and MgO solids have not been reported. Dewing and Richardson have detected and reported a phase transition in MgSO_4 (s) at 1273 K in their differential thermal analysis experiments. In spite of the lack of heat capacity values and reliable data about the phase

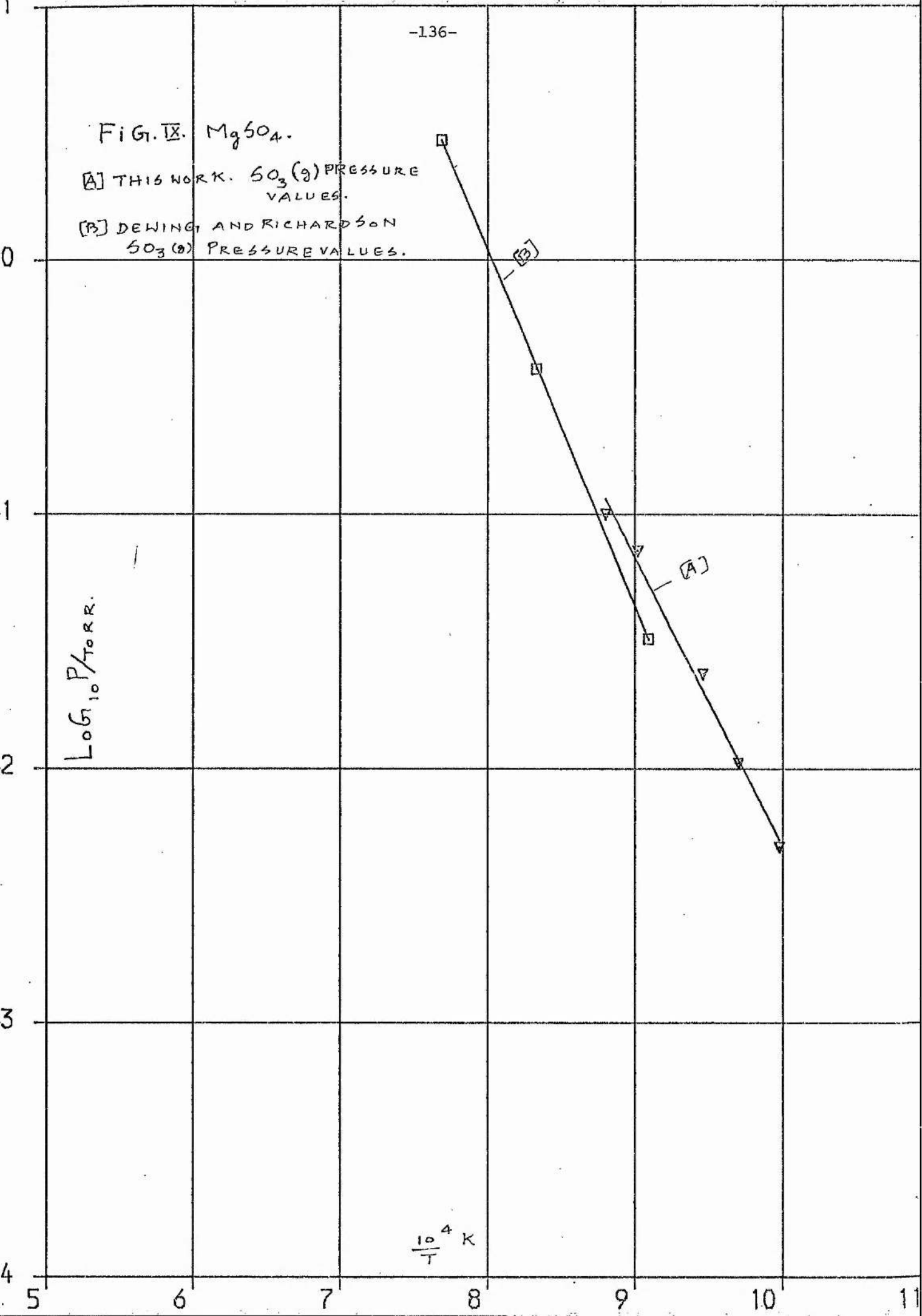
FIG. IX. $MgSO_4$.

[A] THIS WORK. $SO_3(g)$ PRESSURE VALUES.

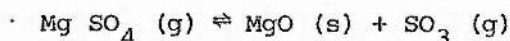
[B] DEWING AND RICHARDSON $SO_3(g)$ PRESSURE VALUES.

$\log_{10} P/Torr.$

$\frac{10^4}{T} K$



transitions for MgSO_4 (s) and MgO (s) there is close agreement between SO_3 (g) pressures of this work and those of Dewing and Richardson's and hence it is reasonable to conclude that the magnesium sulphate decomposes according to the following mechanism

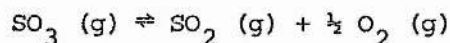


The expression relating the SO_3 (g) vapour pressure dependence on temperature can be represented as follows:

$$* \log_{10} [P/\text{torr}] (950 - 1150 \text{ K}) = 1.136 \pm 0.06 \times 10^4 \text{ K/T} + 3.378 \pm 0.57$$

The ΔH for the above mode of decomposition calculated from the slope yields a value of 217 kJ mol^{-1} .

In spite of the reasonable agreement of the SO_3 (g) pressure values between this work and those of Dewing and Richardson,¹¹⁴ revealed by the above line of argument, the results of the present work are not completely free from criticism. If, as we assumed, SO_3 (g) is the primary product of decomposition from magnesium sulphate and it then dissociates depending upon the Knudsen orifice area, residence time, and temperature, then the slope obtained from $\log P$ vs $1/T$ plot for the largest orifice area ($4.1 \times 10^{-3} \text{ cm}^2$) should be smaller than the slope obtained from the smallest orifice area ($8.9 \times 10^{-4} \text{ cm}^2$) due to the $-\Delta H$ of the following reaction



However, the slopes measured were -1.14 and -1.06 respectively for the largest and smallest orifice area. At present it is not possible to offer any specific explanation for this observation.

SUMMARY

The results of the Knudsen effusion study of calcium and magnesium sulphate reveal that while the high temperature decomposition and thermodynamics of calcium sulphate could be satisfactorily explained both qualitatively and quantitatively the situation is not very clear with respect to magnesium sulphate. However, an attempt has been made to present a reasonably consistent interpretation of the present results. This work has also provided evidence for the hypothesis that both calcium and magnesium sulphate vaporise or decompose with a kinetic barrier or in other words, these substances have low accommodation coefficients and a significant number of gas molecules striking the sample surface do not condense but are reflected back into the gas phase. The complementary effects also shows up in the ionisation mechanism. In the present work it was assumed that SO_3 (g) is the primary product of decomposition of MgSO_4 (s) and that it decomposes within the Knudsen cell to an extent based on the residence time, temperature, and frequency of collision with the walls. This assumption was largely based on the results of Pechkovsky¹²³ and Cubicciotti¹³⁷. If this assumption is right, then further matrix isolation studies with the largest and smallest orifices would provide evidence for this one way or the other. In other words if the SO_3 (g) is the primary product of decomposition, then with the largest orifice area, its residence time within the Knudsen cell would be small compared to the time for the smallest orifice area and would therefore show comparatively more absorbance in the matrix isolation experiments.

APPENDIX I

THERMODYNAMIC FUNCTIONS ESTIMATED FOR GASEOUS Na_2SO_4

Temp (K)	$H_T^{\circ} - H_{298}^{\circ}$ (kcal/mole) ^a	S_T° (gibbs/mole)	$-\left[\frac{G_T^{\circ} - H_{298}^{\circ}}{T} \right]$ (gibbs/mole)
1000	22.98	125.2	102.2
1100	26.57	128.6	104.5
1200	30.19	131.8	106.6
1300	33.84	134.7	108.7
1400	37.50	137.4	110.6
1500	41.18	139.9	112.5
1600	44.86	142.3	114.3
1700	48.56	144.6	116.0

$$^a H_{298}^{\circ} - H_{\text{O}}^{\circ} = 5.40 \text{ k cal mol}^{-1}$$

APPENDIX II

THERMODYNAMIC FUNCTION FOR THE CONDENSED PHASE (Li_2SO_4).

Temp K	$H_T^{\circ} - H_{298}^{\circ}$ (K cal mol ⁻¹)	S_T° cal mol ⁻¹	$-\left[\frac{G_T^{\circ} - H_{298}^{\circ}}{T} \right]$ cal mol ⁻¹
400	3.16	38.10	30.20
500	6.66	45.88	32.56
600	10.53	52.94	35.39
700	14.80	59.51	38.37
800	19.45	65.71	41.40
848 (S1)	21.82	68.59	42.86
848 (S2)	27.93	75.79	42.86
900	30.81	79.09	44.86
1000	36.09	84.66	48.57
1100	41.00	89.34	52.07
1130 (S2)	42.40	90.60	53.07
1130 (L)	44.65	92.57	53.07
1200	48.13	95.55	55.45
1300	53.09	99.52	58.68
1400	58.06	103.20	61.73

APPENDIX III

THERMODYNAMIC FUNCTIONS FOR CONDENSED PHASES

Temp (K)	$H_T^{\circ} - H_{298}^{\circ}$ (kcal/mole)	S_T° (gibbs/mole)	$-\left[\frac{G_T^{\circ} - H_{298}^{\circ}}{T} \right]$ (gibbs/mole)
A: Cs_2SO_4			
400	3.35	60.28	51.91
500	7.03	68.48	54.42
600	11.11	75.92	57.39
700	15.59	82.81	60.54
800	20.46	89.31	63.73
900	25.73	95.51	66.92
940 (S1)	27.95	97.92	68.19
940 (S2)	28.55	98.56	68.19
1000	31.27	101.36	70.09
1100	36.10	105.96	73.15
1200	41.29	110.48	76.07
1274 (S2)	45.37	113.8	78.16
1274 (1)	53.99	120.5	78.16
1300	55.28	121.5	79.02
1400	60.22	125.2	82.19
B: Rb_2SO_4			
400	3.45	57.12	48.49
500	7.20	65.47	57.07
600	11.31	72.96	54.11
700	15.78	79.84	57.30
800	20.60	86.27	60.52
900	25.79	92.37	63.72
931 (S1)	27.47	94.21	64.71
931 (S2)	28.46	95.27	64.71

1000	31.54	98.47	66.93
1100	36.25	102.95	70.00
1200	41.23	107.28	72.93
1300	46.48	111.49	75.73
1339 (S2)	48.60	113.3	76.80
1339 (1)	57.77	119.9	76.80
1400	60.78	122.1	78.73

APPENDIX IV

THERMODYNAMIC FUNCTIONS ESTIMATED FOR THE GASES

Temp (K)	$H_T^{\circ} - H_{298}^{\circ}$ (Kcal/mole)	S_T° (gibbs/mole)	$-\left[\frac{G_T^{\circ} - H_{298}^{\circ}}{T} \right]$ (gibbs/mole)
A: Cs ₂ SO ₄			
298	0	100.6	100.6
400	2.87	108.9	101.7
500	5.94	115.7	103.8
600	9.18	121.6	106.3
700	12.55	126.8	108.9
800	16.00	131.4	111.4
900	19.52	135.6	113.9
1000	23.08	139.3	115.2
1100	26.68	142.7	118.5
1200	30.30	145.9	120.6
1300	33.95	148.8	122.7
B: Rb ₂ SO ₄			
298	0	99.1	99.1
400	2.87	107.3	100.1
500	5.94	114.2	102.3
600	9.18	120.1	104.8
700	12.55	125.3	107.3
800	16.00	129.9	109.9
900	19.52	134.0	112.3
1000	23.08	137.8	114.7
1100	26.68	141.2	116.9
1200	30.31	144.3	119.1
1300	33.95	147.3	121.2

REFERENCES

1. M.A. Soliman, R.H. Carty, W.L. Cogner, and J.E. Funk, *Can.J.Chem. Eng.*, 1975, 53, 164.
2. J.B. Pangborn and D.P. Gregory, "nuclear energy requirements for hydrogen production from water," 9th Inter society energy conversion Engineering Conference, San Francisco, August, 1974.
3. J.B. Pangborn, Personal communication
4. G.V. Jagannathan, G.R. Wolley, and P.A.H. Wyatt, *Annual Reports*, A, The Chemical Society, London, 1974.
5. L. Brewer and A.W. Searcy, *Ann. Rev. Phys. Chem.*, 1956, 7, 259.
6. J.L. Margrave, *Ann. Rev. Phys. Chem.*, 1959, 10, 457.
7. P.W. Gilles, *Ann. Rev. Phys. Chem.*, 1961, 12, 355.
8. R.F. Porter, *Ann. Rev. Phys. Chem.*, 1959, 10, 219.
9. J. Drowart and P. Goldfinger., *Ann. Rev. Phys. Chem.*, 1962, 13, 459.
10. R.J. Thorn, *Ann. Rev. Phys. Chem.*, 1966, 17, 83.
11. J.W. Hastie, R.H. Hauge, and J.L. Margrave., *Ann. Rev. Phys. Chem.*, 1970, 21, 475.
12. W. Buss, *Glas tech. Ber.*, 1962, 35, 167.
13. A.R. Conroy, W.H. Manring, and W.C. Bauer, *The Glass Industry.*, 1966 47, 84.
14. K.D. Carlson, Chapter 5 in "Characterisation of High temperature vapours" (Editor, J.L. Margrave, Wiley, New York, 1967).
15. M. Knudsen, *Ann. Physik.*, 1909, 28, 75.
16. M. Knudsen, *Ann. Physik.*, 1909, 28, 999.
17. E.H. Kennard, *Kinetic theory of Gases.*, McGraw-Hill Book. Co., New York, 1938.
18. P. Clausing, *Ann. Physik.*, 1932, 12(5), 961.
19. J.L.M. Poiseuille, *Compt. Rend.*, 1840, 11, 961, 1041.
20. I. Langmuir, *Phys. Z.*, 1913, 14, 1273.
21. W.C. Demarcus, "The problem of Knudsen flow oak Ridge Gaseous diffusion plant technical report K - 1302, Parts I, II, III, 1956/57.
22. C.I. Whitman, *J.Chem. Phys.*, 1952, 20, 161. 1953, 21, 1407.
23. K. Motzfeldt, *J. Phys. Chem.*, 1955, 59, 139.
24. E.W. Balson, *J. Phys. Chem.*, 1961, 65, 1151.

25. P.I. Ozhegov and A.M. Evseev., zh. Fiz. Khim., 1969, 41, 1809.
26. R.D. Freeman and A.W. Searcy, J. Chem. Phys., 1954, 22, 762.
27. J.Q. Adams, T.E. Phipps and P.G. Wahlbeck, J. Chem. Phys., 1968, 49 1609.
28. J.W. Ward, and M.V. Fraser, J. Chem. Phys., 1968, 49, 3743.
29. V.I. Lozgachev, zh, Fiz. Khim., 1963, 37, 644.
30. E.H. Kennard, Kinetic theory of Gases and Introduction to statistical mechanics (McGraw-Hill Publ. Co., New York, 1938).
31. R.P. Burns, J. Chem. Phys., 1966, 44, 3307.
32. G.M. Rosenblatt, J. Phys. Chem., 1967, 71, 1327.
33. A.N. Nesmeyanov, vapour pressures of the chemical elements (Elsevier Publ. Co. Ltd., London, 1963).
34. G.M. Rosenblatt and Pang. Kai-Lee, J. Chem. Phys., 1970, 52, 1454.
35. G.L. Vidale, U.S. Dept. Com., Office Tech. Serv., PB Report 1960, 153, 300.
36. L. Brewer and J.J. Kane, J. Phys. Chem., 1955, 59, 105.
37. R.G. Bautista and J.L. Margrave. J. Phys. Chem., 1965, 69, 1770.
38. R.J. Thorn and G.H. W. Wilson, J. Chem. Phys., 1957, 26, 186.
39. A.R. Miller, J. Phys. Chem., 1967, 71, 1144.
40. E. Kay and N.W. Gregory, J. Phys. Chem., 1958, 62, 1079.
41. P.E. Hart and A.W. Searcy, J. Phys. Chem., 1966, 70, 2763.
42. A.S. Pashinkin, zh., Fiz. Khim., 1964, 38, 2690.
43. A.S. Pashinkin, zh. Fiz. Khim. 1966, 40, 2611.
44. A.S. Pashinkin, zh, Fiz. Khim., 1968, 42, 1511.
45. J.H. Knox and P.A.H. Wyatt, J.C.S. Faraday I, 1973, 69, 1961.
46. M.G. Rossman and J. Yarwood, J. Chem. Phys., 1953, 21, 1406.
47. C.I. Whitman, J. Chem. Phys., 1953, 21, 1467.
48. H.V. Wartenberg, Z. ElectroChem., 1913, 19, 482.
49. E. Preston, Trans.Faraday. Soc., 1933, 29, 1188.
50. H.W. Melville and S.C. Gray, Trans. Faraday Soc., 1936, 32, 271, 1017, 1026
51. J. Lumsden, Thermodynamics of Alloys., London. Inst. Metals. 1959.
52. H. Braune, Z. Anorg. Allegem. Chem., 1920, 111, 109.

53. C.B. Alcock and G.W. Hopper, Proc. Roy. Soc. (A) 1960, 254, 551.
54. W. Fischer and O. Rahlfs, Z. anorg. Chem., 1932, 205, 1.
55. D. Battat, M.M. Faktor, I. Garret and R.H. Moss, J.C.S. Faraday I., 1974, 70 2267.
56. C. Barthel, and H. Dode, Bul. Soc. Chim. Frank., 1954, 1312.
- 57a. J. Drowart and P. Goldfinger, Agnew. Chem. Inst. Ed. 1967, 6, 581.
- 57b. R.T. Grimley in "The Characterisation of high temperature vapours" Editor, J.L. Margrave. J. Wiley. New York 1967.
- 57c. R.C. Svedberg in Modern aspects of mass spectrometry R.I. Reed. Editor. Plenum Press, New York 1968.
- 57d. H. Hurzeler, M.G. Inghram, J.D. Morrison, J. Chem. Phys., 1958, 28, 76.
58. V.H. Dibeler, R.M. Reese, J. Res. NBS 1964, 68A, 409
59. J. Berkowitz, W.A. Chupka, J. Chem. Phys., 1966, 45, 1287
60. J. Berkowitz, T.A. Walter, J. Chem. Phys., 1968, 49, 1184.
61. T.A. Walter, C. Lifshitz, W.A. Chupka, J. Berkowitz, J. Chem. Phys., 1969, 51, 3531.
62. W.A. Chupka, J. Chem. Phys, 1968, 48, 2337.
63. J. Berkowitz, C. Lifshitz, J. Chem. Phys, 1968, 48, 4346.
64. H. Fujisaki, J.B. Westmore, A.W. Tickner, Can. J. Chem., 1966, 44, 3063.
65. L.N. Sidorov. P.A. Akishin, V.I. Belousov, Russ. J. Phys. Chem., 1969, 43, 39.
66. A. Snelson, J. Phys. Chem., 1969, 73, 1919.
67. L. Andrews, J. Chem. Phys. 1969, 50, 4288.
68. M.J. Linevsky, J. Chem. Phys, 1961, 34, 587.
69. J.L. Margrave, J.W. Hastie, R.H. Hauge, in spectroscopy in Inorganic Chemistry, Vol II, Editors C.N.H. Rao and John Ferrazo. Academic, New York. 1970.
70. H.E. Hallam. Editor. Vibrational spectroscopy of trapped species. John Wiley & Sons, 1973.
71. E.D. Becker and G.C. Pimental, J. Chem. Phys., 1956, 25, 224.
72. M.M. Rochkind, Science., 1968, 160, 196.
73. A.M. Bass, and H.P. Broida, "Formation and trapping of Free Radicals". Academic Press, New York, 1960.

74. G.C. Pimental, and S.W. Charles, *Pure Appl. Chem.*, 1963, 1, 111.
75. J.M.P. Verstegen, H. Goldring, and B. Katz. *J. Chem. Phys.*, 1966, 44, 3216.
76. G.W. Robinson, W.G. Von Holle, *J. Chem. Phys.*, 1966, 44, 410.
77. G.K. Pandey, and S. Chandra, *J. Chem. Phys.*, 1966, 45, 4369.
78. S.W. Charles, and K.O. Lee, *Trans. Faraday. Soc.* 1965, 61, 2081.
79. H.C. Longuet-Higgins, and J.A. Pople, *J. Chem. Phys.*, 1957, 27, 192.
80. G.W. Robinson, *Electronic Spectra in "methods of experimental physics" Editor, D. Williams. Academic Press, New York, 1962, 3, 155.*
81. M. McCarty jr, and G.W. Robinson, *Mol. Phys.*, 1959, 2, 415.
82. L. Brewer, B.A. King, J.L. Wang, B. Meyer, and G.F. Moore, *J. Chem. Phys.*, 1968, 49, 5209.
83. G. Boato, *Cryogenics.*, 1964, 4, 65.
84. G.A. Cook, Editor. "Argon, Krypton and the rare gases" Wiley (Interscience), New York, 1961.
85. G.L. Pollack, *Rev. Mod. Phys.*, 1964, 36, 748.
86. M.T. Bowers, *J. Chem. Phys.*, 1967, 47, 3100.
87. G. Marchal, *Bull. Soc. Chim. Fr.*, 1929, 45, 225.
88. E. Terres, *Brennstoff Chemic.*, 1954, 35, 225.
89. H. Liander, and G. Olsson., 1937, 4, IVA, 145.
90. G. Eyber, *Glastech. Ber.*, 1960, 33, 283.
91. C. Kroger, and J. Stratmann, *Glastech. Ber.*, 1961, 34, 311.
92. R. Bruckner, *Glastech. Ber.*, 1962, 35, 93.
93. M.G. Hocking, Private communication to BGIRA.
94. A.A. Fotiev, and B.V. Slobodin, *zh. Neorg. Khim.*, 1965, 10, 569.
95. S. Holmquist, *The Glass Industry.*, 1968, 49, 143.
96. H.H. Kellog, *Trans. A.I.M.E.*, 1964, 230, 1622.
97. W.H. Manring, and W.C. Bauer, *Bull. Am. Ceram. Soc.*, 1965, 44, 405.
98. L. Brewer and J.L. Margrave, *J. Phys. Chem.*, 1955, 59, 421.
99. P.A.H. Wyatt, Private communication to BGIRA.
100. P.J. Ficalora, O.M. Uy, D.W. Muenow, and J.L. Margrave, *J. Am. Ceram. Soc.*, 1968, 51, 574.

101. T. Kosugi, *Kogyo Kagaku Zasshi.*, 1970, 73, 1087. CA:73:834286.
102. D.G. Powell and P.A.H. Wyatt, *J. Am. Chem. Soc.*, Sec (A) 1971, 4, 3614.
103. D. Cubicciotti, and F.J. Keneshea, *High. temp. sci.*, 1972, 4, 32.
104. F.M. Jaeger, *Z. alleg. chem.*, 1917, 101, 178.
105. N.M. Hopkin, Mellor's comprehensive Treatise on Inorganic and theoretical chemistry, Vol II, Supplement III, Longmans, 1963.
106. V.I. Spitsyn and V.I. Shostak, *Zh. Obstich. Khim.*, 1949, 19, 1801.
107. V.P. Spiridonov, A.H. Khodehenkov, and P.A. Akishn, *J. Struct. Chem. U.S.S.R.*, 1965, 6, 633.
108. A. Buchler, J.L. Stauffer, and W. Klemperer, *J. Chem. Phys.*, 1967, 46, 605.
109. D. Cubicciotti, *High temp. sci.*, 1971, 3, No. 4, 349.
110. K.H. Stern and E.L. Weise, *V.S. Nat. Bur. Stand. Rep.*, NSRDS-NBS7, 1966.
111. C. Tschappat and R. Piece, *Helv. Chim. Acta.*, 1956, 39, 1427.
112. J. Zawadski, *Z. anorg. Chem.*, 1926, 205. 180.
113. G. Marchal, *J. Chim. Phys.*, 1926, 13, 78.
114. E.W. Dewing and F.D. Richardson, *Trans. Far. Soc.*, 1959, 55, 611.
115. J. Rosenquist, *Metals.*, 1951, 3, 535.
116. Richardson, and Jeffes, *J. Iron Steel. Inst.*, 1952, 171, 165.
117. Fyske, *Tidsskr. Kjemi. Bergvesen. Met.*, 1956, 16, 203.
118. Schenck, and Hammerschmidt, *Z. anorg. Chem.*, 1933, 210, 305.
119. A.G. Ostroff, and R.T. Sanderson., *J. Inorg and Nuclear. Chem.*, 1958, 9, 45.
120. J. Cueilleron, and O. Hartmanshenn, *Bull. soc. Chim. Fr.*, 1959, 164.
121. A.Kh. Bononnikov, *Izvest. Vysshikhucheb. Zavendenii.*, *Khim. i. khim. Tekhnol.*, 1961, 4, 433.
122. E. Kowalska, *Przemyst Chem.*, 1956, 35, 442.
123. V.V. Pechkovski, *Sh. Prikl. Khim.*, 1956, 29, 1137. *Uch. zap. Perusk. Gos. Univ.*, 1959, 13, 93.
124. H.J. Knopf, and H. Staude, *Z. Phys. Chem.*, 1955, 204, 265.
125. F.J. Kohl, C.A. Stearns, and G.C. Fryburg, *BLLD IND. Conf. Proc.*, May 1976, Page 53.

126. D.L. Hildenbrand, and E. Murad, J. Chem. Phys., 1970, 53, 3403.
127. R.E. Fryxell, C.A. Trythall and R.J. Perkins, Corrosion., 1973, 29 423.
128. MM. Lucien Denielou, Yan Fournier, Jean-Pierre Petitot, and Christophe Tequi, C.R. Acad. Sc. Paris., 1970, t 270, 1854.
129. F.D. Rossini, D.D. Wagman, W.H. Evans, S. Levine and I. Jaffee, Nat. Bur. Standards 1952. Selected values of chemical thermodynamic properties.
130. W.M. Latimer, J. Am. Chem. Soc., 1951, 73, 1480.
131. I.E. Paukov, L.M. Khriplovich, A.M. Korotkikh, and M.N. Lavrent'Eva, Russ. J. Phy. Chem., 1968, 42, 661, 972.
132. MM. Lucien Denielou, Yan Fournier, Jean-Pierre Petitot, and Christophe Tequi, C.R. Acad. Sc. Paris 1969, t 269, 1577
1970, t 270, 1854.
133. S.M. Skuratov, N.A. Ibrahim, and A.F. Borob'Ev, Russ. J. Inorg. Chem, 1966, 11, 13.
134. D. Cubicciotti, J. Phys. Chem., 1966, 70, No7, 2410.
135. JANAF Thermochemical tables, No. PB-1681370. Edited by D.R. Stull, Dow Chemical Co. Midland, Michigan, 1964.
136. Pirooz Mohazzabi, and A.W. Searcy, Faraday Transactions I., 1976, 2, 290
137. D. Cubicciotti, Private communication